ACTA UNIVERSITATIS SZEGEDIENSIS

ACTA PHYSICA ET CHEMICA

NOVA SERIES

TOMUS XXXIII FASCICULI 1—4.

AUSHAF 33 (1—4) 1987

HU ISSN 0324—6523 Acta Univ. Szeged

HU ISSN 0001—6721 Acta Phys. et Chem.

SZEGED, HUNGARIA

1987

ACTA UNIVERSITATIS SZEGEDIENSIS

ACTA PHYSICA ET CHEMICA

NOVA SERIES

TOMUS XXXIII FASCICULI 1—4.

AUSHAF 33 (1—4) (1987)

HU ISSN 0324—6523 Acta Univ. Szeged

HU ISSN 0001—6721 Acta Phys. et Chem.

SZEGED, HUNGARIA

1987

Adiuvantibus

M. BARTÓK, K. BURGER, L. CSÁNYI, J. CSÁSZÁR, P. FEJES,
P. HUHN, E. KAPUY, I. KETSKEMÉTY, F. SOLYMOSI, et F. SZÁNTÓ

Redigit
MIKLÓS I. BÁN

Edit

Facultas Scientiarum Universitatis Szegediensis de
Attila József nominate

Editionem curant
J. ANDOR, I. BÁRDI, Á. MOLNÁR, et Á. SÜLI

Nota

Acta Phys. et Chem. Szeged

Szerkeszti
BÁN MIKLÓS

A szerkesztő bizottság tagjai:
BARTÓK M., BURGER K., CSÁNYI L., CSÁSZÁR J., FEJES P.,
HUHN P., KAPUY E., KETSKEMÉTY I., SOLYMOSI F., és SZÁNTÓ F.

Kiadja

a József Attila Tudományegyetem Természettudományi Kara
(Szeged, Aradi vértanúk tere 1.)

Szerkesztő bizottsági titkárok:

ANDOR J., BÁRDI I., MOLNÁR Á., és SÜLI Á.

Kiadványunk rövidítése:

Acta Phys et. Chem. Szeged

ISBN 963 481 623 I
Acta Phys. et. Chem Szeged 33 3-10 (1987)

CHANGE CAUSED IN CHARGE DENSITY OF Si BY A HEXAGONAL SITE SELF-INTERSTITIAL

By

G. PAPP[1], P. BOGUSLAWSKI[2] and A. BALDERESCHI[3]

[1] Department of Theoretical Physics, József Attila University Szeged, Aradi vértanuk tere 1., Hungary

[2] Institute of Physics, Polish Academy of Sciences, Warsaw, Poland

[3] Institut de Physique Appliquée, Ecole Polytechnique Federale, Lausanne, Switzerland

Istituto di Fisica Teoretica, Università di Trieste, Italy

(Received 26 April 1987)

The electronic charge density of a self-interstitial at a hexagonal site in Si is investigated. From the results it can be established that the charge density around the self-interstitial atom is metallic-like and the nearest-neighbour bonds are weakened.

Silicon self-interstitials are poorly understood in comparison with other defects (substitutionals or vacancies, for example). Though vacancies and interstitials should be created in equal numbers by irradiation, only vacancies are observed. There is no experimental evidence for the existence of self-interstitials. However, to understand other interstitial impurities, it is instructive to study self-interstitials.

In this paper we present results on the change caused in the charge density of silicon by a self-interstitial at a hexagonal site.

We calculated the electronic structure by using the self--consistent pseudopotential electron-energy approach [1], with the Appelbaum-Hamann soft-core pseudopotential [2]. In this momentum-space formulation, supercells are used to modell the interstitial [3]. The supercell contains sixteen host atoms and a nearest-neighbour - interstitial distance of 7.6 Å. In our calculations a plane wave basis set (about 700 plane wa es) was treated. When this approach is used for pure silicon test calculations, the results are in good agreement with those obtained by more sophisticated methods.

Let us now proceed to the results. In order to examine the nature of the self-interstitial - lattice bonding, in Fig. 1 we show contour plots of the total valence charge density obtained from our calculations.

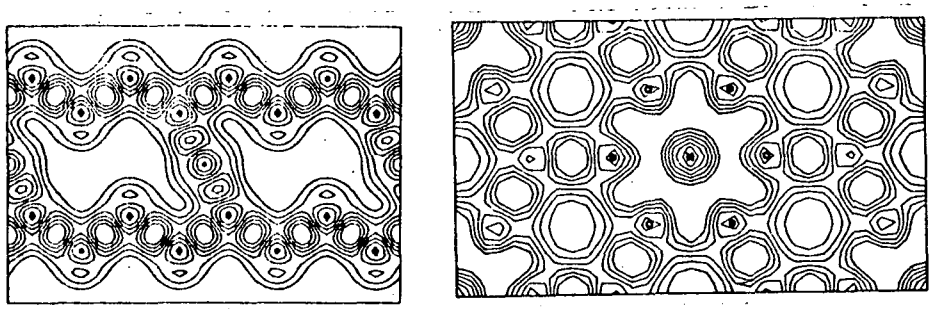

Figure 1: Self-consistent valence charge density contour plot in two different planes: (110) plane (left panel), (111) plane (right panel).

The planes shown are the (110) plane, containing a zigzag chain of atoms (the dark circles) and the self-intersitial (star), and the (111) plane, showing the hexagonal environment. Bonding between the interstitial and the nearest-neighbour atoms is evident, but the charge density accumulation around

the impurity is rather metallic-like. There is a remarkably constant-density region (no contour in the (111) plane) near the Si self-interstitial atom.

Figure 2 shows the $\Delta\rho(\vec{r})$, contour plot for the (110) plane. $\Delta\rho(\vec{r})$ is defined by

$$\Delta\rho(\vec{r})=\rho^{D}(\vec{r})-\rho^{P}(\vec{r}),$$

where $\rho^{D}(\vec{r})$ is the charge density of silicon containing an extra atom, and $\rho^{P}(\vec{r})$ is the pure silicon charge density.

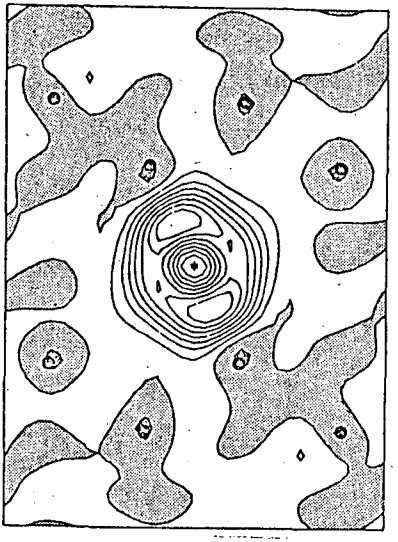

Figure 2: Contour plot of valence charge density difference in (110) plane.

The grey part of Fig. 2 is negative and the remainder is positive. Indifferently, the nearest-neighbour bonds are weakened.

As we have shown earlier [4,5], a hexagnal site self-interstitial produces three main impurity-related states up to the bottom of the conduction band: a hyperdeep state below the valence band, an s-like resonance in the valence band, and a p_z-like bound state in the gap near the top of the valence band. The charge density contour plots in the (110) plane are shown for these states in Fig. 3: the hyperdeep state (panel C), the s-like resonance (panel A) and the p_z-like state (panel B). It can be seen from Fig. 3 that the hyperdeep state and the p_z-like state are well localized around the impurity while the resonance state involves charge

on the nearest neighbours too.

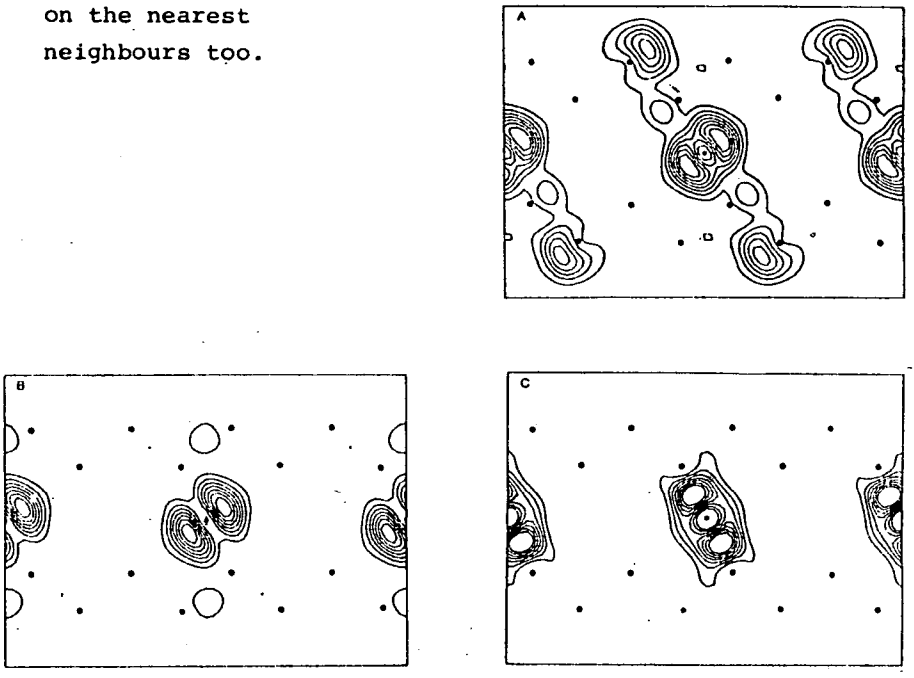

Figure 3: Contour plots of impurity-related states in (110) plane: resonance state (panel A); p_z-like state (panel B); hyperdeep state (panel C).

For the analysis, we decomposed the impurity-related wavefunctions:

$$\psi = P_V \psi + P_C \psi = \psi_V + \psi_C$$

where P_V and P_C are the projectors onto the valence and conduction subspaces, respectively, of perfect Si. In all cases we found that ψ_V consists essentially of host crystal bonding orbitals, and ψ_C corresponds to atomic orbitals of the

self-interstitial orthogonalized to the whole valence states. These results are shown by Figs. 4 and 5 for the hyperdeep state and resonance state in the (211) plane. For the hyperdeep state, contributions from the valence bands dominate, while for the resonance state the effect of the

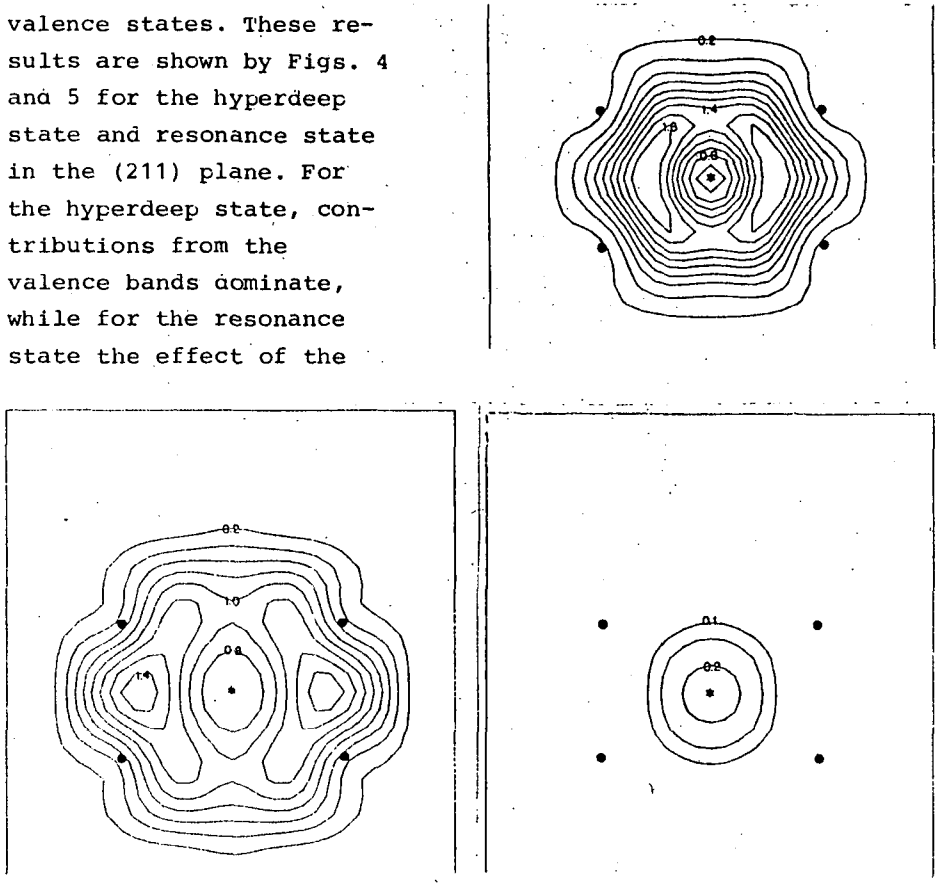

Figure 4: Electron density contour in the (211) plane of the hyperdeep state (top panel), and its projection onto the valence (left panel) and the conduction (right panel) states of perfect Si. Contour values are given in units of one electron/Si unit cell. The self-interstitial and host atoms are indicated by an asterisk and dots, respectively.

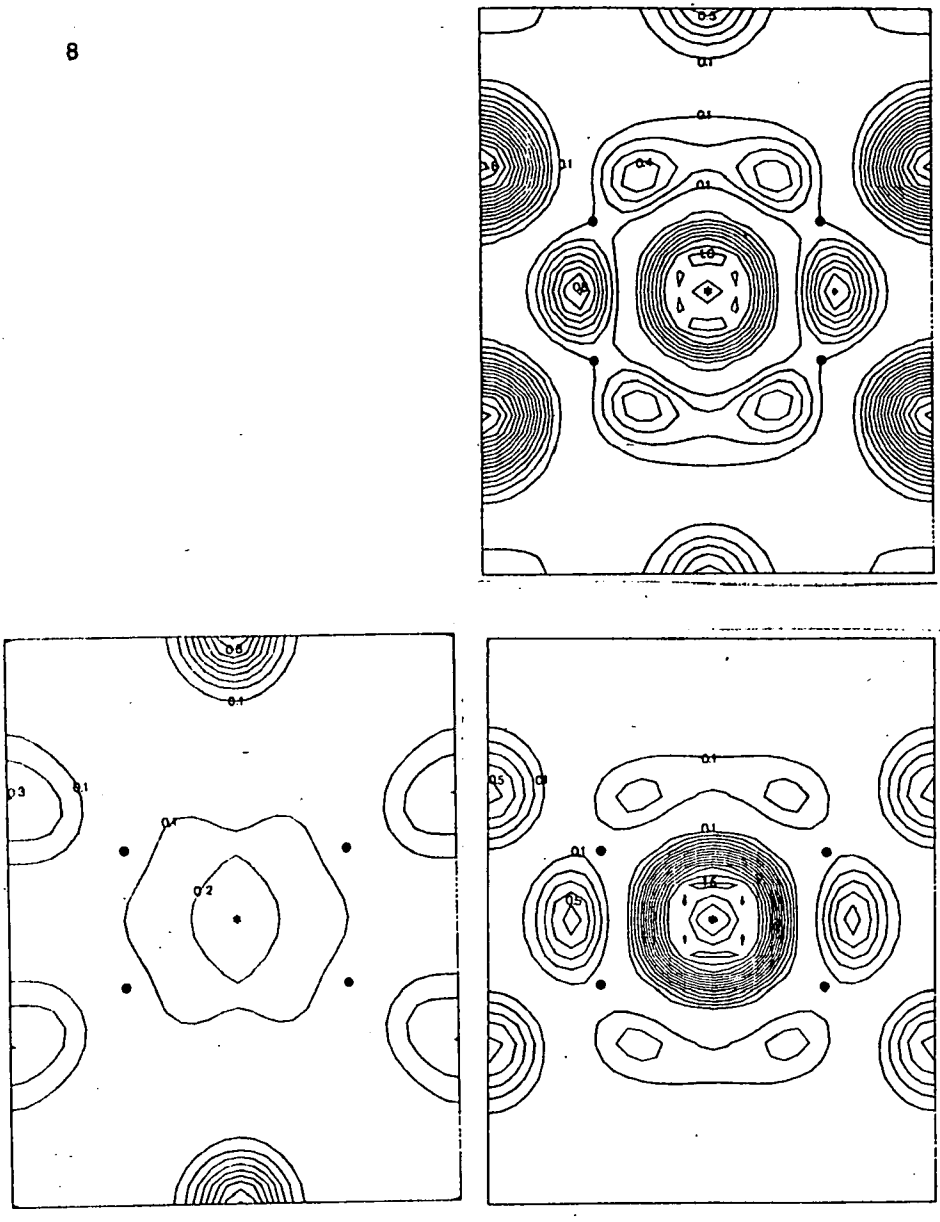

Figure 5: Analysis of the electron density of the s-like resonance state. Same conventions as in Fig. 4.

conduction band is marked. As regards the symmetry properties of the relevant states, we found that the hyperdeep state is a symmetric combination of the nearest-neighbour bonds and the impurity s-orbitals, and the resonance state is an antisymmetric one. Results for the p_z-like state can be found, for example, in [5].

References

[1] *Brust, D.*: Phys. Rev. *A134*, 1337 (1964)

[2] *Appelbaum J.A. and D.R. Hamann*: Phys. Rev. *B8*, 1777 (1973)

[3] Several authors have used the large unit cell approach to study impurity problems. See, for example: *Louie, S.G., M. Schlüter, J.R. Chelikowsky and M.L. Cohen*: Phys. Rev. *B13*, 1654 (1976); *Lindenfelt, U.*: J. Phys. *C11*, 65 and 3651 (1978); *Pickett, W.E., M.L. Cohen and C. Kittel*: Phys. Rev. *B20*, 5050 (1979); *Vanderbilt, D and J.D. Joannopoulos*: Phys. Rev. Lett. *49*, 823 (1982); *Dzwig, P., M.G. Burt, J.C. Inkson and V. Crum*: J. Phys. *C15*, 1187 (1982); *Evarestov, R.A.*: Kvantovokhimicheskie metodi v teorii tverdovo tela, Izdatelstvo Leningradskovo Universiteta (1982)

[4] *Papp, G., P. Boguslawski and A. Baldereschi*: Acta Phys. et Chem. Szeged *32*, 9 (1986)

[5] *Boguslawski, G. Papp and A. Baldereschi*: Solid State Comm. *52*, 155 (1984).

ИЗМЕНЕНИЕ В ПЛОТНОСТИ ЗАРЯДА КРЕМНИЯ ОКАЗЫВАЕМОЙ ГЕКЗАГОНАЛЬНОЙ ТОЧКОЙ САМО-МЕЖДОУЗЛИЯ

Г. Папп, П. Богуславски и А. Балдересски

Исследована плотность электронного заряда само-междоузлия в гекзагональной точке кремния. Из результатов видно, что плотность заряда вокруг атома само-междоузлия и ближайшие связи ослаблены.

ISBN 963 481 624 X
Acta Phys. et Chem. Szeged 33 11-21 (1987)

ON THE SPECTRA OF SOME ACCEPTOR-TYPE POLYNITRO DERIVATIVES OF BIPHENYL, BIPHENYLMETHANE AND BIPHENYLAMINE

By

J. CSÁSZÁR

Institute of General and Physical Chemistry, József Attila University, P.O.B. 105, H-6701, Szeged, Hungary

(Received 1 October 1987)

The UV and visible spectra of nitro and polynitro derivatives of biphenylamine were investigated and the substituent effects were interpreted in comparison with the corresponding biphenyl and biphenylmethane derivatives.

Introduction

It is well known [1-5] that polynitro aromatic compounds act as acceptor molecules and form stable molecular complexes with, for example, aromatic Schiff bases [6-8]. It has been stated that if any nitro group is prevented from assuming a coplanar arrangement with the attached ring, then the polynitro compound will be a less effective complexing agent. For example, trinitrobenzene forms more stable complexes with aromatic hydrocarbons than either trinitrotoluene or picric acid does. Both polar and steric factors may be responsible for this decrease in the complexing ability [9].

We have prepared a series of molecular complexes of aro-

matic Schiff bases as donors with different polynitro compounds as acceptors and studied their UV and visible spectra. The spectra of aromatic Schiff bases have already been discussed in several papers [e.g. 10-12]; in this work, a short review is primarily given of the spectral behaviour of the polynitro acceptor molecules.

Experimental

The compounds investigated were Merck p.a. chemicals. The UV and visible spectra were determined on a SPECORD UV-VIS spectrophotometer, in quartz cells. The solvents were commercially available, spectroscopically pure solvents. The acidic and basis solutions contained 0.1 mol/dm^3 H_2SO_4 or NaOH in methanol.

The twist angles θ_N were calculated by using the formula $\cos^2 \theta_N = \varepsilon / \varepsilon_o$, where ε and ε_o are the molar extinctions of the compound investigated and the planar (quasi-planar) form, respectively.

Results and Discussion

Before a discussion of the spectral behaviour of biphenylamines, it is interesting to compare the corresponding nitro derivatives of biphenyl (BP), biphenylmethane (BPM) and biphenylamine (BPA). Some data are presented in Table I.

The spectrum of BP shows an intense band at 252 nm, which corresponds to the ^1L_a benzene band; the forbidden lower-in-

Table I

λ_{max} and log ε values of BP, BPM, BPA *and their substituted derivatives*

Positions of nitro groups		BP		BPM		BPA
		λ/nm(logε)				
none	a	252(4.26)[13]	c	268(2.61)[16]	d	285(4.31)
2	b	296(3.30)[14]	c	254(3.66)[17]	d	425(3.87)
4	b	295(4.20)[14]	c	278(4.02)[17]	d	392(4.34)
2,2′	b	253(4.10)[15]	c	256(4.00)[18]	d	420(3.97)[19]
4,4′	b	295(4.00)[15]	c	277(4.36)	d	404(4.57)
2,4	b	265(4.02)[15]	d	262(4.12)	c	350(4.23)

a: cyclohexanone; b: isooctane+ 2% CH_2Cl_2; c: ethanol; d: methanol

tensity ^1L_b band is hidden below this band [20].

Pauling [9] suggested that steric interactions between the *ortho* hydrogens should result in a non-coplanar conformation; the interplanar angle in the solution state is about 20° [21]. Theoretically, *cis* and *trans* conformations are possible for 2,2′ derivatives, but electron diffraction data [22, 23] indicate that the 2,2′-dihalogeno-BP derivatives, for example, have a *cis* configuration. The effect of 2,2′ substituents is very important. For instance, 2,2′, 6,6′-tetrachloro-BP is known to be a true biradical [24]. In 4-amino-4′-nitro-BP, the 4′-nitro group exerts a marked effect on the basicity of the 4-NH_2 group, but this effect is diminished by 2 or 2,2′ substituents because these groups block the nitro-amine resonance through the forced non-coplanarity of the conformation of the BP skeleton [25].

Due to the steric interference, the 2,2′ derivative of BP

departs from the coplanar conformation and the resonance is destroyed; the absorption is approximately that of two nitrobenzene molecules. 4,4-Dinitro-BP displays and increased intensity and the band is shifted to longer wavelengths, which can be attributed to the increased polarity of the excited state and to the lowering of the energy required to produce this state [26]. The data in Table I show that for the 2-nitro derivative the band is shifted towards longer wavelengths and the intensity decreases. Similar intensity decreases can be observed for the 2,2' and 2,4 derivatives. The steric inhibition by the bulky nitro groups is obvious, and these compounds have a twisted conformation around the short (1.48 nm [9, 21]) central 1-1' bond. The calculated twist angles θ_N for these three derivatives are 71, 36 and 41°, respectively.

Toluene shows the ^1L_a benzene band at 261 nm ($\log\varepsilon$= 2.35) [14], while BPM has a band at 268 nm ($\log\varepsilon$=2.61) [16]; i.e. the two phenyl rings behave as two separate chromophores. However, a comparison of the spectra of 4-nitrotoluene and 4,4'-dinitro-BPA reveals that this relationship is not valid. Derivatives containing NO_2 groups in the 2 or 2,2' positions also exhibit a decreased intensity compared to that for the 4 or 4,4' derivatives.

The spectrum of aniline contains two bands at 235 (3.98) and 285 (3.22) nm, which correspond to the ^1L_a and ^1L_b bands of benzene, respectively. For the nitro derivatives, the ^1L_a band does not change considerably (223-239 nm), but the longer-wavelength band does. Due to nitro substitution in the *ortho* position in aniline, the $-NH_2$ group is twisted out of the plane of the ring, and the nitrogen bond angles become more pyramidal; consequently, the promotion energy is lowered. For 4-nitroaniline, no steric interference occurs; calculation of the twist angles θ_N from the measured ε_{max} values for 2-, 2,4-, 2,6- and

2,4,6-nitroaniline gives 56°, 32°, 49° and 50°, respectively.

Introduction of a second benzene ring into the aniline system results in a considerable intensity increase, and the new ring may be assumed to be perpendicular or nearly perpendicular to the plane of the C-N bond and the unshared pair [27]. The spectral data on a series of nitro derivatives of BPA are presented in Table II; our data are in accordance with the literature data [e.g. 28-30]. Since the basic and acidic characters of donors and acceptors, respectively, are very important from the aspect of the formation of molecular complexes, Table II also contains the pK_a values of several BPA derivatives.

2,2'-Alkyl substitution generally causes strong hypsochromic shifts, i.e. the steric hindrance and the non-coplanar conformation will raise the potential energy of the excited state, and hence the transition energy will be increased [31].

2-, 2,2'-, 2,6- and 2,2', 6,6'-nitro substitution causes a strong bathochromic shift (~420 nm) and the intensities decrease (Table II). In these cases, due to the steric interference of the nitro groups, ring *B* is not coplanar with the unshared electron pair of the central nitrogen atom, and the molecule has a twisted conformation (Structure I).

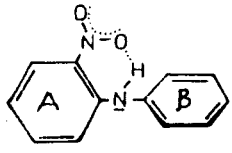

I

In the absence of an *ortho* substituent, e.g. in 4-nitro-BPA, the increased conjugation (which may be crudely represented by resonance form II) tends to change the bonding around the nitrogen atom from a tetrahedral towards a trigo-

Table II

UV and visible spectral data on NO_2 substituted biphenylamines

Positions of nitro groups	Solvent	λ/nm (log ε)			θ_N	pK_a^*
none	MeOH	208(4.33)		285(4.31)		
2	MeOH	220(4.12)	257(4.16)	425(3.87)	53°	17.57
2,2',6,6'	MeOH	229(4.18)		418(3.87)	53°	
2,2'	MeOH	225(4.18)	264(4.22)	420(3.97) [19]	47°	
2,6	MeOH	228(4.18)	256(4.44)	424(3.90)	39°	
2,2',4,4',6,6'	MeOH	208(4.16)		385(4.09)	39°	2.63
2,4,6	EtOH	233(4.29)		367(4.12)	37°	10.38
2,4'	EtOH	245(4.23)	351(4.08)	405(4.14) [19]	35°	13.84
2,2',4	EtOH	228(4.26)	253(4.19)	372(4.16) [19]	33°	
2,2',4,6	MeOH	225(4.21)		374(4.18)	31°	
2,4	EtOH	231(4.11)		350(4.23)	24°	
2,2',4,6,6'	EtOH	234(4.22)		379(4.24)	23°	
2,4,4',6	MeOH	231(4.29)		381(4.29)	12°	8.88
4	MeOH	226(3.80)	257(4.05)	392(4.34)		15.90
4,4'	MeOH	233(4.10)		404(4.57)		14.08
2,4,4'	EtOH	224(4.24)		366(4.33) [19]		12.35
2,2',4,4'	EtOH	219(4.35)	358(4.24)	401(4.36) [19]		10.82
2,2',4,4',6	MeOH	221(4.31)	351(4.25)	409(4.41)		6.72

* Stewart, R., J.P. O'Donnell: J. Amer. Chem. Soc., 84, 493 (1962)

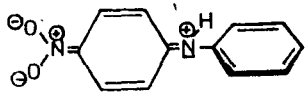

II

nal configuration [27]. This decreases the C-N bond length because of the increased double bond character of the bond, and hence it is more susceptible to steric effects. In contrast, the bands of BPA derivatives containing nitro groups in the 4 or 4,4' positions are shifted hypsochromically, the intensities are slightly decreased and the calculated twist angles are also lower. A similar effect may be observed for the 2,4--dinitro derivative (Structure III).

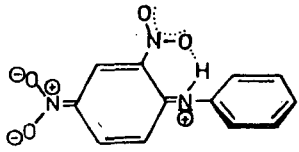

III

The situation more complicated is for this group of compounds relative to the BP and BPM derivatives. In this case the non-bonding electron pair of the central nitrogen atom also participates in the formation of a quinoidal system, which causes a strong bathochromic shift of the bands. The intensity decrease is related to the value $\cos^2\theta$ for the twist angle θ_N [e.g. 14, 32-34]. If we assume that the 285 nm band of BPA corresponds to the band at around 350-420 nm of the nitro derivatives and that BPA is nearly planar, the twist angles can be calculated; the values are presented in Table II. It may be stated that the introduction of the first nitro group into the 2 position causes the greatest twisting; further substitution in the 2' or/and 6,6' positions results in no more change in the conformation, whereas nitro groups in

the 4 or 4,4' positions decrease the twist angle.

In the case of BP derivatives, the steric inhibition of the nitro group(s) is the determinant effect, while for the BPA derivatives the conjugation of the nitro group(s) together with the nitrogen lone pair also plays an important role.

Table III lists the maximum data for the long-wavelength band of 2,2', 4,4',6,6'-hexanitro-BPA (dipicrylamine), measured in different solvents. The solvents can be divided into three groups. In benzene, 1,4-dioxane, chloroform and dichloromethane, the 385 nm band of dipicrylamine does not vary considerably. The intensity is markedly high in chloroform solution, probably due to the intermolecular interaction between the chloroform and the nitro groups [27]. In alcohols, the band shifts in the sequence MeOH < EtOH < n-PrOH < i-PrOH and the intensities alter, too. This sequence is the same as that of the relative permittivities of the alcohols.

Table III

UV and visible spectral data on dipicrylamine in different solvents

Solvent	λ/nm (logε)	Solvent	λ/nm (logε)
Dioxane	378(4.12)	EtOH	406(3.93)
Benzene	383(4.24)	MeOH	385(4.09)
$CHCl_3$	383(4.40)	CH_3CN	423(4.51)
CH_2Cl_2	382(4.27)	DMSO	430(4.72)
i-PrOH	418(4.54)	MeOH/Acid	378(4.10)
n-PrOH	417(4.43)	MeOH/Base	420(4.43)

It seems that the polarization effect of the solvent molecules plays an important role, but the active hydrogen atom of the alcohols must also be taken into account. Higher bathochromic shifts are observed in DMF and DMSO solutions, which may be interpreted via the high polarization effects of these solvents, as a result of which an increased conjugated system is formed. A similar situation can be observed in strong basic solution, in which dipicrylamine is present almost entirely as an anion [35], while in acidic medium the spectrum does not change significantly.

References

[1] *Briegleb, G., J. Czekalla*: Angew. Chem. *72*, 401 (1960).
[2] *Briegleb, G., H. Delle*: Z. Elektrochem., *64*, 347 (1960).
[3] *Briegleb, G., J. Czekalla*: Z. physik. Chem., N.F. *24*, 37 (1960).
[4] *Foster, R., T.J. Thomson*: Trans. Farad. Soc., *59*, 2287 (1961).
[5] *Foster, R., C.A. Fyfe*: Trans. Farad. Soc., *61*, 1626 (1965).
[6] *Issa, R.M., M. Graber, A.L. El-Ansary, H.F. Rizk*: Bull Soc. Chim. France, 173 (1985).
[7] *Hindawey, A.M., Y.M. Issa, R.M. Issa, H.F. Rizk*: Acta Chim. Hung.,Budapest, *112*, 415 (1983).
[8] *Issa, Y.M.*: Spectrochim. Acta, *40A*, 137 (1984).
[9] *Pauling, L.*: The Nature of the chemical Bond, 2nd ed., Cornell Univ. Press, Ithaca, 1942., p. 220
Newman, M.S.: Steric Effects in Organic Chemistry., J. Wiley and Sons, N.Y. 1956. p. 473.
[10] *Császár, J.*: Acta Phys. Chem., Szeged, *25*, 137 (1979).
[11] *Császár, J., J. Balog, A. Makáry*: Acta Phys. Chem., Szeged, *24*, 473 (1978) and references cited therein
[12] *Brocklehurst, P.*: Tetrahedron, *18*, 299 (1961)
[13] *Friedel, R.A., M. Orchin*: Ultraviolet Spectra of Aromatic Compounds., J. Wiley and Sons, N.Y. 1951.
[14] *DeTar, D.F., H.H. Scheifele*: J. Amer. Chem. Soc., *73*, 1442 (1951).

[15] *DeTar, D.F., A.A. Kazini*: J. Amer. Chem. Soc., *77*, 3842 (1955).
[16] *Habert, R., J. Derkoch*: Monatsh. Chem., *88*, 47 (1957).
[17] *Dewar, M.J.S., D.S. Orel*: J. Chem. Soc., 3079 (1958).
[18] *Margerum, J.D., L.J. Miller, E. Saito, M.S. Brown, H.S. Mosher, R. Hardwick*: J. Phys. Chem. *66*, 2434 (1962).
[19] *Schroeder W.A., P.E. Wilcox, K.N. Trueblood, A.O. Dekker*: Anal. Chem., *23*, 1740 (1951).
[20] *Jaffé, H.H., M Orchin*: Theory and Application of Ultraviolet Spectroscopy., J. Wiley and Sons, N.Y. 1964. p. 408.
[21] *Suzuki, H.*: Bull. Chem. Soc. Japan, *32*, 1340 (1959).
[22] *Bastiansen, O.*: Acta Chem. Scand., *3*, 408 (1949).
[23] *Bastiansen, O., L. Snodvik*: Acta Chem. Scand., *8*, 1593 (1954).
[24] *Müller, E.*: Chem. Ber., *72*, 2063 (1939).
[25] *Sherwood, D.W., M. Calvin*: J. Amer. Chem. Soc., *64*, 1350 (1942).
[26] *Radebush, W.H.*: Chem. Rev., *41*, 317 (1947).
[27] *Balasubramanian, A., J.B. Capindale, W.F. Forbes*: Canad. J. Chem., *42*, 2674 (1964).
[28] *Stewart, R.S., J.P. O'Donnell*: Canad. J. Chem., *42*, 1681 (1964).
[29] *Bell, M.G.W., M. Day, A.T. Peters*: J. Chem. Soc., 132 (1967).
[30] *Balaban, A.T., P.T. Frangopol, M. Frangopol, N. Negoiță*: Tetrahedron, *23*, 4661 (1967).
[31] *Remington, W.R.*: J. Amer. Chem. Soc., *67*, 1838 (1945).
[32] *Beale, R.N., E.M.F. Roe*: J. Amer. Chem. Soc., *74*, 2302 (1952).
[33] *Hawthorne, F., D.J. Cram*: J. Amer. Chem. Soc., *74*, 5859 (1952).
[34] *Braude, E.A., F. Sondheimer*: J. Chem. Soc., 3754 (1955).
[35] *G. Schill*: Anal. Chim. Acta, *21*, 341 (1959).

О СПЕКТРАХ НЕКОТОРЫХ ПОЛИНИТРО ПРОИЗВОДНЫХ АКЦЕПТОРНОГО ТИПА БИФЕНИЛА, БИФЕНИЛМЕТАНА И БИФЕНИЛАНИЛИНА

Й. Часар

Изучены спектры интро- и полинитро производных бифенилаанилина в ультрафиолетовой и видимой областях и рассмотрено влияние заместителей при сравнении с соответствующими бифенил и бифенилметановыми производными.

ISBN 963 481 626 6
Acta Phys. et Chem. Szeged 33 23-36 (1987)

SPECTRAL STUDIES OF MOLECULAR COMPLEXES OF AROMATIC SCHIFF BASES WITH PICRIC ACID

By

J. CSÁSZÁR

Institute of General and Physical Chemistry, József Attila University, P.O.B. 105, H-6701 Szeged, Hungary

(*Received 1 October 1987*)

Twenty-six 1:1 molecular complexes of Schiff bases (formed from salycilaldehyde, ortho-vanillin, iso-vanillin and aniline derivatives) with picric acid were prepared and their UV, visible and IR spectral behaviour was investigated. The results suggested that the molecular complexes are formed via π-π* charge-transfer interactions.

Introduction

The formation of molecular complexes of aromatic hydrocarbons as donors with polynitrobenzenes as acceptors has been the subject of several studies [1-7]. It has been pointed out on the basis of visible, IR and ^{1}H NMR data that the following differentiation can be made: (a) charge-transfer (π-π*) complexes, (b) proton-transfer interaction, and (c) molecular complexes involving n - π* or hydrogen-bonds besides a π - π* interaction [e.g. 6]. Similar derivatives of aromatic Schiff bases have received relatively little attention from this point of view [8, 9]. According to Issa [10], the aniline

moiety of the Schiff bases is the donor centre, because the anilines have lower ionization potentials than the benzaldehyde derivatives.

In the present paper we discuss the preparation and the UV, visible and IR spectra of 1:1 molecular complexes of Schiff bases of salicylaldehyde, ortho-vanillin, iso-vanillin and aniline derivatives as donors (I) with picric acid as acceptor (Table I).

Experimental

The studied complexes were prepared by mixing hot methanolic solutions of the donor and the acceptor in a 1:1 mole ratio. On cooling, the complexes separated out as fine crystals having different colours. The products were recrystallized from a 1:1 acetone-methanol mixture. The m.p. and analytical data are listed in Table II. It is also possible to prepare 1:2 complexes, but the present paper discusses only the 1:1 complexes.

The visible and UV spectra were recorded on a SPECORD UV-VIS spectrophotometer; the solvents were spectroscopically pure. The reflection spectra were measured on a BECKMAN DU spectrophotometer against MgO standard. The IR spectra were measured on a ZEISS UR-10 instrument, in KBr discs.

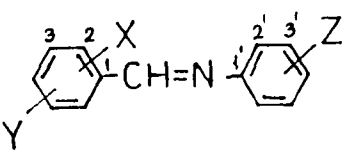

I.

Table I.

Positions of the substituents in the donor molecules and the numbering of their molecular complexes in the text

No.	X	Y	Z	No.	X	Y	Z
I	2-OH	H	4'-$N(CH_3)_2$	XIV	2-OH	H	3'-OCH_3
II	2-OH	H	4'-OH	XV	2-OH	H	4'-OCH_3
III	2-OH	H	4'-OC_4H_9	XVI	2-OH	H	3',4'-$(OCH_3)_2$
IV	2-OH	H	4'-CH_3	XVII	2-OH	3-OCH_3	H
V	2-OH	H	H	XVIII	2-OH	3-OCH_3	2'-OCH_3
VI	2-OH	H	4'-$NHCOCH_3$	XIX	2-OH	3-OCH_3	3'-OCH_3
VII	2-OH	H	4'-Cl	XX	2-OH	3-OCH_3	4'-OCH_3
VIII	2-OH	H	4'-Br	XXI	2-OH	3-OCH_3	3',4'-$(OCH_3)_2$
IX	2-OH	H	4'-I	XXII	4-OH	3-OCH_3	H
X	2-OH	H	4'-$COCH_3$	XXIII	4-OH	3-OCH_3	2'-OCH_3
XI	2-OH	H	4'-CN	XXIV	4-OH	3-OCH_3	3'-OCH_3
XII	2-OH	H	4'-NO_2	XXV	4-OH	3-OCH_3	4'-OCH_3
XIII	2-OH	H	2'-OCH_3	XXVI	4-OH	3-OCH_3	3',4'-$(OCH_3)_2$

Results and Discussion

The first series of complexes studied involves 4-X-N(2-hydroxybenzylidene)aniline derivatives (I-XII); the compounds are yellow in colour, except for I and X, which are brown and reddish-brown, respectively. The m.p.'s of the molecular complexes are higher than those of the parent components, except for XII, which has a lower m.p., similarly as for the molecular complexes of the aniline derivatives [7]. Relatively low m.p.'s were measured for the molecular complexes of benzylideneanilines with trinitrotoluene, for example, where

Table II

Analytical data on the molecular complexes

No	M.p.	Colour	C%		H%	
			Calcd.	Found	Calcd.	Found
I	154.0	P	53.73	53.70	4.08	4.02
II	184.9	GY	51.59	51.49	3.19	3.16
III	142.0	GY	55.42	55.40	4.45	4.40
IV	179.6	LY	54.55	54.49	3.66	3.65
V	157,8	LY	53.53	53.48	3.31	3.26
VI	205.7	LY	52.18	52.13	3.54	3.55
VII	169.7	LY	49.53	49.49	2.84	2.80
VIII	167.1	LY	45.17	45.11	2.59	2.55
IX	166.1	LY	41.33	41.25	2.37	2.38
X	141.0	BR	53.85	53.77	3.44	3.38
XI	145.2	GY	53.22	53.21	2.90	2.81
XII	136.8	OY	49.70	48.36	2.71	2.71
XIII	184.0	LY	52.64	52.47	3.53	3.50
XIV	175.5	GY		52.51		3.45
XV	172.0	LY		52.44		3.49
XVI	165.0	BY	51.86	51.77	3.73	3.68
XVII	176.5	O	52.64	52.60	3.53	3.50
XVIII	190.5	LY	51.86	51.74	3.73	3.69
XIX	137.0	BY		51.75		3.70
XX	121.0	BY		51.80		3.68
XXI	118.0	BR	51.17	51.08	3.90	3.88
XXII	201.0	LY	52.64	52.55	3.53	3.47
XXIII	171.5	BR	51.86	51.77	3.73	3.66
XXIV	167.0	OY		51.69		3.68
XXV	212.0	OY		51.71		3.61
XXVI	182.5	O	51.17	51.06	3.90	3.90

P: purple; GY: greenish-yellow; LY: lemon-yellow; BR: brick-red; OY: orange-yellow; BY: brownish-yellow; O: orange;

neither n-π^* interaction nor proton-transfer is possible, and only π-π^* charge-transfer takes place [7, 9]. The interaction between the studied Schiff bases and picric acid in solution is weak, and thus considerable changes in the UV and visible spectra are not probable; however, a comparison of the spectral behaviour of the components with that of their molecular complexes is of interest.

The solution spectra of the yellow compounds in chloroform show a sharp band at about 340 nm, with a small bathochromic shift relative to the spectra of the corresponding Schiff base, and a well-defined inflection ($\log\varepsilon \sim 2$-2.5) in the range 420-440 nm. Salicylideneanilines give a band at around 420 nm in hydrogen-bond forming solvents (e.g. methanol), due to the formation of an intermolecular six-membered ring with guinoidal structure [11]. However, in chloroform this band is absent, and the inflection is therefore assigned to the molecular complexes formed (Table III).

In the spectra of I and X, a well-defined band occurs in the visible range (Fig. 1). The spectral data measured in different solvents are presented in Table IV. It can be seen that the intensities of the main band (520-540 nm) do not vary considerably, whereas the structures and positions of the bands do. In solvents with low (< 10) permittivity, well-defined inflections are observed on both the long and short-wavelength sides of the main band, but in higher-permittivity solvents only a single band can be observed between 510 and 520 nm (Fig. 2). No correlation can be found between the characteristics of the solvents and the spectral data; this problem necessitates further investigations. The reflection spectrum of X contains only one inflection, at about 545 nm.

When the spectra of our molecular complexes are compared

Table III

UV and visible data on the complexes, measured in chloroform

No.	λ/nm (log ε)			
Picric acid	~260	336(3.66)		
I	---	~340	387(4.26)	485(3.72)
II	274(4.32)	~320	348(4.30)	~430
III	265(4.28)	~325	350(4.27)	~420
IV	270(4.31)	~320	343(4.26)	~430
V	270(4.36)	~320	338(4.21)	~420
VI	271(4.55)	~330	348(4.51)	~430
VII	272(4.43)	~325	344(4.30)	~420
VIII	272(4.40)	~325	343(4.28)	~420
IX	---	~330	346(4.34)	~430
X	280(4.44)	---	340(4.33)	530(2.94)
XI	275(4.47)	~325	346(4.26)	~430
XII	---	---	335(4.33)	---

with those of complexes containing dipicrylamine as acceptor, the similarity is obvious; for I and X, a visible band appears. In the latter case, proton-transfer is improbable, and consequently the band above 500 nm must be due to $\pi-\pi^*$ charge-transfer. In the case of 4-nitro-N-(2-aminobenzylidene)aniline, for example, the formation of an intramolecular hydrogenbond is impossible. The molecular complexes of these compounds with picric acid have intense colour and considerable absorbancy above 400 nm, and the $\nu=\overset{\oplus}{N}H$ band is absent from the IR spectra.

The second series comprises the molecular complexes of Schiff bases containing a methoxy group(s) on the aldehyde

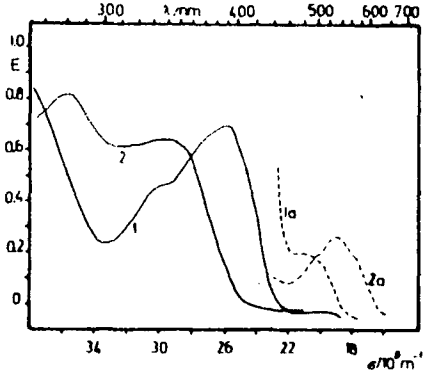

Figure 1: UV and visible spectra in chloroform of I (1, 1a), $c=3.8.10^{-4}$, and X (2, 2a), $c=3.10^{-4}$ mol/dm^3; d=0.1 cm (1, 2) and 1.0 cm (1a, 2a).

Table IV

Visible spectral data on X, measured in different solvents

Solvent	λ/nm (log ε)		
1,4-Dioxane	500(2.83)	536(2.91)	~570
Benzene	~500	534(2.98)	~575
Chloroform	500(2.96)	526(3.09)	558(2.95)
Chlorobenzene	~500	529(3.02)	~562
Dichloroethane	~505	532(3.05)	---
Benzyl alcohol	---	530(3.00)	~560
Cyclohexanol	~495	521(2.99)	~550
Acetone	---	513(3.02)	---
Methanol	---	515(3.03)	---
Acetonitrile	---	511(3.03)	---
DMSO	---	523(2.96)	---

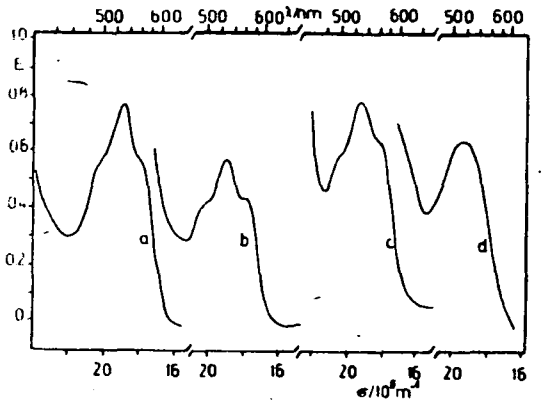

Figure 2: Visible spectra of X, measured in a: chloroform; b: chlorobenzene; c: cyclohexanol; d: acteone; $c=6.4.10^{-4}$ mol/dm^3, d=1.0 cm.

or/and on the aniline rings (XIII-XXVI). The data in Table V reveal that the spectra in chloroform solution are characterized by two high-intensity bands; the structures of the spectra are very similar to those of the parent Schiff bases (see e.g. Figs 3 and 4). The two main bands appear between 268-280 and 310-350 nm, respectively, but these bands have higher intensities than in the case of the Schiff bases. The wavelength ratios do not change considerably: they vary between 1.15 and 1.35.

The 400-450 nm range is characteristic of the spectra of the complexes studied. In every spectrum, a well-defined medium-intensity inflection appears at about 430-450 nm. On the basis of our results and literature data [8, 12], this band is assigned to π-π^* charge-transfer processes from the higher occupied state of the donor to the lowest unfilled state of the acceptor ($\pi_{HOMO_D} - \pi_{LUMO_A}$).

Table V

Spectral data on XIII-XXVI, *measured in chloroform*

No	λ/nm (log ε)		
XIII	268(4.27)	345(4.22)	~440
XIV	270(4.38)	344(4.28)	~430
XV	269(4.19)	353(4.32)	~430
XVI	~265	352(4.29)	~430
XVII	276(4.35)	319(4.25)[a]	~470
XVIII	270(4.24)	342(4.14)	~480
XIX	275(4.38)	336(4.23)	~470
XX	273(4.34)	339(4.24)	~470
XXI	273(4.29)	337(4.32)	~460
XXII	275(4.26)	315(4.12)	~380
XXIII	~270	338(4.22)	~450
XXIV	277(4.27)	335(4.25)[a]	~380
XXV	~280	350(4.30)	396(4.23)
XXVI	~270	350(4.31)	405(4.13)

a: broad band

The IR data on I-XII are listed in Table VI. In the range 3000-3200 cm^{-1}, a diffuse band system appears which is assigned to the stretching vibration of the OH group on the aldehyde part of the schiff base. The range of appearance and the diffuse structure of this band suggest that an intramolecular hydrogen-bond is also formed in the molecular complexes, similarly to the former observation in connection with the interaction between Schiff bases with p-nitrophenol [13].

No band can be observed in the range 2500-2900 cm^{-1}. In the IR spectra of the molecular complexes, e.g. benzyl-

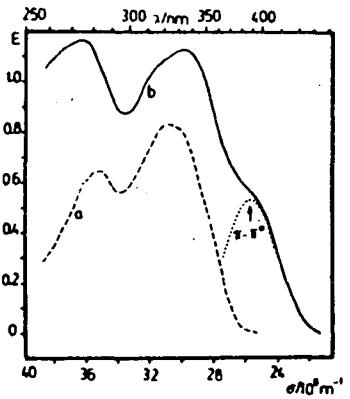

Figure 3: Spectra of the Schiff base (a), $c=6.05.10^{-4}$, and its complex XXIV (b), $c=6.17.10^{-4}$ mol/dm^3, in $CHCl_3$, d=0.1 cm.

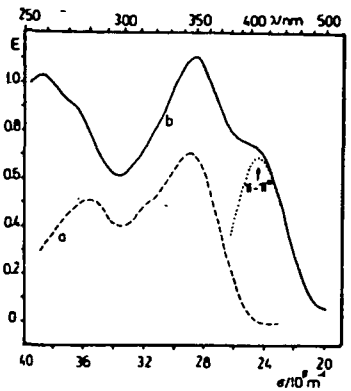

Figure 4: Spectra of the Schiff base (a), $c=4.55.10^{-4}$, and its complex XXVI (b), $c=5.42.10^{-4}$ mol/dm^3 in $CHCl_3$; d=0.1 cm.

ideneanilines with picric acid, a characteristic band is found in this range, due to the $\nu=\overset{\oplus}{N}H$ vibration, as a consequence of a proton-transfer from the phenolic OH group to the basic centre $\rangle C=N-$ of the donor. On the basis of the above data, we presume that the formation of the intramolecular six-membered ring prevents the intermolecular proton-transfer.

The $\nu_{as}NO_2$ band of picric acid contains two components, but for the complexes only a single, very intense band occurs, probably due to the destruction of the intramolecular hydrogen-bond in picric acid. The band generally shifts to higher frequencies. The ν_sNO_2 band shifts in the opposite direction, as a result of the increased π-electron density

Table VI

IR data on complexes I-XII

No.	νOH	$\nu_{as}NO_2$	ν_sNO_2	γCH	γ_sNO_2
Picric acid	3122s	1570s, 1550s	1352s	790m	735m, 712m
I	3140m	1588s	1340s, 1328s	776m, 758m	715m
II	3120m	1572s	1328s	778m, 756m	712s
III	3090m	1572s	1332s	780m, 772m	720s
IV	3090m	1578s	1321s	770m, 749m	710s
V	3080m	1577s	1330s	772m, 760m	718s
VI	3110m	1578s	1335s	778m, 766m	715s
VII	3100m	1570s	1338s	770m, 759m	718s
VIII	3100m	1570s	1338s	770m, 758m	718s
IX	3080m	1572s	1336s	772m, 756m	716s
X	3100m	1581s	1344s, 1328s	760m, 748m	719s
XI	3060m	1575s	1341s	769m, 758m	722s
XII	3120m	1575s	1350s	777m, 728m	728s

m: medium, s: strong

on the acceptor. It is noteworthy that in the case of IV and X the ν_sNO_2 band splits.

The γCH bands of the acceptor are shifted to lower wavenumbers. Issa et al. [9] suggested that the shift of this band of the anilino moiety is higher than that the aldehyde moiety, because the former is were the center contributing to the intermolecular charge-transfer, which takes place from the HOMO state of the donor to the LUMO state of the acceptor. An n-π* interaction is improbable, due to the blocking of the nitrogen lone pair through the intramolecular hydrogen-bond.

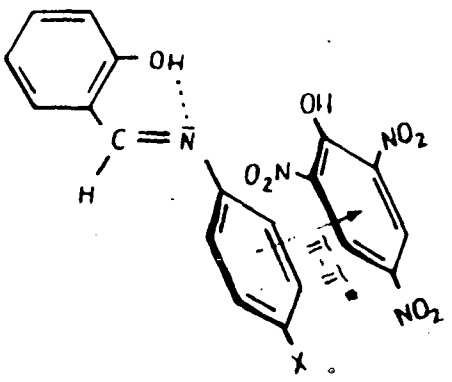

II.

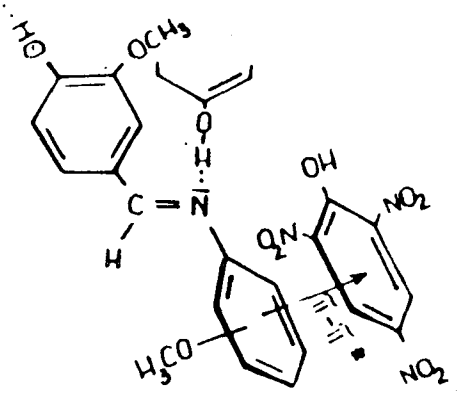

III.

It was earlier discussed [e.g. 14] that the aniline ring is twisted out from the plane of the molecule. On the other hand, Ross and Labes [15] have suggested that in the case of molecular complexes of anilines with 1,3,5-trinitrobenzene the two aromatic rings are parallel to each other. On the basis of these statements and the above experimental findings, we propose Structure II. for the complexes of the 2-hydroxy derivatives (I-XXI). The problem is more complicated in the case of the 4-hydroxy derivatives (XXII-XXVI). We presume that an intermolecular interaction may be possible with the neighbouring molecules via the 4-OH group and the azomethine nitrogen atom (Structure III).

Further investigations of our molecular complexes are in progress by means of ^{1}H NMR and electrochemical methods.

References

[1] *Briegleb, G., J. Czekalla*: Angew. Chem., *72*, 401 (1960).
[2] *Briegleb, G., H. Delle*: Z. Elektrochem., *64*, 347 (1960).
[3] *Briegleb, G., J. Czekalla*: Z. physik. Chem. N.F., *24*, 37 (1960).
[4] *Foster, R., T.J. Thomson*: Trans. Farad. Soc., *59*, 2287 (1963).
[5] *Foster, R., C.A. Fyfe*: Trans. Farad. Soc., *61*, 1626 (1965).
[6] *Issa, R.M., M.M. El-Essawey*: Z. physik. Chem., *253*, 36 (1973).
[7] *Hindawey, A.M., A.M.G. Nassar, R.M. Issa*: Acta Chim. Hung., Budapest, *92*, 263 (1977); *88*, 341 (1977).
[8] *Issa, R.M., M. Graber, A.L. El-Ansary, H.F. Rizk*: Bull. Soc. Chim. France. 173 (1985).
[9] *Hindawey, A.M., Y.M. Issa, R.M. Issa, H.F. Rizk*: Acta Chim. Hung., Budapest, *112*, 415 (1983).
[10] *Issa, Y.M.*, Spectrochim. Acta, *40 A* 137 (1984).
[11] *Császár, J.*: Acta Phys. Chem., Szeged *28*, 135 (1982).
[12] *Issa, Y.M., A.E. El-Kholy, A.L. El-Ansary*: Acta Chim. Hung., Budapest, *118*, 43 (1985).
[13] *Kovacic, J.E.*: Spectrochim. Acta, *23A*, 183 (1967).
[14] *Császár, J., J. Balog, A. Makáry*: Acta Phys. Chem., Szeged, *24*, 473 (1978).
[15] *Ross, S., M. Labes*: J. Amer. Chem. Soc., *77*, 4926 (1955).

СПЕКТРАЛЬНОЕ ИЗУЧЕНИЕ МОЛЕКУЛЯРНЫХ КОМПЛЕКСОВ АРОМАТИЧЕСКИХ ШИФФОВЫХ ОСНОВАНИЙ С ПИКРИНОВОЙ КИСЛОТОЙ

Й. Часар

Синтезированы и изучены ультрафиолетовые, видимые и инфракрасные спектры двадцати шести комплексов Шиффовых оснований, образованных из салицилальдегидных, орто-ванилиновых, изо-ванилиновых и анилиновых производных и пикриновой кислоты, состава I : I. Результаты показывают, что эти молекулярные комплексы, вероятно, образовались при взаимодействиях π - π^* переходов заряда.

ISBN 963 481 625 8
Acta Phys. et Chem. Szeged 33 37-51 (1987)

SPECTROSCOPIC STUDY OF MOLECULAR COMPLEXES OF AROMATIC SCHIFF BASES WITH POLYNITRO COMPOUNDS

By

J. CSÁSZÁR and N. M. BIZONY

Institute of General and Physical Chemistry, József Attila University, P.O.B. 105, H-6701, Szeged, Hungary

(Received 1 October 1987)

Schiff bases were formed from salicylaldehyde an aminopyridines and their methyl derivatives and molecular complexes of these Schiff bases with 2,4-dinitroaniline, picric acid and dipicrylamine were prepared. The spectral behaviour of the parent Schiff bases and their molecular complexes was studied and discussed.

Introduction

Molecular complexes of polynitro compounds with Schiff bases as π-donor systems are an interesting group of compounds, which have recently been widely studied [1-5]. Issa and El-Essawey [6] found that the type and structure of these complexes may be studied well via UV, IR and ^{1}H NMR-spectroscopy.

As a continuation of our earlier work, we have prepared molecular complexes of Schiff bases as donors (formed from salicylaldehyde and 2-aminopyridine, its methyl derivatives

and 3-aminopyridine) with aromatic polynitro compounds as acceptors. The present paper reports a spectral study of the parent Schiff bases and their molecular complexes.

Experimental

The donors were Schiff bases having the general structures I and II.

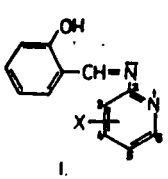

I.

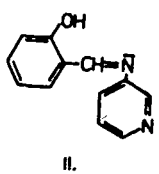

II.

1 X = H
3 X = 3-CH_3
4 X = 4-CH_3
5 X = 5-CH_3
6 X = 6-CH_3

2

The acceptors used were 2,4-dinitroaniline (DNA), picric acid (PA) and dipicrylamine (DPA).

All chemicals were pure lab. grade BDH products. The preparation of the molecular complexes was described previously [4, 5]. The analytical data are listed in Table I; these data are in good agreement with the expected compositions for a donor:acceptor stoichiometric ratio of 1:1 (DNA and PA) or 1:2 (DPA).

The UV and visible spectra were recorded on a SPECORD UV-VIS spectrophotometer, using spectroscopically pure solvents. The IR spectra were measured on a ZEISS UR-20 spectrophotometer, in KBr discs; the ^1H NMR spectra were observed on

Table I

Analytical data on the molecular complexes studied

Acceptor	Donor	M.p.*		Colour**	C% Calcd.	C% Found	C% Calcd.	C% Found
DNA	1	178.5	(64.1)	LY	56.69	56.48	3.96	3.96
	2	120.5	(57.0)	LY		56.50		3.91
	3	113.5	(80.3)	O	57.72	57.66	4.33	4.30
	4	93.5	(99.4)	LY		57.69		4.28
	5	96.0	(100.5)	BY		57.71		4.30
	6	178.5	(65.8)	LY		57.66		4.26
PA	1	218.5		LY	50.59	50.50	3.07	3.01
	2	165.0		LY		50.52		3.05
	3	218.5		LY	51.71	51.66	3.43	3.40
	4	218.0		LY		51.61		3.38
	5	228.5		LY		51.65		3.41
	6	202.5		LY		51.60		3.37
DPA	1	177.5		R	40.16	40.01	1.87	1.77
	2	136.5		R		39.96		1.80
	3	197.5		BB	40.75	40.15	2.03	1.98
	4	196.5		O		40.33		2.00
	5	175.5		SC		40.51		1.88
	6	186.5		SC		40.55		1.78

* the data in parentheses are the m.p.s. of the Schiff bases

** LY: lemon-yellow; O: orange; BY: brownish-yellow; R: red; BB: bluish-brown; SC: scarlet

a JEOL 60 MHz instrument in CCl_4, with TMS as internal standard.

Discussion

Spectra of Schiff bases. The absorption spectra were similar to those of other Schiff bases of salicylaldehyde and aromatic amines [7-10]. Three main bands appear, at 270-280, 300-320 and 320-360 nm (Fig. 1, curves a,c), which may be assigned to $\pi^* \leftarrow \pi$ transitions of the aromatic systems. The positions and intensities of the bands measured in chloroform, benzene, hexane, etc. did not vary considerably (Table II).

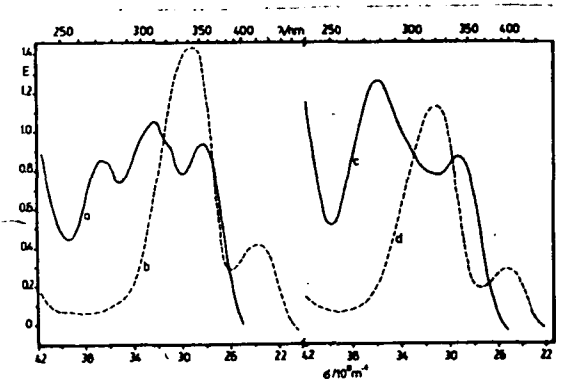

Figure 1: UV spectra. a: 1 in $CHCl_3$, c=8.07.10^{-4}, b: 1 in conc. H_2SO_4, c=7.57.10^{-4}; c: 2 in $CHCl_3$, c=8.58.10^{-4}; d: 2 in conc. H_2SO_4, c=8.07.10^{-4} mol/dm^3. d=0.1 cm.

Table II

UV and visible spectral data on the Schiff bases, measured in different solvents

No.	Solvent*	λ/nm (log ε)			
1	M	270(4.03)	303(4.07)	345(4.02)	450(2.10)
	Chl	270(4.03)	310(4.12)**	353(4.06)	~460
	B	270(4.00)	307(4.07)	352(4.04)	---
	S	---	---	341(4.26)	419(3.74)
2	M	276(4.06)	---	340(3.88)	---
	Chl	279(4.17)	---	344(4.01)	---
	B	281(4.04)	---	343(3.92)	---
	S	---	---	322(4.14)	398(3.56)
3	M	271(4.04)	315(4.06)	346(4.08)	445(2.47)
	Chl	274(4.01)	313(4.05)**	355(4.08)	~460
	B	270(4.12)	320(4.18)	356(4.22)	---
	S	---	---	329(4.07)	412(3.60)
4	M	272(4.04)	302(4.06)	345(4.01)	440(2.20)
	Chl	274(4.06)	309(4.16)**	352(4.13)	~460
	B	272(3.95)	305(4.10)	353(4.06)	---
	S	---	---	331(4.18)	414(3.72)
5	M	269(4.04)	310(4.08)	347(4.06)	450(2.20)
	Chl	272(4.09)	320(4.15)**	351(4.17)	~460
	B	275(3.94)	312(4.06)	353(4.10)	---
	S	---	---	342(4.26)	414(3.74)
6	M	269(4.07)	310(4.10)	343(4.09)	444(2.30)
	Chl	273(4.11)	319(4.14)**	354(4.16)	~460
	B	275(3.94)	312(4.06)	353(4.10)	---
	S	---	---	341(4.29)	415(3.76)

* M: methanol; Chl: chloroform; B: benzene; S: concentrated sulphuric acid

** double band

We presume that the same transitions are involved in the spectra of all the Schiff bases studied; the wavelength ratios ν_3/ν_2 are between 1.10 and 1.16, and the solvent effect does not appreciably influence the relative energies of the ground and excited states of the chromophores. However, in methanol, or in other hydrogen-bond forming solvents, a band can be detected between 400 and 450 nm, which is absent from the spectra of the benzene or hexane solutions. These medium--intensity bands can be interpreted in terms of a benzoid/quinoid tautomeric equilibrium (Structure III) [10]. Similar phenomena can be observed in the photochromic [11, 12] and thermochromic [e.g. 13-15] transformations of the Schiff bases in the solid state.

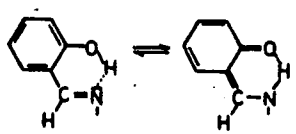

III.

Totally different spectral behaviour can be observed for 2; the visible band disappears almost completely. The nitrogen atom in the "meta" position decreases the charge density on the azomethine nitrogen to nearly the same extent as a nitro group; the probability of the above equilibrium is very small. The K values calculated for the methyl derivatives 3-6 vary in the sequence 3 < 6 < 4 < 5; owing to its steric effect, the methyl group in position 3 twists the pyridine ring out of the plane and thereby hinders extension of the quinoidal structure over the entire molecule; the value of K is the lowest. The different behaviour of 2 is also well seen from the low δCHN and high νCHN frequencies (Table III).

In concentrated sulphuric acid solution, the $>C=\overset{\oplus}{N}H-$ protonated forms of the Schiff bases are present, and the molecules have a planar or nearly planar conformation [16, 17]. Table II shows that the intensity of the third band is

increased considerably compared, for example, to the spectra of the methanolic solutions (Fig. 1, curves b, d). Ont the basis of the intensity differences, the twist angle θ_N of the aniline ring can be calculated [18-20] (Table III); the values differ only slightly, and the different positions of the methyl group scarcely influence the conformation.

The OH proton signals are in the interval 12.4-13.7 ppm; the lowest value is observed for 2. We found that the ppm values and the intensities of the advanced visible bands change in parallel. The 6.5-9.5 ppm region is extremely complicated, the signals of the aldehyde and pyridine ring protons appear with significant couplings in this range.

Spectra of the molecular complexes. DNA, PA and DPA differ considerably in their acidic character (pK_a = 15.0, 2.68 and 1.0, respectively). The donors have a basic character, and thus their behaviour towards the acceptors used differs. In the case of DNA and DPA, only a charge-transfer (CT) interaction is expected, but in the case of PA proton-transfer is also possible theoretically.

The three groups of molecular complexes studied show different spectral behaviour; characteristic data on the complexes DNA/1-6 and PA/1-6 are presented in Table IV.

The absorption spectra of DNA/1-6 display two high-intensity bands, at around 260-265 and 330-335 nm; in the longer-wavelength region, an inflection is also found. On the basis of the positions and intensities of the main bands, we assigned these to $\pi^* \leftarrow \pi$ transitions in the aromatic systems, while the inflection is due to CT processes between the aromatic rings of the donor and acceptor. Table IV shows that the solvent effect is not so important.

It is remarkable that the spectra of DNA and its complexes are practically the same. However, the formation of molecular complexes is supported by the facts that the inten-

Table III

Characteristics of the Schiff bases

No.	δOH^a	δCHN^a	δCH_3^a	νCHN^b	K^c	$\theta_N{}^d$
1	13.11	9.47		1618s	4.0	81
2	12.46	8.60		1629s	-	-
3	13.69	9.40	2.49	1620s	2.0	74
4	13.23	9.50	2.38	1603s	5.7	80
5	13.19	9.43	2.33	1619s	8.6	80
6	13.26	9.47	2.55	1619s	4.6	79

a: measured in CCl_4; b: in KBr discs; c: in methanol/benzene mixtures see e.g.[8,9]; d: calculated via the intensity of the protonated form.

sities are higher than that of DNA and the predicted one, and the analytical data also correspond to the formation of 1:1 complexes.

Ross and Labes [21] suggested that in the molecular complexes of aniline with 1,3,5-trinitrobenzene the two aromatic rings are parallel to each other. We propose an analogous structure (Structure IV), in which the DNA molecule and the pyridine ring of the Schiff base lie parallel, and only a $\pi - \pi^*$ interaction need be taken into account.

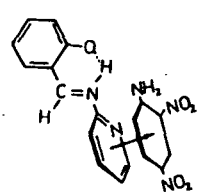

IV

The high similarity of the measured spectra to the one calculated on the basis of the additivity suggests that in solutions corresponding to the equilibrium $D.A \rightleftharpoons D^+ + A^-$ the sum of the spectra of the donor and acceptor is measurable (Fig.2).

Table IV

UV and visible spectral data on the molecular complexes of DNA *and* PA

Acceptor	Donor	Solvent*	λ/nm (log ε)		
DNA	1	Chl	262(4.34)	331(4.47)	~380
		AcCN	261(4.30)	333(4.49)	~380
	2	Chl	263(4.47)	334(4.48)	~380
		AcCN	263(4.42)	335(4.43)	~370
	3	Chl	262(4.43)	333(4.53)	~380
		AcCN	264(4.44)	331(4.50)	~380
	4	Chl	263(4.42)	334(4.52)	~370
		AcCN	263(4.43)	333(4.53)	~380
	5	Chl	263(4.42)	333(4.54)	~380
		AcCN	261(4.42)	335(4.50)	~380
	6	Chl	262(4.42)	331(4.53)	~380
		AcCN	261(4.45)	330(4.51)	~380
PA	1	MeOH	~315	354(4.41)	~390
		Chl	~318	344(4.28)	411(4.01)
		AcCN	310(4.06)	369(4.29)	~410
	2	MeOH	252(4.47)	349(4.44)	~400
		Chl	252(4.08)	341(3.94)	~410
		AcCN	243(4.49)	374(4.45)	~420
	3	MeOH	314(4.28)	357(4.40)	~410
		Chl	323(4.30)	346(4.32)	412(4.02)
		AcCN	307(4.11)	367(4.34)	~420
	4	MeOH	311(4.11)	358(4.32)	~420
		Chl	~315	350(4.28)	414(4.01)
		AcCN	303(4.01)	369(4.34)	~410
	5	MeOH	~325	357(4.33)	~400
		Chl	338(4.25)	~350	414(3.93)
		AcCN	~318	369(4.33)	~415
	6	MeOH	320(4.24)	358(4.30)	~400
		Chl	326(4.29)	~340	406(4.06)
		AcCN	313(4.12)	372(4.35)	~420

*MeOH: methanol; Chl: chloroform; AcCN: acetonitrile.

It must be mentioned that the possibility for intermolecular n - π* bonding between the amino and nitro groups should not be excluded [22], but our results do not support this possibility.

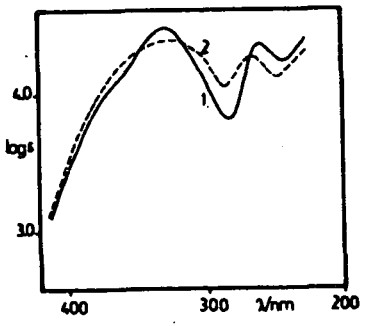

Figure 2: UV spectra of DNA/1 in $CHCl_3$. 1: measured, 2: calculated spectrum.

The chloroform solutions of complexes PA/1-6 also show two intense bands; a well-defined band appears at around 400 nm (Fig. 3). This band corresponds unambigously to the molecular complex, and is also due with high probability to π - π* processes. In methanol or in acetonitrile, the long-wavelength band disappears and an inflection is observed in the same region. If the spectral data and the changes are taken into account, it may be presumed that the structures of the molecular complexes are similar to those discussed above; only the π - π* CT process is possible; the intramolecular hydrogen-bond in the Schiff bases prevents intermolecular proton-transfer [e.g. 1-3]; the characteristic frequencies of the $\rangle C=\overset{\oplus}{N}H-$ group are absent from the solid-state IR spectra.

It has long been known that DPA yields slightly-soluble compounds with, for example, quaternary ammonium compounds [23] and different organic bases [24, 25]. While the complexes discussed above are yellow or orange, the molecular complexes of DPA are brick-red, scarlet or violet. Since it is obvious from the structure of DPA that donor ← acceptor proton trans-

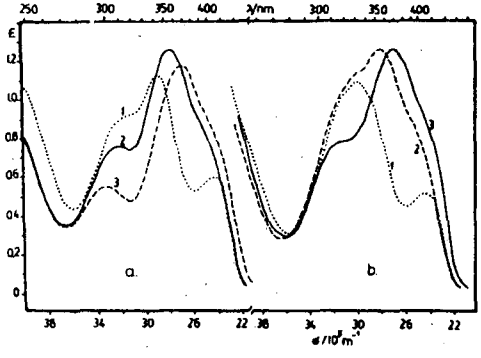

Figure 3: UV and visible spectra. a) PA/4 in 1: $CHCl_3$, $c=5.89.10^{-4}$; 2: CH_3OH, $c=5.89.10^{-4}$; 3: AcCN, $c=5.44.10^{-4}$. b) PA/5 in 1: $CHCl_3$, $c=6.12.10^{-4}$; 2: CH_3OH, $c=5.89.10^{-4}$; 3: AcCN, $c=5.89.10^{-4}$ mol/dm^3. d=0.1 cm.

fer is impossible, in this case only CT processes need be taken into account; typical spectra are shown in Fig. 4.

In methanol or acetonitrile the molecular complexes DPA/1-6 show a broad high-intensity band between 420 and 430 nm; this band corresponds to the characteristic 383 nm band of DPA (Table V) [26]. The longer-wavelength side of this band is asymmetric, which indicates the presence of a covered band. In chloroform or dioxane solutions, the maximum is situated at around 380 nm, with an inflection in the interval 440-460 nm. The higher-energy band appears at 290-320 nm.

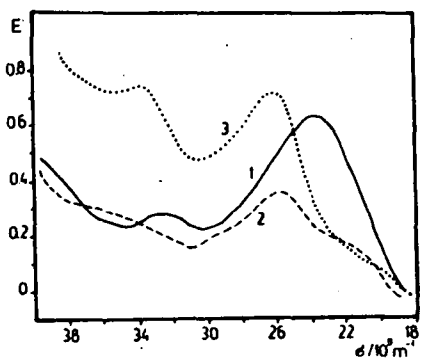

Figure 4: UV spectra of DPA/2 in 1: CH_3OH, $c=1.02.10^{-4}$; 2: $CHCl_3$, $c=8.82.10^{-5}$; 3: 1,4-dioxane, $c=1.10.10^{-4}$ mol/dm^3, d=0.1 cm.

We presume that the inflection appearing next to the 383 nm band ($\log\varepsilon \approx 3.5$-4.0) corresponds to $\pi - \pi^*$ CT processes; the CT bands occur in a similar range in the spectra of molecular complexes of other Schiff bases [1, 2].

According to Issa [27], the aniline ring is primarily the centre contributing to the intermolecular CT interaction, but in the case of 1:2 donor:acceptor complexes the aldehyde ring, takes also part in the formation of complexes. On the basis of these findings, the analytical data, the intensity relations and the intense colours, we assume that 1:2 donor:acceptor complexes are formed, i.e. the aniline and aldehyde rings of the Schiff bases bind two acceptor molecules via $\pi - \pi^*$ CT (Structure V). The formation of a 2:1 donor:acceptor complex is improbable, because of the steric inhibition. The structural considerations are very problematic, because

Table V

Spectral data on the molecular complexes of DPA

Donor	Solvent*	λ/nm (log ε)		
1	MeOH	310(4.62)	---	421(4.92)
	Chl	~280	384(a)	~460
	Diox	295(4.58)	380(4.51)	~460
	AcCN	298(4.43)	---	423(4.84)
2	MeOH	305(4.45)	---	419(4.79)
	Chl	~280	386(4.60)	~460
	Diox	294(4.82)	383(4.81)	~460
	AcCN	300(4.26)	---	423(4.70)
3	MeOH	315(4.46)	---	422(4.74)
	Chl	~280	389(4.42)	~440
	Diox	297(4.64)	380(4.58)	~460
	AcCN	304(4.32)	---	426(4.72)
4	MeOH	318(4.41)	---	420(4.73)
	Chl	~280	385(4.33)	~460
	Diox	300(4.52)	381(4.49)	~480
	AcCN	313(4.34)	---	425(4.79)
5	MeOH	311(4.68)	---	420(5.02)
	Chl	~280	384(a)	~470
	Diox	296(4.62)	382(4.57)	~460
	AcCN	302(4.26)	---	425(4.72)
6	MeOH	261(4.72)	350(4.59)	420(4.58)
	Chl	278(4.78)	350(4.66)	~390
	Diox	278(4.80)	346(4.69)	~390
	AcCN	273(4.69)	347(4.63)	423(4.60)

*

* MeOH: methanol; Chl: chloroform; Diox: 1,4-dioxane; AcCN: Acetonitrile; a) very low solubility

the DPA acceptor molecule, as discussed previously [22], is a twisted one due to the high steric interference of the nitro groups in the 2,2', 6,6' positions.

Detailed investigations of DPA complexes by means of different physico-chemical methods are in progress.

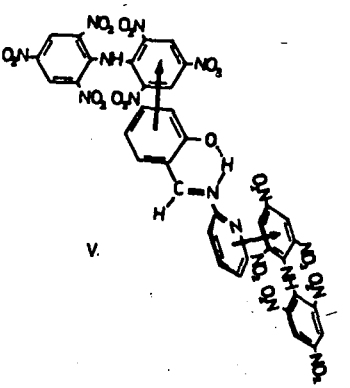

V.

References

[1] *Issa, R.M., M. Gaber, A.I. El-Ansary, H.F. Rizk*: Bull. Soc. Chim. France, No.2., 173 (1985).

[2] *Hindawey, A.M., Y.M. Issa, R.M. Issa, H.F. Rizk*: Acta Acad. Sci. Hung., *112*, 415 (1983).

[3] *Issa, Y.M., A.E. El-Viholy, A.L. El-Ansary*: Acta Acad. Sci. Hung., *118*, 43 (1985).

[4] *Császár, J.*: Acta Phys. Chem. Szeged, in press.

[5] *Dale, B., R. Foster, D. LL. Hammick*: J. Chem. Soc., 3986 (1954); *R. Foster, D. LL. Hammick, P.J. Placito*: J. Chem. Soc., 3881 (1956).

[6] *Issa, R.M., M.M. El-Essawey*: Z. physik. Chem., *253*, 96 (1973).

[7] *Császár, J.*: Acta Phys. Chem., Szeged, *28*, 135 (1982).

[8] *Császár, J.*: Acta Phys. Chem., Szeged, *27*, 47 (1981).

[9] *Császár, J.*: Acta Phys. Chem., Szeged, *25*, 137 (1979).

[10] *Császár, J., J. Balog, A. Makáry*: Acta Phys. Chem., Szeged, *24*, 473 (1978).

[11] *Lewis, J.W., C. Sándorfy*: Canad. J. Chem., *60*, 1738 (1982).

[12] *Yoshida, M., M. Kobayashi*: Bull. Chem. Soc. Japan, *54*, 2395 (1981).
[13] *Cohen, M.D., G.M.T. Schmidt*: J. Phys. Chem., *66*, 2442 (1962).
[14] *Cohen, M.D., G.M.T. Schmidt, S. Flavian*: J. Chem. Soc., 2041 (1964).
[15] *Cohen, M.D., G.M.T. Schmidt*: In Reactivity of Solids., Ed. J.H. de Boer, Elsevier, Amsterdam, 1961. p. 556.
[16] *Brocklehurst, P.*: Tetrahedron, *18*, 299 (1961).
[17] *Minkin, V.I., Yu. A. Zhdanov, E.A. Megyantzeva, Yu. A. Ostroumov*: Tetrahedron, *23*, 3651 (1967).
[18] *Braude, E.A., F. Sondheimer*: J. Chem. Soc., 3754 (1955).
[19] *Kraszovickij, B.M., B.M. Bolomin, R.N. Nurmahatmetev*: Zh. Obsch. Khim., *34*, 3786 (1964).
[20] *Császár, J.*: Acta Phys. Chem. Szeged, *29*, 133 (1983); *32*, 17 (1986).
[21] *Ross, S., M. Labes*: J. Amer. Chem. Soc., *77*, 4916 (1955).
[22] *Hindawey, A.M., A.M.G. Nassar, R.M. Issa*: Acta Acad. Sci., Hung., *88*, 341 (1976).
[23] *Ackerman, D., H. Maner*: Z. physik. Chem., *279*, 114 (1943).
[24] *Kertes, S.*: Anal. Chim. Acta, *15*, 73 (1956).
[25] *Kertes, S., V. Kertes*: Anal. Chim. Acta, *15*, 154 (1956)
[26] *Császár, J.*: Acta Phys. Chem., Szeged, *33*, 11 (1987).
[27] *Issa, Y.M.*: Spectrochim. Acta, *40A*, 137 (1984).

СПЕКТРОСКОПИЧЕСКОЕ ИЗУЧЕНИЕ МОЛЕКУЛЯРНЫХ КОМПЛЕКСОВ АРОМАТИЧЕСКИХ ШИФФОВЫХ ОСНОВАНИЙ С ПОЛИНИТРОСОЕДИНЕНИЯМИ

Й. Часар и Н.М. Бизонь

Синтезированы молекулярные комплексы Шиффовых оснований образованные из салицилальдегида, амино пиридонов, а также их метиловых производных с 2,4-динитроанилином, пикриновой кислотой и дипикриламином. Изучены и обсуждены спектральные свойства исходных оснований и их молекулярных комплексов.

ISNB 963 481 627 4
Acta Phys. et Chem. Szeged 33 53-67 (1987)

FURTHER DATA RELATING TO THE INTERPRETATION OF SOLVENT EFFECTS OBSERVED IN THE ABSORPTION SPECTRA OF SCHIFF BASES

By

P. NAGY and R. HERZFELD

Department of Chemistry, Juhász Gyula Teachers' Training College,
P.O.Box 396, H-6701 Szeged, Hungary

(Received 15. October 1987)

The solvent effects observed in the absorption spectra of N-(2-hydroxybenzylidene)amine and N-(4-hydroxybenzylidene)amine were studied in various solvent mixtures. Good correlations were found between the intensity of the band at around 400 nm and the E_T^N and B_{KT} values of the solvents.

Introduction

It is known that, in the case of Schiff bases in which the aldehyde component contains an OH group in the o- or p-position, a characteristic solvent effect can be observed in the absorption spectra. For instance, on the addition of alcohol or water a new band (the "fore-band") appears at around 400 nm, which cannot be detected in an apolar solvent. Since this phenomenon was first observed [1-4], many different suggestions have been put forward concerning its investigation and interpretation. The phenomenon has been linked with an intramolecular and with an intermolecular

hydrogen-bond [5-10].

Dudek [11] and Ledbetter [12] interpreted the phenomenon in terms of the development of a benzoid-quinoid tautomeric equilibrium depending on the solvent. The effects of substituents [13] and various salts on the solvent effect [14] are in agreement with this supposition. The equilibrium constant of the process can be calculated for the solvent mixtures [15-17], as can the concentration of the quinoid form in some cases [18].

However, recent investigations have led some research workers to discount the formation of the quinoid form; instead, they presume a twin-ionic structure [19-21]. On the other hand, other authors consistently interpret the solvent effect in terms of the benzoid-quinoid equilibrium [23].

Thus, though it has been widely investigated, the problem is not yet solved. The present paper reports on a study of the correlation between the solvent effect and the acidity and basicity parameters of the solvent. The results provide further data promoting a better understanding of the solvent effect observed in the absorption spectra of Schiff bases.

Experimental

The Schiff bases were prepared by mixing ethanolic solutions of the components. Their purities were checked via melting point measurements after recrystallization. The solvents were purified by means of the methods customary in spectroscopy, and carefully dried. VSU-2P and Spektromom 195

spectrophotometers were used to determine the absorption curves. The values of the acidity parameter (E_T^N) and the basicity parameter (B_{KT}) [23-25] of the solvents were measured and calculated as described earlier [26]. The measurements were carried out at 25 °C.

Results and discussion

The experiments revealed that the solvent effect observed for the above Schiff bases can be characterized by an A ⇌ B equilibrium process, which is dependent on the temperature. The position of the equilibrium varies with the examined compound and the solvent used. This is demonstrated by the well-defined isosbestic points of the absorption curves determined in different solvents, which can be seen in Figures 1. and 2. (The Figures clearly show that $CaCl_2$, similarly to the solvent, but more significantly, influences the A ⇌ B equilibrium.) The structure of form B is debatable. Either the quinoid (B_1) or the twin-ionic (B_2) structure can be supposed:

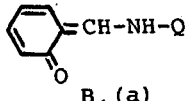

B_1(a)

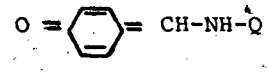

B_1(b)

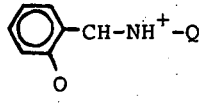

B_2(a)

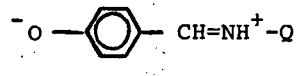

B_2(b)

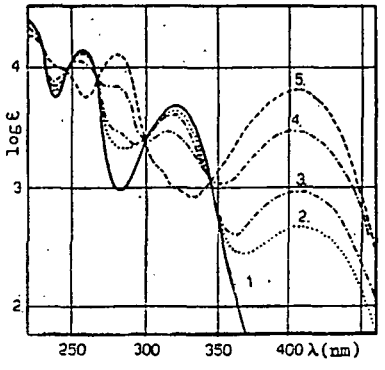

Figure 1.: Absorption curves of N-(2-hydroxybenzylidene) benzylamine in different solvents. Solvents: 95 % hexane-ethanol (1); ethanol (2); methanol (3); 40 % water-methanol (4); 1.5 mol/dm^3 $CaCl_2$ in ethanol (5).

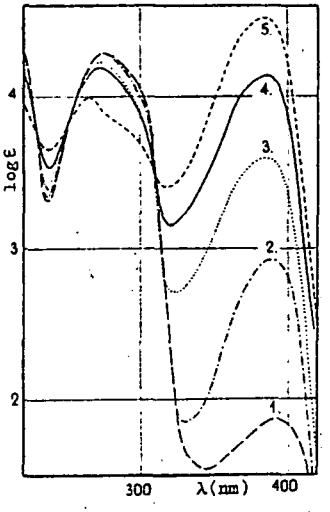

Figure 2.: Absorption curves of N-(4-hydroxybenzylidene) benzylamine in different solvents. Solvents: 95 % hexane-ethanol (1); ethanol (2); 40 % water-ethanol (3); 0.3 mol/dm^3 $CaCl_2$ in ethanol (4); 1.5 mol/dm^3 $CaCl_2$ in ethanol (5).

The equilibrium constant for the A ⇌ B process is:

$$K = \frac{\varepsilon - \varepsilon_A}{\varepsilon_B - \varepsilon} \quad ; \quad \log K = \log \frac{\varepsilon - \varepsilon_A}{\varepsilon_B - \varepsilon} \qquad (1)$$

where ε_A and ε_B are the molar absorption coefficients of forms A and B, and ε is the molar absorption coefficient of the equilibrium mixture at the wavelength corresponding to the band maximum at around 400 nm. Thus, the solvent applied influences the equilibrium constant value.

The two or multiple-parameter regression equations [27-29] involving the solvent parameters can be well applied for different kinds of solvent-dependent equilibrium processes. If this method is applied for the examined equilibrium, using the E_T^N and B_{KT} values:

$$\log K = b_1 E_T^N + b_2 B_{KT} + a' \qquad (2)$$

and taking (1) into consideration:

$$\log \frac{\varepsilon - \varepsilon_A}{\varepsilon_B - \varepsilon} = b_1 E_T^N + b_2 B_{KT} + a' \qquad (3)$$

can be determined directly in various solvents. However, ε_A is nearly zero, since these compounds do not exhibit appreciable absorption in the region of the "fore-band" in apolar solvents. This was confirmed by the method of Berstein and Kaminckij [30] and is illustrated in Figures 3 and 4. These Figures present the absorption measured in the region of the "fore-band" in different solvents (characteristic of form B) in comparison with the absorption measured at the maximum of the band characteristic of form A. It can be seen that the resulting straight lines cross the x-axis at one point, which means that only form A absorbs in the region of the "fore--band", i.e. $\varepsilon_A = 0$ in Eq. (3). For the Schiff bases of 2- and 4-hydroxybenzaldehyde with aliphatic amine and benzylamine, we have determined the values of ε_B as well [31], applying the salt effect which influences the position of the A $\rightleftharpoons$ B equilibrium. However, in the case of aromatic Schiff bases the equilibrium is strongly shifted in the direction of the bottom arrow.

Therefore, this method cannot be used, though it is probable

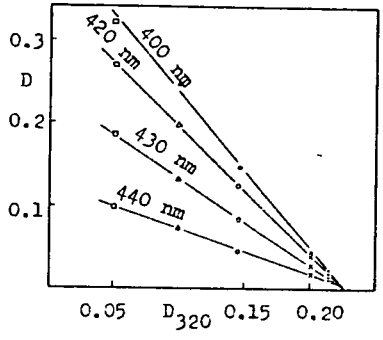

Figure 3.: Change in absorption measured in the region of the fore-band as a function of the absorption at 320 nm in solutions of N-(2-hydroxybenzylidene)benzylamine in different solvents.
$c=5.10^{-4}$ mol/dm^3, l=0.1 cm.
Solvents: ethanol (.); methanol (x); 40%= water-ethanol (o); 2 mol/dm^3 $CaCl_2$ in methanol (Δ); 1.5 mol/dm^3 $CaCl_2$ in ethanol (□)

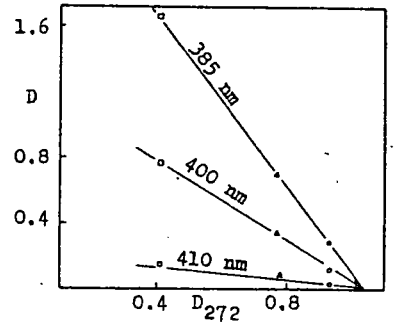

Figure 4.: Change in absorption measured in the region of the fore-band as a function of the absorption at 272 nm in solutions of N-(4-hydroxybenzylidene) benzylamine in different solvents.
$c=5.10^{-4}$ mol/dm^3, l=0,1 cm.
Solvents: ethanol (.); 40 % water-ethanol (o); 0.3 mol/dm^3 $CaCl_2$ in ethanol (Δ); 1.5 mol/dm^3 $CaCl_2$ in ethanol (□).

that the ε_B values of these compounds are at least as high as they are for the compounds of the corresponding aldehyde with aliphatic amines. Thus, for the examined Schiff bases and solvents ε_B, and therefore Eq. (3) can be applied as

$$\log \varepsilon = b_1 E_T^N + b_2 B_{KT} + a \qquad (4)$$

where $a = a' + \log \varepsilon_B$.

In the case of Schiff bases, we have measured the values of ε, E_T^N and B_{KT} in different solvent mixtures. They are collected in part in our earlier papers [26, 32] and in part in Tables I and II.

Table I

Molar absorption coefficients of N-(2-hydroxybenzylidene)-benzylamine *at 405 nm and those of* N-(4-hydroxybenzylidene) benzylamine *at 385 nm in different solvent mixtures /t=25°C/*

$\varepsilon_B(405) = 8180$ $\varepsilon_B(385) = 55930$

[ethanol] mol/dm^3	ethanol-hexane		ethanol-benzene		ethanol-acetone	
	ε_{405}	ε_{385}	ε_{405}	ε_{385}	ε_{405}	ε_{385}
0.000	3.3	2*	14.4	5.0	36.8	9.2
1.704	51.2	80	76	54.4	69.6	29.6
3.409	104.8	144	130	103.2	100	62.4
6.817	196	268	216	222.4	170	144
10.226	292	400	320	374	252	276
13.635	380	566	412	568	356	484
17.044	480	820	480	820	480	820

*extrapolated value

We have used the data obtained to calculate the constans of Eq. (4) and the multiple correlation coefficients for various types of Schiff bases by applying the least squares method. In order to make a better comparison of the effects of E_T^N and B_{KT}, the regression coefficients were calculated for the

Table II

E_T^N and B_{KT} values (t=25 °C) of ethanol-acetone *mixtures*

[ethanol] mol/dm^3	E_T^N	B_{KT}	[ethanol] mol/dm^3	E_T^N	B_{KT}
0.000	0.355*	0.54	10.226	0.640	0.63
1.704	0.537	0.55	11.931	0.643	0.65
3.409	0.580	0.56	13.635	0.648	0.68
5.113	0.610	0.58	15.340	0.647	0.70
6.817	0.625	0.59	17.044	0.650	0.77
8.522	0.634	0.61			

* literature data [23]

"beta coefficients" [33]. By normalizing β_1 and β_2, we have obtained in percentages the distribution of the effects of acidity and basicity in relationship (4). The calculated data are listed in Table III.

From the data in Table III, it can be seen that, for the compounds examined, according to Eq. (4) there are good correlations between the "fore-band" intensity and the E_T^N and B_{KT} values of the solvents.

The correlations between the E_T^N and B_{KT} values for the three solvent mixtures in Table III are as follows: good in the ethanol-benzene mixture (r=0.980), weak in the ethanol--hexane misture (r=0.922), and very bad in the ethanol--acetone mixture (r=0.653). Accordingly, in the ethanol--benzene mixture there is a good correlation:

$$\log \varepsilon = b_E E_T^N + a_E \qquad (5)$$

Table III

Solution of regression equation (4) for the following Schiff bases in different solvent mixtures:

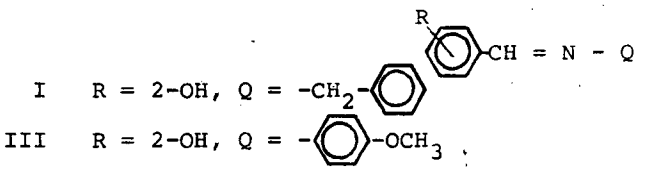

Compound	Solvent	b_1	b_2	a	β_1(%)	β_2(%)	n	R
I	ethanol-hexane	5.460	-1.191	0.098	73.64	26.36	7	0.9860
II		6.092	-1.124	-0.160	76.76	23.24	7	0.9946
III		3.732	-1.079	0.723	67.82	32.18	7	0.9769
IV		4.582	-1.380	0.048	66.92	33.08	7	0.9832
I	ethanol-benzene	1.308	1.227	0.897	42.89	57.11	7	0.9994
II		2.048	1.616	0.295	47.17	52.83	7	0.9993
III		0.483	1.243	0.985	21.49	78.51	7	0.9992
IV		0.485	1.902	0.010	15.09	84.91	7	0.9996
I	ethanol-acetone	2.012	2.663	-0.622	48.95	51.05	7	0.9899
II		3.706	4.350	-2.760	51.95	48.05	7	0.9912
III		0.940	2.626	-0.316	31.82	68.18	7	0.9889
IV		1.796	4.194	-2.489	35.83	64.17	7	0.9912

and

$$\log \varepsilon = b_B B_{KT} + a_B \qquad (6)$$

which is slightly worse than that in Eq. (4). However, in the ethanol-hexane, and especially the ethanol-acetone mixtures, the correlation according to regression equations (5) and (6) is considerably worse than that based on relationship (4). Figures 5 and 6 illustrate the measured log ε values and those calculated via the regression equations for N-(4-hydroxybenzylidene)butylamine solutions. Thus, it is to be expected that the position of the A ⇌ B equilibrium characteristic of the solvent effects of the Schiff

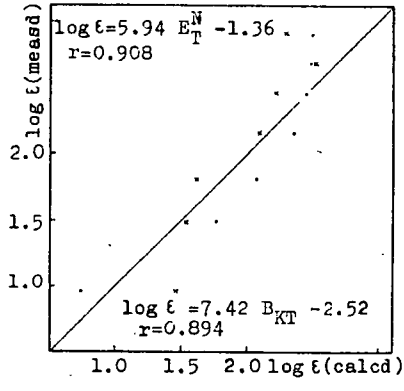

Figure 5.: Measured log ε and values calculated from Eq. (5) (.) and Eq. (6) (x) in ethanol-acetone solution of N-(4-hydroxybenzylidene)benzylamine

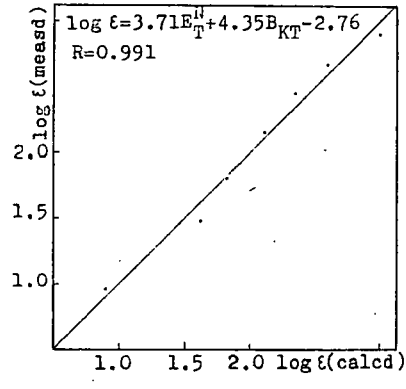

Figure 6.: Measured log ε and values calculated from Eq. (4) in ethanol--acetone solution of N-(4-hydroxy-benzylidene) benzylamine

bases studied is influenced by both the acidity and the basicity parameters. This is valid for both the 2- and the 4-hydroxy derivatives, i.e. the possible intramolecular hydrogen-bond in the case of the 2-hydroxy derivatives does not cause any significant change in the phenomenon described. In Table III there is no significant difference between the data on compounds I and II and those on compounds III and IV. Slight differences can be seen between the Schiff bases formed with benzylamine and those with the aromatic amine (I, II and III, IV, respectively). In the latter case, the effect of the basicity (β_2') is higher for every solvent mixture, while the effect of the acidity (β_1') on the process is lower. This is presumably connected with the lower electron density of the azomethine-nitrogen of the aromatic derivatives. It is noteworthy that in these compounds the A ⇌ B equilibrium is generally shifted strongly in the direction of the bottom arrow in every solution.

We have investigated the applicability of relationship (4) in pure solvents as well. The results are summarized in Table IV.

From use of the data in the Table, the regression equations (5), (6) and (4) are as follows:

$$\log \varepsilon = 3.376\ E_T^N + 0.566 \qquad r = 0.9623$$

$$\log \varepsilon = 2.029\ B_{KT} + 0.845 \qquad r = 0.8616$$

$$\log \varepsilon = 2.556\ E_T^N + 0.723\ B_{KT} + 0.498 \qquad R = 0.9827$$

It can be seen that the correlations with E_T^N or with B_{KT} are worse than with the multiple-parameter equation.

Table IV

Molar absorption coefficients of N-(2-hydroxybenzylidene)-benzylamine *at 405 nm in different solvents at 25 °C*

ε_B = 8150 [31]

Solvent	ε	E_T^N [23]	B_{KT} [25]
n-hexane	3.3	0.074	0.00
benzene	14.4	0.127	0.08
acetone	36.8	0.355	0.54
terc. buthanol	212	0.407	0.95
sec. buthanol	300	0.506	0.90
n-buthanol	412	0.602	0.85
ethanol	480	0.654	0.77
methanol	940	0.765	0.62

This also indicates that both the acidity and basicity of the solvents play roles in the examined process.

We earlier [14, 18, 31] reported that some salts ($CaCl_2$, NaI, LiCl) in ethanolic solution exert a considerable influence on the solvent effect in the absorption spectra of N-(2-hydroxybenzylidene)amine and N-(4-hydroxybenzylidene)amine. Depending on the salt concentration, the A $\rightleftharpoons$ B equilibrium is shifted markedly in the direction of the upper arrow. These observations led us to investigate whether there is any salt effect during the determination of E_T^N values. Figure 7 illustrates the increase in the E_T^N value of ethanol on the action of NaI. The ε values [14] of the "fore-band" maxima of N-(2-hydroxybenzylidene)amine and N-(4-hydroxybenzylidene)amine are shown in the Figure,

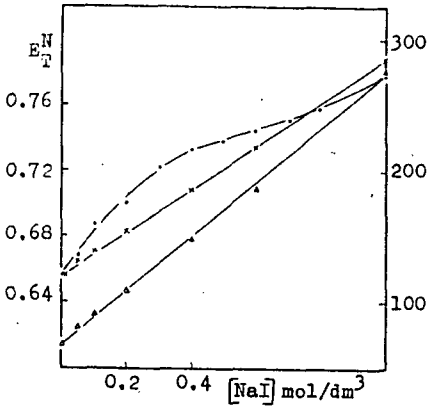

Figure 7.: Changes in the E_T^N value of ethanol (.), the ε_{436} (x) value of N-(2-hydroxybenzylidene) aniline and the ε_{420} (Δ) value of N-(4-hydroxybenzylidene)aniline as functions of the NaI concentration (t=25 °C)

too. Equation (5) indicates a good correlation between the corresponding data for both N-(2-hydroxybenzylidene)aniline (r=0.9869) and N-(4-hydroxybenzylidene)aniline (r=0.9947). It is very likely that there is a certain degree of similarity between the Schiff bases examined and the mechanism of the solvent effect of the betaine dye used to measure E_T^N. Further investigations are required to clarify this problem.

References

[1] *Tsuhida, R., T. Tsumaki*: Bull. Soc. Chem. Japan *13*, 537 (1938).
[2] *Kiss, A., G. Auer*: Z. Phys. Chem. *A.189*, 344 (1941).

[3] *Kiss, A., G. Bácskai, E. Varga*: Acta Chem. et Phys. Szeged, *1*, 155 (1943).
[4] *Kiss, A., R. Paunez*: Acta Chem. et Phys. *3*, 83 (1948).
[5] *Gaouck, V., R.J.W. Le Févre*: J. Chem. Soc. 741 (1938).
[6] *Cohen, M.O., J. Hirschberg, G.M.J. Schmidt*: Hydrogen Bonding. London, 293 (1959).
[7] *Hires, J.*: Kandidátusi disszertáció. Szeged, (1959).
[8] *Hires, J., P. Nagy*: Ped. Főisk. Évk. 183, (1960).
[9] *Hires, J.*: Acta Phys. et Chem. Szeged, *4*, 120 (1958).
[10] *Hires, J., L. Hackl*, Acta Phys. et Chem. Szeged, 519 (1959).
[11] *Dudek, G.O., E.P. Dudek*: J. Amer. Chem. Soc. *86*, 4283 (1964); 88, 2407 (1966).
[12] *Ledbetter, J.W.*: J. Phys. Chem. *70*, 2245 (1966); *71*, 2351 (1967); *72*, 4111 (1968).
[13] *Nagy, P.*: Magy. Kém. Folyóirat *71*, 11 (1965); *72*, 108 (1966).
[14] *Nagy, P.*: Szegedi Tanárképző Főisk. Tud. Közl. 167 (1965).
[15] *Nagy, P.*: Szegedi Tanárképző Főisk. Tud. Közl. 209 (1970).
[16] *Császár, J., M. Novák-Bizony*: Acta Chim. Hung. *86*, 9 (1975).
[17] *Császár, J., J. Balog*: Acta Chim. Hung. *86*, 101 (1975).
[18] *Nagy, P., E. Kövér*: Magy. Kém. Folyóirat *77*, 100 (1971).
[19] *Lewis, J.W., C. Sandorfy*: Can. J. Chem. *60*, 1720 (1982).
[20] *Lewis, J.W., C. Sandorfy*: Can. J. Chem. *60*, 1727 (1982).
[21] *Ledbetter J.W.*: J. Phys. Chem. *86*, 2449 (1982).
[22] *Ranganathan, H., T. Ramasami, D. Ramaswancy, M. Santappa*: Indian J. Chem. *25A*, 127 (1986).
[23] *Reichardt, C., E. Harbusch-Görnert*: Liebigs. Ann. Chem. 721 (1983).
[24] *Kamlet, M.J., R.W. Taft*: J. Amer. Chem. Soc. *98*, 377 (1977).
[25] *Krygowski, T.M., E. Milczarek, P.K. Wrona*: J.C.S. Perkin II. 1563 (1980).
[26] *Nagy, P., R. Herzfeld*: Acta Phys. et Chem. Szeged, *31*, 735 (1985).
[27] *Svoboda, P., P. Pytela, M. Vecera*: Coll. Czechoslovak Chem. Commun. *48*, 3287 (1983).
[28] *Bekárek, V.*, J. Chem. Soc. Perkin Trans II. 1293 (1983).
[29] *Reichardt, C.*: Molecular Interactions, Wiley, Chichester, New York, Vol. 3, p. 241 (1982).
[30] *Berstein, Ja.I., Ju.L. Kaminszkij*: Opt. Spekt. *15*, 705 (1963).
[31] *Nagy, P.*: Szegedi Tanárképző Főisk. Tud. Köz. 123 (1968).

[32] *Nagy, P., R. Herzfeld*: Acta Phys. et Chem. Szeged, *32*, 33 (1986).
[33] *Krygowski, T.M., W.R. Fawcet*: J. Amer. Chem. Soc. *97*, 2143 (1975).

НОВЫЕ ДАННЫЕ К ПОНИМАНИЮ ВЛИЯНИЯ РАСТВОРИТЕЛЯ В АБСОРЦИОННЫХ СПЕКТРАХ ОСНОВАНИЙ ШИФФА

П. Надь и Р. Герцфельд

Авторы исследовали влияние растворителя в абсорционных спектрах N-/2-гидрокси-бензилиден/амина и N-/4-гидрокси-бензилиден/амина. Нашли хорошую корреляцию между данными интенсивности полосы около 400 нм и E_T^N растворителей а также B_{KT}.

ISBN 963 481 629 0
Acta Phys. et Chem. Szeged 33 69-97 (1987)

INVESTIGATIONS ON THE ACIDITIES OF DIFFERENT TYPES OF ZEOLITES

By

I. KIRICSI*, GY. TASI*, H. FÖRSTER** and P. FEJES*

* Applied Chemistry Department, József Attila University, Rerrich Béla tér 1., H-6720 Szeged, Hungary

** Institute of Physical Chemistry, University of Hamburg, Bundesstrasse 45., D-2000 Hamburg 13, Federal Republic of Germany

(*Received 12 October 1987*)

Different zeolites were characterized by means of X-ray diffraction, derivatography and infrared spectroscopy. The acidities of the zeolites were determined by pyridine adsorption. The literature data concerning the absorption coefficients of pyridine adsorbed on acidic sites are critically evaluated.

Introduction

The characterization of zeolite catalysts used for investigations of the mechanisms and kinetics of hydrocarbon transformation is indispensable, and includes (i) an estimation of the number and nature of potential active sites; (ii) determination of the temperature range of operation in which no essential structural changes occur in the catalysts.

Kinetic data, i.e. apparent rate constants and activa-

tion energies, usually obtained from kinetic experiments supplemented with the predetermined physical properties of the catalysts, may provide a promising data-set for the computer optimization of kinetic models.

The present study deals with the acidities and partly also with the thermal stabilities and crystallinities of the zeolites used in adsorption, kinetic and spectroscopic measurements with the aim of investigation of the kinetics and mechanisms of the cracking of short-chain paraffins.

Derivatography, X-ray diffraction and ir spectroscopy were used to acquire data for catalyst characterization.

Experimental

NH_4^+-zeolites were prepared from their sodium forms. In order to obtain samples with different ammonium ion contents, NaY (Linde) was ion-exchanged with NH_4Cl solutions of different concentrations for 12 h at 350 K.

NH_4^+-mordenite was obtained by ion-exchange of Na-mordenite (Norton) in 0.1 mol/dm^3 NH_4Cl solution at 350 K for 12 h (the procedure was repeated three times with fresh solutions).

In the case of zeolite ZSM-5, the following procedure was used. The starting material, the zeolite ZSM-5 "as synthesized", was baked out at 770 K in flowing air for 12 h in order to burn off the organic template. This raw material was converted into its sodium form by repeated ion-exchange in 0.1 mol/dm^3 NaCl solution at room temperature, and then washed with water. NH_4^+-ion-exchange of NaZSM-5 was performed

at room temperature and repeated three times following the preparation procedure proposed by Dwyer [1].

After ion-exchange, the NH_4^+ forms of the zeolites were carefully washed with distilled water until the filtrate was Cl^--free, then dried and stored over saturated NH_4Cl solution to obtain samples with a standard water content.

The compositions of the samples were determined by neutron activation analysis (Y and mordenite) and atomic absorption spectroscopy (ZSM-5), and are given in Table I.

Table I

Unit cell compositions of the zeolites under study

Sample	Unit cell composition	Water content, m %
NaY	$Na_{58}Al_{58}Si_{134}O_{384}$	28
H1Y	$(NH_4)_5Na_{53}Al_{58}Si_{134}O_{384}$	+
H2Y	$(NH_4)_{32}Na_{26}Al_{58}Si_{134}O_{384}$	+
H3Y	$(NH_4)_{42}Al_{16}Al_{58}Si_{134}O_{384}$	+
NaM	$Na_{6.5}Al_{6.5}Si_{41.5}O_{96}$	12
HM	$(NH_4)_{6.3}Na_{0.2}Al_{6.5}Si_{41.5}O_{95}$	+
NaZSM-5	$Na_{1.08}Al_{1.08}Si_{94.9}O_{192}$	6
HNaZSM-5	$(NH_4)_{1.02}Na_{0.006}Al_{1.08}Si_{94.9}O_{192}$	+

+ The water content was not available for these samples.

Results and Discussion

Characterization of samples by X-ray and ir spectroscopy

To check the crystallinity of each catalyst sample, and its change under the conditions of preparation and activation, X-ray diffraction and ir spectroscopy (in the range of framework vibration, 400-1300 cm^{-1}) where used. X-ray diffraction analysis was carried out at ambient temperature, with a DRON-3 diffractometer. For the KBr pellet technique, a SPECORD-75 IR spectrophotometer was utilized. In each case, wafers of 1 m % zeolite in KBr were recorded vs. an empty KBr pellet.

Figure 1 shows a set of diffractograms selected to demonstrate the characteristic reflexions of the zeolites tested. No change in crystallinity due to ion-exchange was detected. In contrast, the removal of the organic template influenced the X-ray pattern of ZSM-5, as can be seen in Figure 1. The change in intensity of reflexions as a result of template removal is well known and has been discussed in the literature [2-7].

The ir spectra show obvious differences, depending on the structures of the zeolites used (see Figure 2). The frequencies observed are in good agreement with the literature data [8-12]; they are listed in Table II. According to Flanigen [13], absorptions at around 1100, 700 and 450 cm^{-1} are assigned to internal vibrations of the tetrahedra. The bands at 650-550 cm^{-1} are characteristic of the presence of double-rings of tetrahedra. Absorption in the range 1000-1200 cm^{-1} are due to external asymmetric motions.

The method of Coudurier [11], according to which the ratio of the absorbances of the bands at 650-550 and 480--440 cm^{-1} is a good measure of the crystalline fraction of

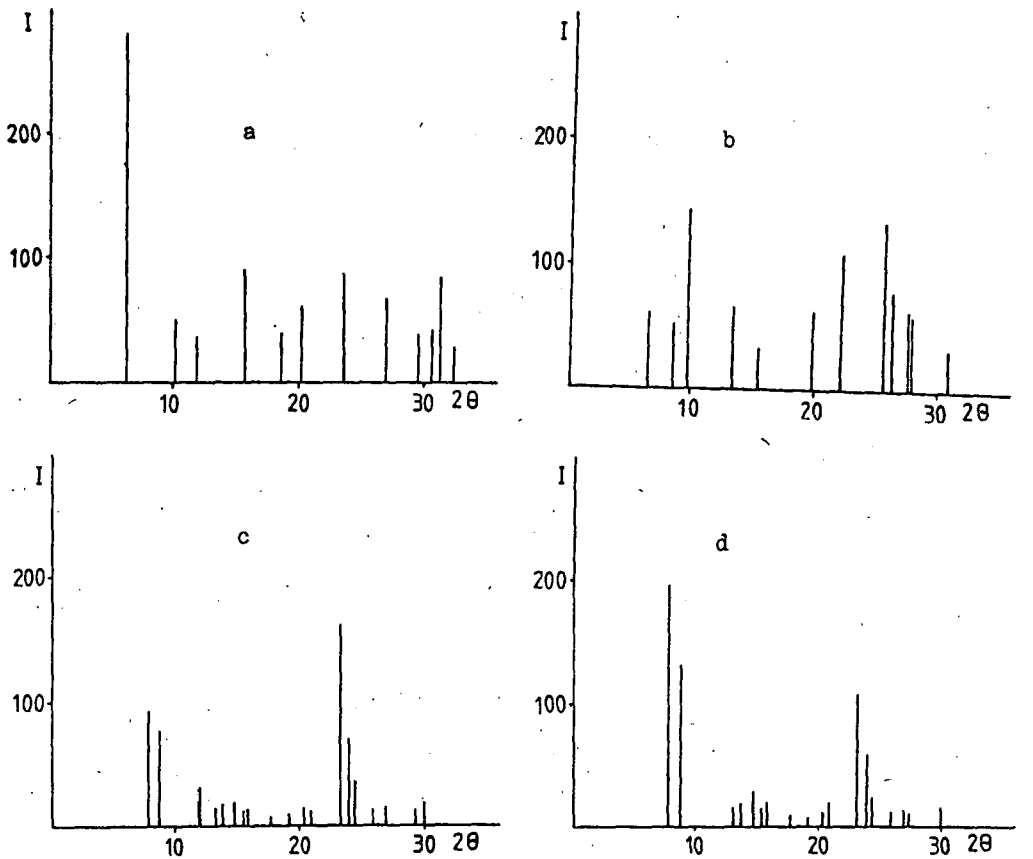

Figure 1.: X-ray diffractograms of zeolites tested:
a/ NH_4NaY, b/ NH_4Na-mordenite,
c/ ZSM-5 "as synthesized", d/ NH_4ZSM-5

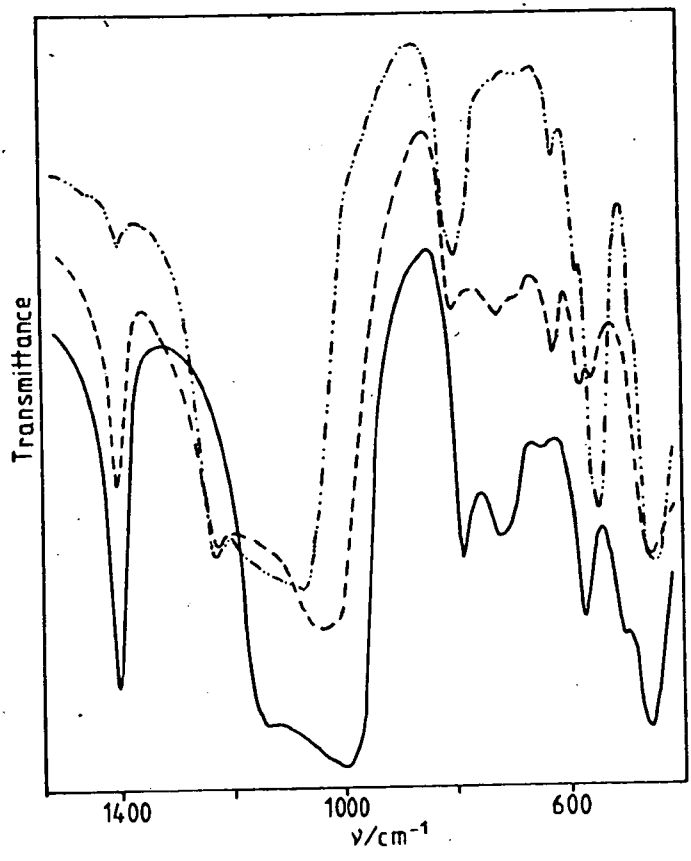

Figure 2.: Ir spectra of NH_4NaY (------), NH_4Na-mordenite (- - - - -) and NH_4ZSM-5 (-..-..-) in the range of framework vibration.

Table II

Observed bands in the range of framework vibrations

Zeolite	Frequencies, cm^{-1}							
NH_4NaY	460	505	575	640	720	785	980	1140
NH_4NaM	460	520	545	625	730	805	1005	1230
$NH_4NaZSM5$	450	546	585	626	680	800	1080	1230

a given zeolite, results in characteristic ratios of 0.24, 0.51 and 0.72 for the zeolites; these should be compared with the values we obtained: 0.19, 0.49 and 0.78 for mordenite, zeolite Y and ZSM-5, respectively.

Comparison of the ammonium contents of the samples obtained from their chemical analysis and those determined from the absorbance of the NH_4^+ band at 1400 cm^{-1} (0.67, 0.5 and 0.04 for NH_4NaY, NH_4NaM and $NH_4NaZSM-5$, respectively) shows a good linear relationship.

Thermogravimetric investigations

Derivatographic experiments were performed with a DERIVATOGRAPH-Q instrument. Zeolites were placed on platinum plates. The thermograms were recorded in air at a heating rate of 5 K/min. Information obtained from these measurements can only be regarded as approximate, as the transformations taking place in zeolites under high-vacuum conditions (especially in the case of NH_4^+ forms) depend strongly on the experimental conditions, i.e. heating rate, atmosphere over the sample, thickness of the zeolite layer, etc. [14-19].

A typical derivatographic pattern of zeolite NH_4NaY is depicted in Figure 3. The TG curve shows three, not clearly

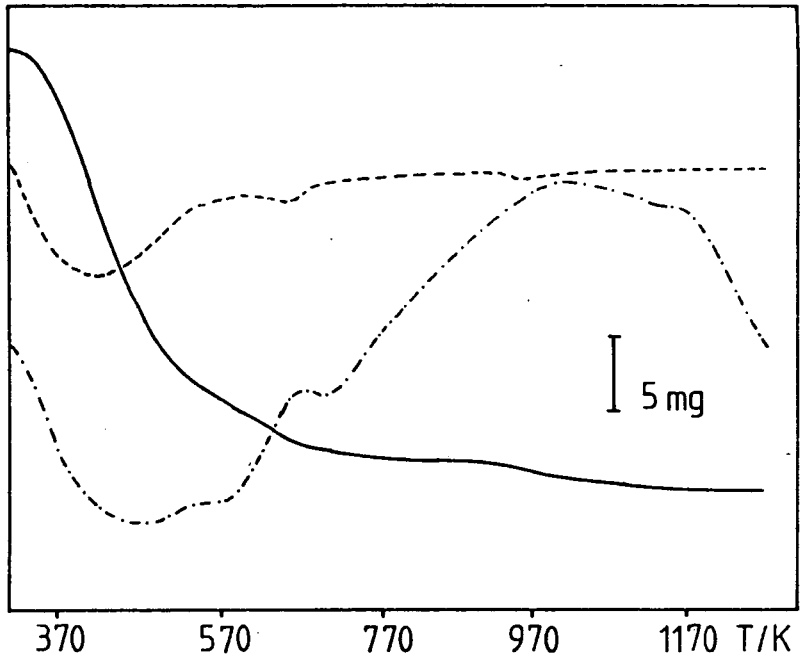

Figure 3.: Derivatographic pattern of NH_4NaY: TG ———; DTG - - - -; and DTA -.-.-.

separated steps, at 410, 640 and 950 (as can be seen in the DTG, too). The large and broad endotherm at 480 K (see DTA) is due to dehydration, which is not complete prior to deammonization.

Under the experimental conditions used in these measurements, the deammonization of NH_4NaY can be characterized by an exotherm and an endotherm, at 580 and 660 K, respec-

tively. It was reported earlier that the deammonization of zeolites in an inert atmosphere shows no exotherm, while in the presence of oxygen there is a more or less pronounced exotherm, depending on the oxygen content of the eluent gas [20-23].

Figure 4 shows the TG curves of NaM and NH_4NaM. After the dehydration of NaM, no further weight loss could be ob-

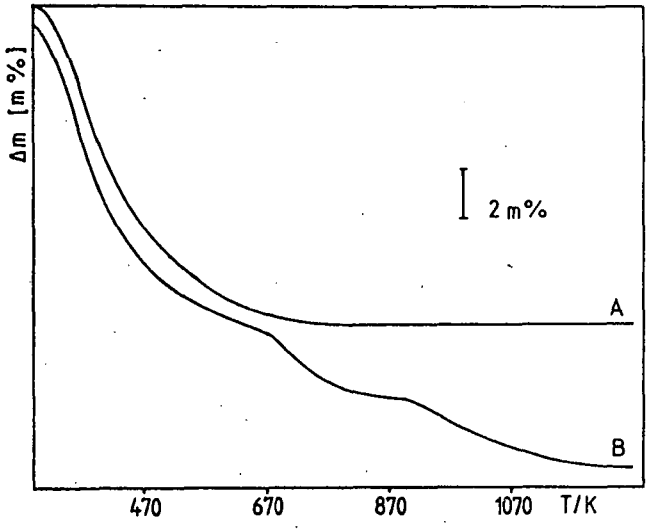

Figure 4.: TG curves of Na-mordenite (A) and NH_4Na-mordenite (B)

served up to 1270 K, the highest temperature obtained with our equipment. From the TG curve of NH_4NaM, it can be inferred that the deammonization and dehydroxylation are better

resolved then for NH_4NaY. Therefore, the ammonium ion content of this sample could be determined from the weight loss due to deammonization (1.8 mmol/g), and was in good agreement with the value derived from chemical analysis (2.1 mmol/g).

The thermal behaviour of the ZSM-5 samples is shown in Figure 5. The TG curve of ZSM-5 "as synthesized" shows two overlapping steps, reflecting the weight loss upon removal

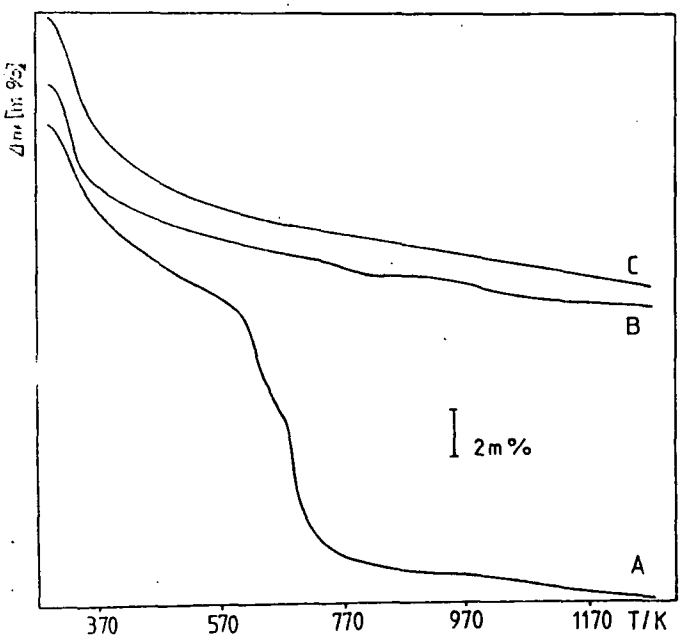

Figure 5.: TG curves of ZSM-5 "as synthesized" (A), $NH_4NaZSM-5$ (B) and NaZSM-5 (C)

of the organic template. At higher temperatures, a slight, but continuous decrease in weight was detected. The TG curve of NH_4NaZSM-5 also contains two steps due to deammonization and dehydroxylation, at 770 and 1030 K, respectively, while in curve B only a slight weight loss can be observed.

Thermoanalytical investigations on NH_4NaY showed an exothermic peak at 1170 K, due to collapse of the crystal lattice. Since this temperature is much higher than that used for activation of the zeolites applied for the acidity measurements (870 K was the highest), no appreciable loss of crystallinity should be expected, although slight changes cannot be excluded. Some loss of crystallinity of NH_4NaM, which is regarded as much more stable than the Y type, was found by Weeks et al. [20]. Their explanation was that deposition of amorphous alumina takes place upon heat treatment, and simultaneously a unit cell contraction occurs. Details on the compositions of aluminium compounds formed upon different heat treatments were given by Barrer [64].

Upon the pretreatment of NH_4 forms of zeolites in high vacuum, similar transformations occur in the framework as under deep- or shallow-bed conditions, but there can be large deviations as concerns the extents of these reactions. Removal of aluminium from the framework of ZSM-5 can also take place during treatment at high temperatures. However, in our case, where each unit cell of ZSM-5 contains approximately only one aluminium ion, the formation of multinuclear aluminium complexes may be excluded for topological reasons.

Acidity measurements

In general, two main types of hydroxy groups can be distinguished in zeolites. The first type absorbs in the range 3730-3750 cm^{-1} and is assigned to nonacidic OH groups, the origin of which is still ambiguous [24, 25]. The second type concerns the acidic OH groups, as these can easily react with base molecules such as pyridine [26-29], piperidine [30], alkylamines [31, 32], etc. Depending on the type of zeolite, the cations introduced by ion-exchange and the pretreatment conditions, one or more acidic OH groups are formed in the zeolite, as proved by the respective number of ir bands in the OH stretch region [33-39].

There are two possible ways to characterize Brönsted acidity. The first is to measure the intensities of the OH bands themselves. Although this method seems to be rather approximate, and can provide only some ideas on the trend of the change in acidity for the same zeolitic type and cation form, some very careful investigations are to be found in the literature, the aim of which was to make this method more accurate [40, 41].

The second way to analyse the surface acidities of both Brönsted and Lewis sites is based on the selective adsorption of bases on both types of sites, giving rise to distinct ir absorptions. Various bases have been used as probes for the characterization or quantitative determination of the concentrations of acidic centres in zeolites [25, 42-48]. Selection of the most suitable probe molecule seems to be very difficult, since each procedure has certain disadvantages. As pyridine has been used for decades for this purpose, and as there is a great body of literature

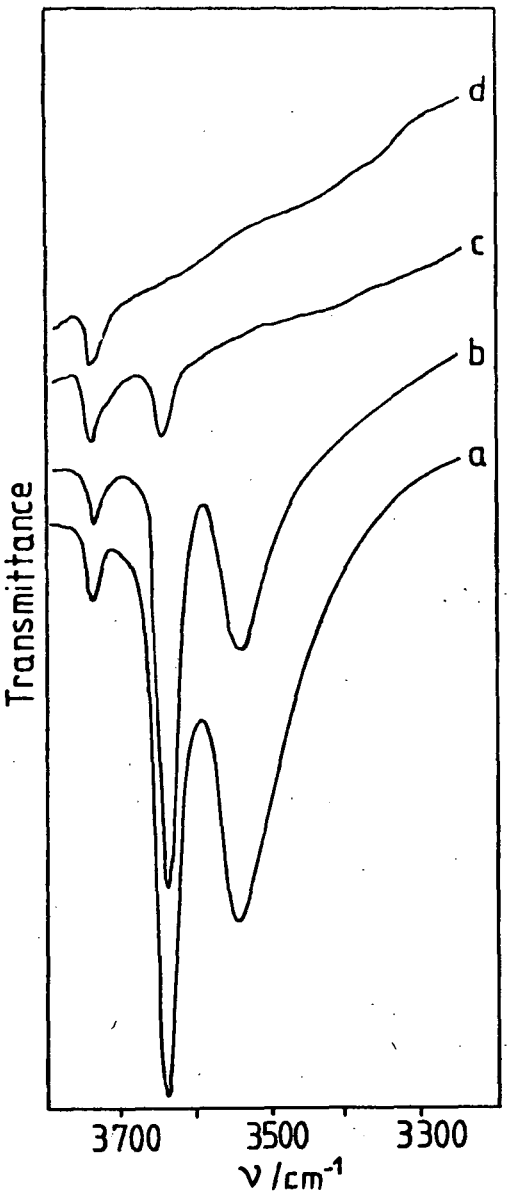

supplying a very good and useful background of knowledge, this "traditional" molecule was chosen for our investigations. It should be mentioned that the literature contains no uniform procedure which could be regarded as a standard method with pyridine.

Self-supporting wafers 5-7 mg/cm^2 in thickness were prepared, inserted into a gold holder, and placed in the ir cell connected to the vacuum/dosing system.

Figure 6.: Ir spectra in the range of OH stretching vibrations of the H3Y sample treated in vacuo at 450 (a), 670 (b), 770 (c) and 870 K (d)

The specimens were degassed for 12 h at different temperatures in high vacuum. The final pressure was lower than $5x10^{-7}$ Torr. The spectra were recorded at beam temperature with a PERKIN-ELMER 225 spectrometer

Figure 6 shows the spectra of H3Y activated at 450, 670, 770 and 870 K. For the sample evacuated at 450 K, OH bands were detected at 3740, 3650 and 3550 cm^{-1}. Upon elevation of the activation temperature, the bands at 3650 and 3550 cm^{-1} decreased as a result of dehydroxylation, the Brönsted sites being converted into Lewis sites. After evacuation at 770 K, only the high-frequency band at 3650 cm^{-1} and the nonacidic OH band at 3740 cm^{-1} were observed. Treatment in high vacuum at 870 K resulted in an almost complete disappearance of acidic OH groups. From this it should be concluded that this sample did not contain any Brönsted acidity, although, as will be demonstrated later, this assumption proves to be only a very approximate one.

Adsorption of pyridine was carried out at beam temperature. In order to accelerate this process, the wafers were treated with pyridine at temperatures high enough for complete pyridine chemisorption. For zeolites Y and ZSM-4 450 K was chosen, and for mordenite 570 K.

With the exception of mordenite, whose acidity had been investigated very carefully by Karge, the temperature of pyridine desorption was studied, too [49, 50]. As the concentration of acid sites is calculated from the absorbance of Brönsted- (BPy) and Lewis-bound pyridine (LPy), which depends strongly on the desorption temperature used, determination of the optimum conditions for pyridine desorption seemed to be of high importance.

Figure 7 shows the integral absorption of BPy and LPy as functions of the desorption temperature. It can be seen

that pyridine is desorbed more easily from Brönsted sites than from Lewis sites with increasing temperatures. Similar results were obtained for ZSM-5 samples pretreated at 670 and 770 K. On the basis of these investigations, 530 K was chosen as the temperature for the desorption of pyridine.

Beamont et al. published an excellent paper on the acidities of Y-type zeolites with different aluminium contents [51]. The ready desorption of BPy was observed above 570 K. In high vacuum, after the pyridine had been pumped off for 1 h at 450 K, some physically adsorbed pyridine remained on the sample, which was not the case at 530 K. Therefore, for Y-type zeolites 530 K was used as the temperature for desorption.

For the determination of mordenite acidity, the Karge procedure could be applied [49, 50], with desorption at 470 K.

Upon the adsorption of pyridine on the activated samples at beam temperature, numerous ir absorption were detected, from which the bands at 1540 and 1450 cm^{-1} are assigned to the BPy and LPy, in accordance with the literature [52-56]. In addition, a third band, at 1490 cm^{-1}, due to an overlapping band of pyridine interacting with Brönsted and Lewis acid sites, is also frequently used for analysis [57]. Figure 8 shows ir absorptions upon the adsorption of 1.33 kPa pyridine for 1 h at beam temperature on Y-type zeolites degassed at different temperatures.

As a result of the adsorption of pyridine on NaY at beam temperature, sharp bands were obtained at 1445, 1490, 1577 and 1623 cm^{-1}. They disappeared almost completely upon evacuation at 530 K, where only very weak bands remained, proving that this sample contained only few Lewis acid sites (see Figure 8, spectrum a). Pyridine bound to Na^{+} ions, giv-

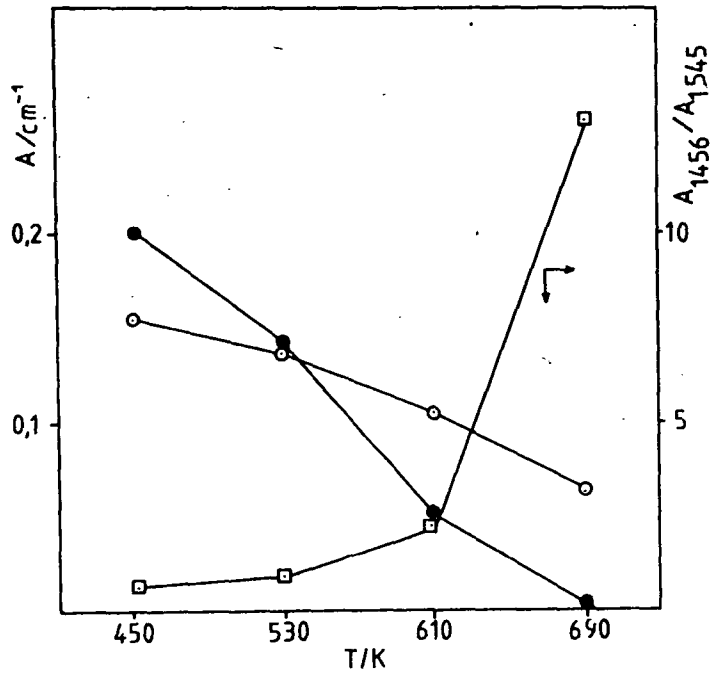

Figure 7.: Integral absorbance of the bands of Lewis- and Brönsted-bound pyridine and their ratio as functions of the desorption temperature.

○ BPy
● LPy
⊡ Ratio of LPy to BPy

ing rise to a band at 1445 cm^{-1}, could be removed by evacuation at 530 K for every sample tested, as seen in Figure 8. After desorption of pyridine from HY zeolites pretreated at different temperatures, bands characteristic of Brönsted (1540 cm^{-1}) and Lewis (1455 cm^{-1}) acid sites were observed, the intensities of which varied with the activation tem-

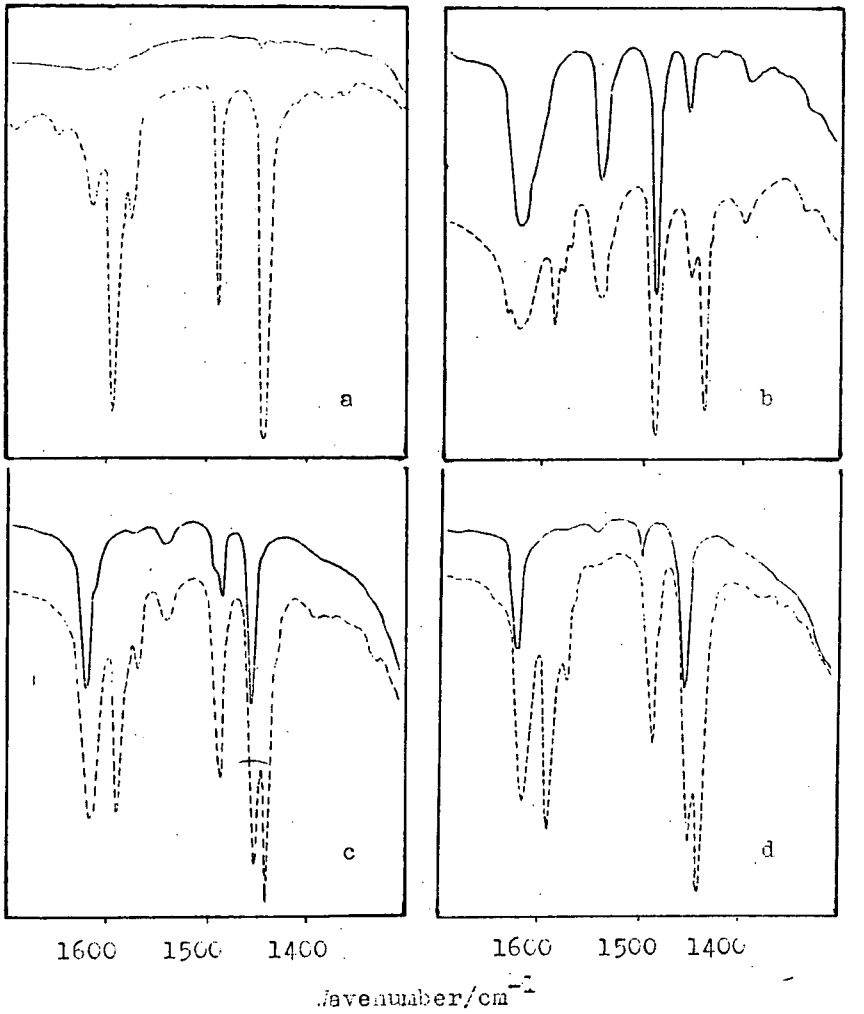

Figure 8.: Ir absorption due to adsorbed pyridine on Y-type zeolites (a) NaY, (b-d) H3Y activated at 670, 770 and 870 K. Dashed-line spectra and full-line spectra refer to adsorbed pyridine before and after evacuation at 410 K.

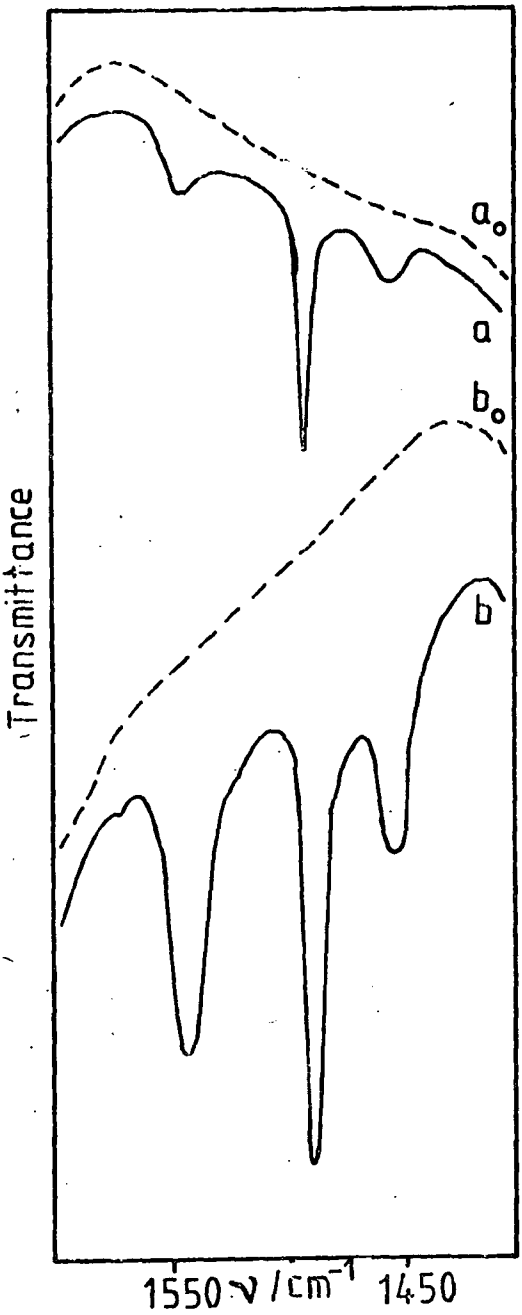

perature. In case of the sample pretreated at 870 K in high vacuum, the BPy band could be observed too, although no acidic OH bands could be detected in the ir spectrum. This proves that the application of probe molecules improved the sensitivity of detection of surface acidity.

Figure 9.: Infrared spectra of adsorbed pyridine on zeolites HZSM-5 and H--mordenite. a_o and a: spectra of HZSM-5 before and after pyridine adsorption; b_o and b: spectra under similar conditions for H--mordenite.

In Figure 9, spectra of adsorbed pyridine on H-mordenite and HZSM-5 can be seen. In both cases, Brönsted and Lewis acid sites were detected. Comparison of the band intensities shows that the concentration of acid centres is higher for mordenite than for ZSM-5.

The band frequencies of adsorbed pyridine for the investigated zeolites are listed in Table III.

Table III

Band frequencies of adsorbed pyridine for the studied samples (cm^{-1})

	Zeolite		
	HZSM-5	HNaM	HNaY
BPy	1545	1542	1545
LPy	1456	1454	1454

Estimation of the concentrations of acid sites from the spectra of adsorbed pyridine

The integral absorbance of a band between ν_1 and ν_2 is given by

$$E_{int} = \int_{\nu_1}^{\nu_2} \log (T_0/T)\, d\nu \qquad (1)$$

This represents a more unobjectionable measure for absorption and is correlated with the absorbance E_ν:

$$E_\nu = \log (T_0/T) \qquad (2)$$

where T_0/T is the ratio of the intensities of the incident

and transmitted radiation. The concentration c of the absorbed species can be determined via the Beer-Lambert law:

$$c = E/\varepsilon \cdot l \qquad (3)$$

where l is the path length and ε the extinction coefficient. In the case of self-supporting wafers, the molar amount per square area d (or, if more convenient, the mass per square area) can be used in place of $c \cdot l$, by means of which the extinction coefficient

$$\varepsilon_\nu = E_\nu/d \qquad [m^2 \cdot mol^{-1}] \qquad (4)$$

or the integral extinction coefficient

$$\varepsilon_{int} = E_{int}=d \qquad [m \cdot mol^{-1}] \qquad (5)$$

can be determined.

The following factors influence the accuracy of determination of the number of acidic centres. The determination of band intensities is usually straightforward, but for zeolites where the spectrum is obscured by additional bands of framework vibrations in the range 1400-1600 cm^{-1}, more attention should be paid to the establishment of the baseline. Furthermore, determination of the extinction coefficient of a surface species is in general difficult, as the simultaneous measurement of ir intensity and adsorbed amount is necessary, provided that only one surface compound is formed. If the extinction coefficients were identical for both species of adsorbed pyridine the ratio of the band absorbances would yield the ratio of the concentrations of Brönsted and Lewis acid sites. However, this is generally not

the case, and different approaches have been used to overcome this problem. A number of papers deal with this fundamental question; of these only the most important will be mentioned, in order to show the great efforts which had to be made in this field.

Ward suggested utilization of the fact that, upon heat treatment, two Brönsted acid sites are converted into one Lewis acid site, keeping the sum of 2 Lewis sites + 1 Brönsted site constant, while their ratio will change with the temperature of pretreatment [58]. Thus, from measurements of pyridine adsorption on two samples activated at different temperatures, $\varepsilon_L/\varepsilon_B$ and the ratio of acid sites can be determined. This method was succesfully applied to Y-type zeolites, but it cannot be applied to mordenites, where this conversion does not follow the stoichiometry mentioned above.

Basila and co-workers studied the contributions of LPy and BPy to the intensity of the common band at 1490 cm^{-1} [59]. For investigations on potassium-poisoned silica--alumina, the ratio of the extinction coefficients $\varepsilon_{1490}/\varepsilon_{1450}$ was found to be 0.25 and the ratio of Lewis to Brönsted acid centres was estimated via

$$\frac{LPy}{BPy} = \frac{1.5\ E_{1450}}{E_{1490}-1.5\ E_{1450}}$$

Recently, Riseman et al. reinvestigated this problem [60], and the relationship

$$\frac{LPy}{BPy} = \frac{6.035\ E_{1450}}{E^{T}_{1490}-0.35\ E_{1450}}$$

was found to be valid, where E^{T}_{1490} means the total absorbance of the 1490 cm^{-1} band. From a comparison of these two equations, their analogy becomes obvious. Although the applicability of this method (based on the assumption that the ratio of the extinction coefficients $\varepsilon_{1490}/\varepsilon_{1450}$ is the same for alumina, silica-alumina and zeolites) seems to be proved, the fundamental question of whether the extinction coefficients of BPy and LPy are independent of the strengths of the acid sites present in different solids has not been completely clarified.

Direct determination of the extinction coefficients of LPy and BPy requires two extremely different samples, one containing only Brönsted, and the other only Lewis acidity. Preparation of these samples is difficult, though not impossible [50]. With these samples available, the extinction coefficients can be determined. This was done by Datka, who obtained 0.084 and 0.059 $cm^2/\mu mol$ for BPy and LPy, respectively, on HNaY [61], and 0.058 $cm^2/\mu mol$ for LPy on HNaZSM-5 [62]. These nearly identical values of LPy support the above assumption that it is almost independent of the zeolite (and/or silica-alumina). In constrast to Datka's results, Stock et al. obtained significant differences as concerns the extinction coefficients of BPy even for zeolites HNaY and HNaX [40].

Take determined the extinction coefficients of BPy and LPy for HZSM-5. The value for BPy was similar to those of Stock et al. and Hughes and White [30], but that for BPy was somewhat smaller than that for LPy [63].

Table IV. lists the extinction coefficients found in the literature.

Table IV

Extinction coefficients of pyridine adsorbed on Brönsted and Lewis acid sites, taken from the literature

B	L	References
0.084 $cm^2/\mu mol$	0.059 $cm^2/\mu mol$	61
-	0.058 $cm^2/\mu mol$	62
1.31 $cm/\mu mol$	1.42 $cm/\mu mol$	30
1.11-1.49 $cm/\mu mol$	-	40
1.3 $cm/\mu mol$	1.5 $cm/\mu mol$	63

It was difficult to select the extinction coefficients for both kinds of surface acidity and the procedure for their determination from the literature. Finally, we chose the integral extinction coefficients published by Take [63], simply because these were the most recent data in the literature. The concentrations of acid sites calculated as described in this paper can be found in Table V. for the zeolites applied.

Our acidity measurements permit the conclusion that the higher the ammonium ion content of the sample, the larger the number of acid sites formed in the zeolite during deammoniation.

For mordenite and zeolites Y, it was found that the concentration of Lewis acid sites passes through a maximum at 770 K with increasing pretreatment temperature. The same was found by Karge for zeolite NH_4M [50]. According to his explanation, the reason for the decrease in Lewis acidity above 770 K is that the increasing amount of $[AlO^+]$ species formed during dehydroxylation hinders the diffusion of pyr-

Table V

Concentrations of acidic sites for the zeolites tested in this study

Sample	Temperature of vacuum treatment	Concentration of acid sites in mol/kg	
		Brönsted	Lewis
NaY	770	-	detectable
H1Y	670	0.078	0.013
H2Y	670	0.275	0.093
H2Y	770	0.014	0.151
H3Y	670	0.441	0.082
H3Y	770	0.058	0.305
H3Y	870	0.007	0.156
HM	670	0.695	0.193
HM	770	0.212	0.460
HM	870	0.023	0.182
HZSM-5	670	0.033	0.008
HZSM-5	770	0.028	0.013
HZSM-5	870	0.018	0.015

idine in the pore system of mordenite. Recently, Shannon et al. investigated the nature of the nonframework aluminium species in HY zeolite [65], and concluded that similar residual nonframework aluminium species are present in both HY dehydroxylated at 920 K in vacuo and HY steamed at 1160 K. However, in the latter in increased degree of condensation and an increased number of nonframework aluminium species were found. A boehmite-like phase could be identified, which is present in the supercages and has dimensions fitting the supercage of Y-type zeolites.

This boehmite-like phase can be formed through the clustering of smaller Al-containing species during dehydroxylation. These results indicate that dehydroxylation is accompanied by condensation of aluminium-containing species (at least of boehmite structure). Therefore, the higher the temperature, the greater the degree of condensation and consequently, the more increased the hindrance for pyridine diffusion, even in the case of HY zeolite. On the other hand, if the species formed during dehydroxylation are not large enough, they could act as multiple adsorption sites for two or three pyridine molecules. However, as these types of interactions are improbable because of steric hidrance, the decreasing number of Lewis acid sites above 770 K seems to be explainable in terms of the formation of aluminium-containing clusters.

Summary

Zeolite catalysts have been characterized by X-ray diffraction, derivatography and ir spectroscopy. The X-ray measurements showed that the crystallinity of the tested zeolites was well-preserved. Ir spectroscopic investigations in the range of framework vibrations supplemented this finding. The absorptions observed for these samples are in good agreement with literature data.

The acidities of the zeolites were determined by means of pyridine adsorption. For mordenite and zeolite Y, the number of Lewis acid sites passed through a maximum at 770 K,

while a monotonous decrease in the number of Brönsted acid sites was found with increasing pretreatment temperature. The decrease in the number of Lewis acid centres above 770 K was explained by the enhanced formation of nonframework aluminium-containing clusters generated during dehydroxylation.

Acknowledgements

We thank Dr. K. Zietlow and Mrs. M. Hemmert for zeolite analyses and M. J. von Pat preparation of the ZSM-5 sample. The scholarship for I. K. by the Alexander von Humboldt Foundation is gratefully acknowledged. We are indebted to the Deutsche Forschungsgemeinschaft for financial support.

References

[1] *Dwyer, F.G.*: ACS Symp. Ser. *218*, 59 (1983).
[2] *Olson, D.H., G.T. Kokotailo, S.L. Lawton, W.M. Meier*: J. Phys. Chem. *85*, 2238 (1981).
[3] *Price, G.D., J.J. Pluth, J.V. Smith, J.M. Bennett, R.L. Patton*: J. M. Chem. Soc. *104*, 5971 (1982).
[4] *Lermer, H., M. Draeger, J. Steffen, K.K. Unger*: Zeolites *5*, 131 (1985).
[5] *Chao, K.J., J.C. Lin, Y. Wang, G.H. Lee*: Zeolites *6*, 35 (1986).
[6] *van Koningsveld, H., H.van Bekkum, J.C. Jansen*: Acta Cryst. *B43*, 127 (1987).
[7] *Rohrman, A.C., Jr. R.B. LaPierre, J.L. Schlenker, J.D. Wood, E.V. Valyocsik, M.K. Rubin, J.B. Higgins, W.J. Rohrbaugh*: Zeolites *5*, 352 (1985).
[8] *Flanigen, E.M., H. Khatami, H.A. Szymanski*: Molecular Sieves Zeolites I., ACS *101*, 1971, p. 201

[9] *Shiralkar, V.P., S.B. Kulkarni*: Z. Phys. Chemie N.F. *447*, 213 (1982).
[10] *Lohse, U., E. Alsdorf, H. Stach*: Z. anorg. allg. Chem., *447*, 64 (1978).
[11] *Coudurier, G., C. Naccache, J.C. Vedrine*: J. Chem. Soc. Chem. Comm. 1982, 1413
[12] *Jansen, J.C., F.J. van der Gaag, H. van Bekkum*: Zeolites *4*, 369 (1984).
[13] *Flanigen, E.M.*: Zeolite Chemistry and Catalysis, ed. J.A. Rabo, Am. Chem. Soc. Eashongton, ACS Monograph 171, 1976, p. 80
[14] *Benesi, H.A.*: J. Catalysis *8*, 368 (1967).
[15] *Beyer, H., J. Papp, D. Kallo*: Acta Chim. Acad. Sci. Hung. *85*, 7 (1975).
[16] *Cattanach, J., E.L. Wu, P.B. Venuto*: J. Catalysis, *11*, 342 (1968).
[17] *Kristof, J., Gy. Gardos, A. Redey*: J. Thermal Anal. *22*, 123 (1981).
[18] *Bolton, P.A., M.A. Lanewala*: J. Catalysis, *18*, 154 (1970).
[19] *Lai, P.P., L.C.V. Rees*: JCS Faraday I. *72*, 1840 (1976).
[20] *Weeks, T.J., Jr., H.F. Hillery, P.A. Bolton*: JCS Faraday I., *71*, 2051 (1975).
[21] *Beyer, H.K., J. Mihalyfi, A. Kiss, P.A. Jacobs*: J. Thermal Anal. *20*, 351 (1981).
[22] *Chu, P.*: J. Catalysis *43*, 346 (1976).
[23] *Hopkins, P.D.*: J. Catalysis *12*, 325 (1968).
[24] *Jacobs, P.A., R. von Ballmoos*: J. Phys. Chem. *86*, 3050 (1982).
[25] *Quin, G., L. Zheng, Y. Xie, Ch. Wu*: J. Catalysis, *95*, 609 (1985).
[26] *Liengme, B.V., W.K. Hall*: Trans. Faraday *62*, 3229 (1966).
[27] *Ghosh, A.K., G. Curthoys*: JCS Faraday I. *79*, 805 (1983); JCS Chem. Comm. 1983, 1271
[28] *Freude, D., W. Oehme, H. Schmiedel, B. Staudte*: J. Catalysis *49*, 123 (1977).
[29] *Bremer, H., D. Freude, F. Hoffmann, H. Pfeifer, B. Staudte, F. Vogt*: Z. anorg. allg. Chem. *481*, 168 (1981).
[30] *Hughes, T.R., H.M. White*: J. Phys. Chem. *71*, 2129 (1967).
[31] *Meinhold, R.H., L.M. Parker, D.M. Bibby*: Zeolites *6*, 491 (1986).
[32] *Ghosh, A.K., G. Curthoys*: JCS Faraday I, *79*, 147, 2569 (1983); JCS Faraday I, *80*, 99 (1984).
[33] *Lercher, J.A., G. Rumplmayr*: Z. Phys. Chem. N.F. *146*, 113 (1985).

[34] *Datka, J., E. Tuznik*: Zeolites 5, 230 (1985)
[35] *Uytterhoeven, J.B., L.G. Christner, W.K. Hall*: J. Phys. Chem. *69*, 2117 (1965).
[36] *Jacobs, P.A., J.B. Uytterhoeven*: JCS Faraday I., *69*, 359, 373 (1973).
[37] *Karge, H.*: Z. Phys. Chem. N.F., *76*, 133 (1971).
[38] *Mirodatos, C., B.H., Ha, K. Otsuka, D. Barthomeuf*: Prod. of the Fifth Intern. Conf. on Zeolites, ed, L.V. Rees, Heyden, 1980, p. 382.
[39] *Karge, H., J. Ladebeck, Z. Sarbak, K. Hatada*: Zeolites *2*, 94 (1982).
[40] *Stock, Th. D. Dombrowski, J. Hoffmann, J. Fruwert*: Z. Phys. Chem., Leipzig, *265*, 551 (1984).
[41] *Dombrowski, D., J. Hoffmann, J. Fruwert*: JCS Faraday I. *81*, 2257 (1985).
[42] *Ratov, A.N., A.A. Kubasov, K.V. Topchieva, E.N. Rosolovskaja, V.P. Kalinin*: Kinetika i Kataliz, *14*, 1024 (1973).
[43] *Ione, K.G., V.G. Stepanov, G.V. Echevskii, A.A. Shubin, E.A. Paukshtis*: Zeolites *4*, 114 (1984).
[44] *Bosacek, V., D. Freude, W. Gründer, W. Meiler, H. Pfeifer*: Z. Phys. Chem., Leipzig, *265*, 241 (1984).
[45] *Barthomeuf, D.*: J. Phys. Chem. *88*, 42 (1984).
[46] *Vedrine, J.C., A. Auroux, V. Bolis, P. Dejaifve, C. Naccache, P. Wierzchowski, E.G. Derouane, J.B. Nagy, J.-P. Gilson, J.H.C. van Hoof, J.P. van den Berg, J. Wolthuizen*: J. Catalysis *59*, 248 (1979).
[47] *Mirodatos, C., D. Barthomeuf*: J.C.S. Chem. Comm. 1981, 39.
[48] *Lunsford, J.H., W.P. Rotwell, W. Shen*: J. Am. Chem. Soc. *106*, 1540 (1985).
[49] *Karge, H.K. Klose*: Z. Phys. Chem. N.F. *83*, 100 (1973).
[50] *Karge, H.*: Z. Phys. Chem. N.F., *122*, 103 (1980).
[51] *Beaumont, R., P. Pichat, D. Barthomeuf, Y. Tambouze*: Catalysis, ed. W. Hightower, North Holland Publk. Comp., Amsterdam, London, American Elsevier Company INC, New York, 1973. Vol. 1. p. 343.
[52] *Eberly, P.E., Jr.*: J. Phys. Chem., *72*, 1042 (1968).
[53] *Hata, K., Y. Ono, Y. Ushiki*: Z. Phys. Chem. N.F., 117, 37 (1979).
[54] *Watanabe, Y.H.W. Habgood*: J. Phys. Chem. *72*, 3066 (1968).
[55] *Jacobs, P.A., H.K. Beyer*: J. Phys. Chem. *83*, 1174 (1979).
[56] *Auroux, A.V. Bolis, P. Wierzchowski, P.C. Gravelle, J.C. Vedrine*: JCS Faraday Trans II. *75*, 2544 (1979).
[57] *Lefrancois, M., G. Malbois*: J. Catalysis, *20*, 350 (1971).

[58] *Ward, J.W.*: J. Catalysis *12*, 271 (1969).
[59] *Basila, M.R., T.R. Kantner*: J. Phys. Chem. *70*, 1981 (1966).
[60] *Riseman, S.M., F.E. Massoth, G.M. Dhar, E.M. Eyring*: J. Phys. Chem. *86*, 1760 (1982).
[61] *Datka, J.*: JCS Faraday I., *76*, 2437 (1980); JCS Faraday I. *77*, 2877 (1981)
[62] *Datka, J.E. Tuznik*: J. Catalysis, *102*, 43 (1986).
[63] *Take, J., T. Yamaguchi, K. Miyamoto, H. Ohyama, M. Misono*: Proc. of the 7th Intern. Zeolite Conference, Tokyo, August 17-22. 1986, Kodansha-Elsevier, Amsterdam-Tokyo, ed. Y. Murakami et al., p. 495.
[64] *Barrer, R.M.*: Zeolites and Clay Minerals as Sorbents and Molecular Sieves, Academic Press, London, 1978, Ch. 7, p. 339.
[65] *Shannon, R.D., K.H. Gardner, R.H. Staley, G. Bergeret, P. Gallezot, A. Auroux*: J. Phys. Chem. *89*, 4778 (1985).

ИЗУЧЕНИЕ КИСЛОТНОСТИ ЦЕОЛИТОВ РАЗНОГО ТИПА

И. Киричи, Г. Таши,
Г. Фёрстер и П. Феешм

Определены характеристики различных цеолитов с помощью рентгеновской дифракции, дериватографии и инфракрасной спектроскопии. Кислотность цеолитов определялась адсорбцией пиридина. Критически рассмотрены литературные данные, относящиеся к адсорбционным коэффициентам пиридина на кислых местах цеолитов.

ISBN 963 481 628 2
Acta Phys. et Chem. Szeged 33 99-107 (1987)

ADSORPTION OF PROPENE IN NaA ZEOLITE IN HENRY'S - LAW REGION

By

GY. TASI, I. KIRICSI, F. BERGER and P. FEJES

Applied Chemistry Department, József Attila University, Szeged
Rerrich Béla tér 1, Hungary

(Received 1 October 1987)

Adsorption equipment designed for the performance of adsorption measurements in the pressure range 10^{-3}-10^{3} Torr is described. Its applicability is demonstrated on the example of the adsorption of propene in NaA zeolite at low coverages. Henry's constant was determined at different temperatures.

Introduction

The theoretical adsorption isotherms derived from different gas-solid adsorption models include the Henry's law constant as parameter [1, 2]. In certain cases it is very important to estimate this constant, irrespective of any a priori adsorption model. Examples of the theoretical calculation of Henry's constant can be found in the literature only for simple molecules (such as CH_4) and for the noble gases [3]. Isotherms are the most promising means for its experi-

mental determination, provided the isotherms are measured at low coverages. For this purpose, a well-calibrated adsorption equipment is needed and the measurements should be performed very accurately.

This preliminary paper reports on a precise adsorption equipment designed for adsorption measurements in a wide pressure range, and its applicability is demonstrated by results obtained in an investigation of the adsorption of propene in NaA zeolite at low coverages.

Experimental

An outline of the volumetric adsorption equipment can be seen in Fig. 1.
With this set-up, adsorption measurements could be performed in the pressure range 10^{-3}-10^{3} Torr[+]. Two types of heaters were applied. During activation, the sample holder was heated by an electrical oven and the temperature could be stabilized within $\pm$ 1 K at 673 K. A thermostat filled with silicone oil was used to adjust the temperature of the sorbent within $\pm$ 0.1 K between 293 K and 523 K. The McLeod manometer and the mercury gas burette were tempered at 313 $\pm$ 0.1 K. During the measurements, the temperature of the sorbent was continuously checked with a Ni-CrNi thermocouple.

[+] 1 Torr = 101325/760 Pa

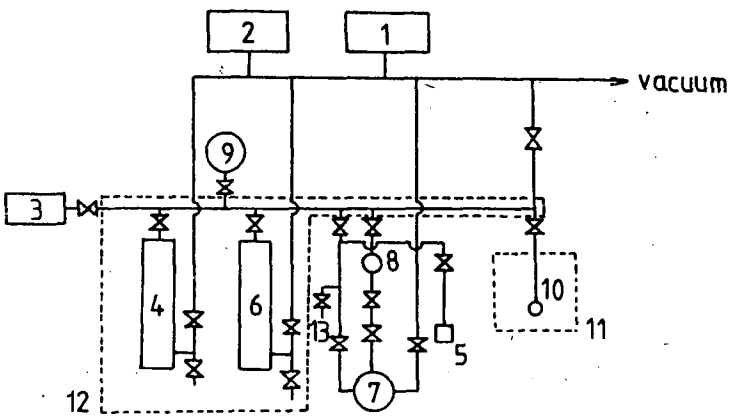

Figure 1.: Outline sketch of the volumetric adsorption apparatus.
1. Penning gauge; 2. Pirani gauge;
3. Barocel electronic manometer; 4. McLeod gauge;
5. Mercury manometer; 6. Mercury gas burette;
7. Propene storage; 8. Dosing part;
9. Helium storage; 10. Adsorber;
11. Silicone oil thermostat; 12. Water thermostat;
13. Gas inlet

Helium was used to determine the dead volume of the sample container.

The commercial NaA (Linde 4A) was exchanged in

0.1 mol/dm^3 NaCl solution in order to obtain a homoionic sample. Zeolite powder was stored in an exsiccator over saturated NH_4Cl solution.

Fresh samples of adsorbent (0.2-0.5 g) were used in each experiment.

The adsorbent placed into the sample container was dehydrated at 673 K for 12 h under high vacuum (the final vacuum was better than $1x10^{-6}$ Torr).

After pretreatment, the adsorbent was cooled to the desired temperature under continuous evacuation. In order to stabilize the temperature, the sorbent was equilibrated for 2 h prior to the measurements.

No change in crystallinity during activation could be observed by means of XRD, TG and IR.

For adsorption measurements, commercial propene (Merck, 99 %) was purified further with Linde 3A molecular sieve.

In the calculation of the adsorbed amounts, propene was regarded as a slightly imperfect gas [4]. The thermal transpiration effect for propene can be considered via the Takaishi-Sensui equation at low pressures [7,8].

Results and discussion

Figures 2 and 3 show the isotherms of propene over NaA at low coverages in the temperature range 343-493 K. Inspection of the Figures permits the following conclusions:

(i) Independently of the temperature, the accuracy and reproducibility of the measurements are good.

(ii) The adsorption of propene is reversible and non-dissociative, in accordance with the IR and GC investiga-

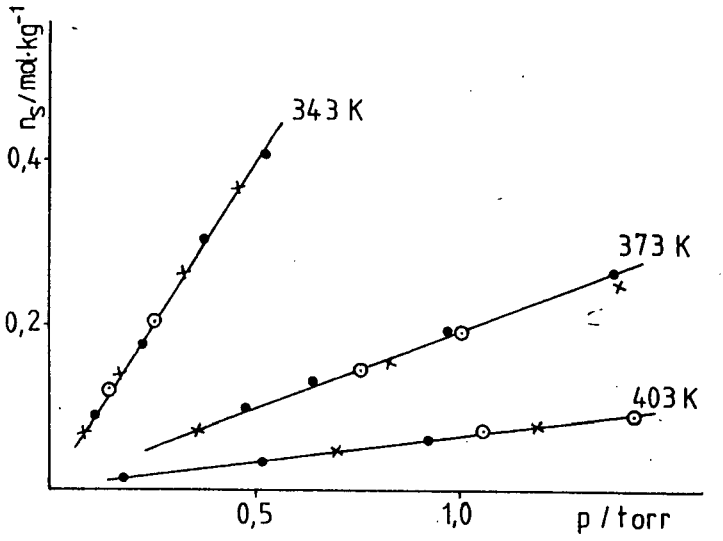

Figure 2.: Propene adsorption isotherms on NaA at low coverages. ●, x: adsorption points; ⊙: desorption points

tions [5, 6].

At low coverages, under conditions of no adsorbate-adsorbate interactions, a linear relationship exists between the specific adsorbed amount (n_s) and the equilibrium pressure (p): $n_s = K_H p$, where K_H is Henry's constant [9]. For the estimation of K_H, several independent ad- and desorption data sets were used at each temperature. The estimated values of K_H obtained with the ordinary least squares method are listed in Table I. In all cases the linear correlation

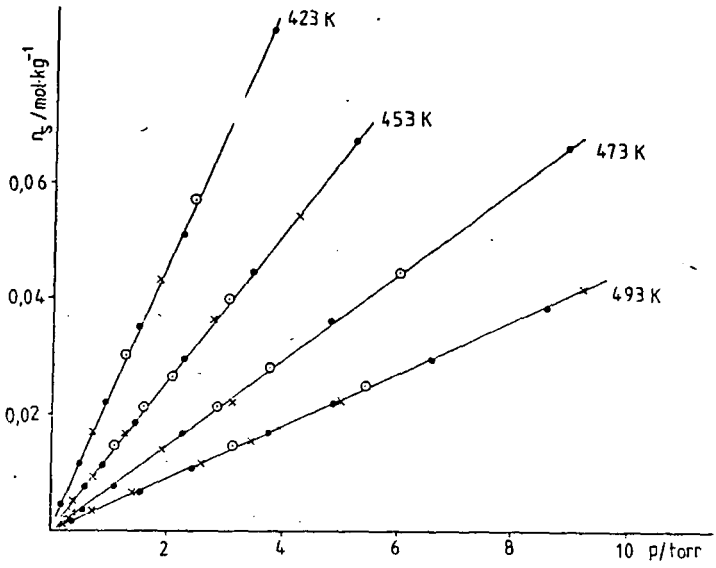

Figure 3.: Propene adsorption isotherms on NaA at low coverages. ●, x: adsorption points; ⊙: desorption points

coefficient was found to be > 0.995.

The temperature-dependence of K_H can be given by the van't Hoff equation:

$$K_H = K_o \exp [q_o/RT]$$

where q_o is the isosteric heat of adsorption at low coverages. The log K_H vs. 1/T plot is depicted in Fig. 4. Curve-fitting by the weighted least squares method resulted in the following values:

$$q_o = 47.83 \pm 0.13 \text{ kJ/mol}$$

$$K_o = 2.979 \times 10^{-10} \pm 6.6 \times 10^{-12} \text{ mol.kg}^{-1}.\text{Pa}^{-1}.$$

Table I

Henry's constants determined at different temperatures

Temperatures/K	K_H/mol.kg^{-1}.Pa^{-1}	S.E*[K_H]/mol.kg^{-1}Pa^{-1}
343	5.72×10^{-3}	3.5×10^{-5}
373	1.48×10^{-3}	2.0×10^{-5}
403	4.79×10^{-4}	1.0×10^{-5}
432	1.69×10^{-4}	1.7×10^{-6}
453	9.55×10^{-5}	6.0×10^{-7}
473	5.60×10^{-5}	4.0×10^{-7}
493	3.45×10^{-5}	2.0×10^{-7}

* Standard error of K_H [10]

The linear correlation coefficient was found to be 0.9997.

The adsorption of propene in A-type zeolites of different cationic forms (such as Li^+, Ca^{2+}, Mg^{2+}, Co^{2+}, Ni^{2+} and Mn^{2+}) was also investigated by means of IR spectroscopy and volumetry.

The results and their detailed discussion will be described in later papers.

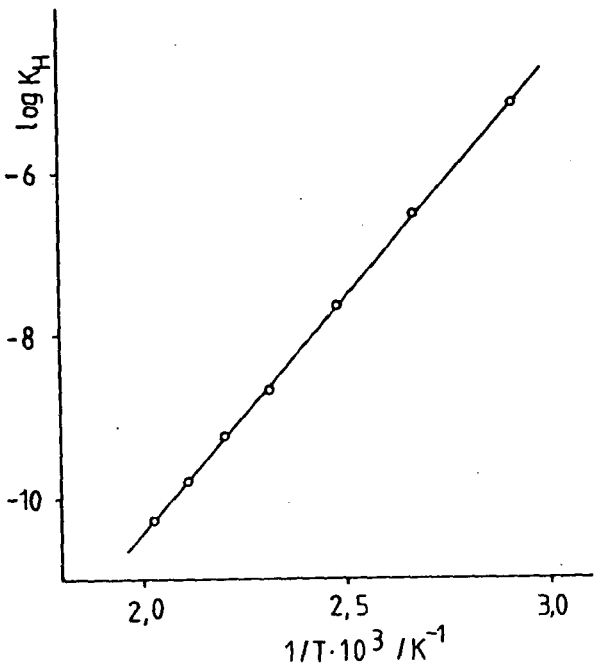

Figure 4.: Plots of log K_H against reciprocal absolute temperature.

References

[1] *Barrer, R.M.*: Zeolites and Clay Minerals as Sorbents and Molecular Sieves, Academic Press, London, 1978.
[2] *Ruthven, D.M.*: Principles of Adsorption and Adsorption Processes, John Wiley, New York, 1984.

[3] *Bezus, A.G., M. Kocirik and E.A. Vasilyeva*: Zeolites, *7*, 327 (1987) and other references therein.
[4] *Guggenheim, E.A.*: Thermodynamics, North-Holland Publ. Company, Amsterdam, 1977.
[5] *Förster, H., J. Seebode*: Zeolites, *3*, 63 (1983).
[6] *Fejes, P., I. Kiricsi, Gy. Tasi and K. Varga*: Acta Phys. et Chem. Szeged (Proc. of Intern. Symp. on Zeolite Catalysis) *31*, 405 (1985).
[7] *Takaishi, T., Y. Sensui*: Trans. Faraday Soc. *84*, 2503 (1963).
[8] *Yasumoto, I.*: J. Phys. Chem. *84*, 589 (1980).
[9] *Steele, W.A.*: The Interaction of Gases with Solid Surfaces, Pergamon, Oxford, 1974.
[10] *Box, G.E.P., W.G. Hunter and J.S. Hunter*: Statistics for Experimenters, Wiley, New York, 1978.

АДСОРБЦИЯ ПРОПЕНА НА ЦЕОЛИТЕ ТИПА NaA В ОБЛАСТИ ДЕЙСТВИЯ ЗАКОНА ГЕНРИ.

Г. Таши, И. Киричи,
Ф. Бергер и П. Феешл

Описан прибор для проведения адсорбционных измерений в интервале давлений 10^{-3} – 10^{3} торр. Пригодность прибора показана на примере адсорбции пропена на цеолите типа NaA при низких степенях покрытия. Определены константы Генри при различных температурах.

ISBN 963 481 633 9
Acta Phys. et. Chem. Szeged 33 109-118 (1987)

ON THE ISOMERIZATION OF ALLENE TO PROPYNE OVER A-TYPE ZEOLITES

By

P. KÓS, I. KIRICSI, K. VARGA, and P. FEJES

Department of Applied Chemistry, József Attila University
Szeged, Hungary

(Received 12 October 1987)

The allene to propyne isomerization was investigated over different cationic exchanged forms of A-type zeolite. All of the investigated catalyst samples proved to be active to various extents, but the isomerization was accompained by side-reactions in most cases. Purified $Na_{12}A$ zeolite ($A=Al_{12}Si_{12}O_{48}$) offered the conversion and selectivity required for investigations of the kinetics of the isomerization.

Introduction

In heterogeneous catalytic reactions, the interconversion of the reactants takes place in the adsorbed layer on the surface of the catalysts. As concerns the overall process, the reaction A ⇌ B is one of the most simple types, even though it passes through at least three distinct steps:

$$A + X \rightleftharpoons AX \rightleftharpoons B + X$$

where the first step is the adsorption of reactant A on the active site X of the catalyst, the second one is the surface interconversion, and product B desorbs into the gas phase in the last step.

The overwhelming majority of heterogeneous catalytic reactions are much more complex than the hypothetical one characterized by the above reaction steps. In theoretical investigations, it is sometimes advisable to search for a particular reaction that proceeds exclusively through the three steps mentioned.

The allene to propyne isomerization is a reversible reaction. It is of first order in both directions, and thus it can be regarded as an ideal reaction for kinetic studies in the sense outlined. It can be observed merely in the gas phase, above 900 K, without catalysts [1-4]. Its kinetics has already been investigated with the use of homogeneous catalysts such as iodine vapour [5], or even different metal oxides as catalysts [6-8].

Zeolites are frequently used as catalysts in a wide range of reactions of different hydrocarbons, because of their well-defined crystalline structures and ion-exchange properties. Different cationic forms of type-A zeolites were chosen as potential catalysts of the allene isomerization on the basis of experience gained earlier in studies of the cyclopropane to propene transformation over this type of catalyst [9].

In this work we attempted to find a catalyst that accelerates the allene to propyne reaction without resulting in unwanted by-products. We also aimed to establish precise conditions leading to the acquisition of data suitable for later quantitative evaluation.

Method and materials

The compositions of the catalysts can be seen in Table I. They were prepared by ion-exchange of LINDE 4A zeolite. The Co^{2+} content of CoNaA was determined by polarography; other catalysts were analysed by neutron activation.

Table I

Zeolite	Unit cell composition of catalyst used
NaA	$Na_{12}A$ $(A=Al_{12}Si_{12}O_{48})$
ZnNaA	$Zn_{5.4}Na_{1.2}A$
LiNaA	$Li_{9.6}Na_{2.4}A$
CaA	Ca_6A
CoNaA	Co_5Na_2A

From the powders, pellets were prepared by applying pressures of the order of 10^8 Pa. The pellets were crushed, and the 0.16-0.2 mm sieve-fraction was selected and stored over saturated ammonium chloride solution until use.

The allene was a MATHESON product of 99.3 % purity, which was used without further purification.

The experiments were carried out in a recirculatory batch reactor. A 100 mg sample of catalyst was put into the reactor and was heated to 678 K at a pressure of 1 Pa for 4 hours. It was then cooled down to the reaction temperature, which varied between 395 K and 460 K. The reaction temperature was continuously recorded via a Na-CrNi thermo-

couple reaching the middle of the catalyst bed. A large amount of nitrogen was used as diluting gas (up to 99 %) to maintain isothermicity in spite of the heat of sorption of allene.

Gas samples were taken from the reactor with a Carlo-Erba sampling valve and were analysed by means of GC with a column filled with 30 % DMS on CHROMOSORB-P; the carrier gas was nitrogen.

Experimental results

The kinetic curves obtained over CoNaA zeolite demonstrate that the isomerization of allene was accompained by side-reactions, as shown in Fig. 1. At 395.5 K, the amounts of allene and propyne as functions of time are characterized by monotonously decreasing and increasing curves, respectively. Since no other products but allene and propyne can be detected in the gas phase, the sum of their concentrations (i.e. partial pressures) should not change after sorption equilibrium is reached. Actually, the shape of the overall mass balance curve c unambiguously shows that the amount of the gas phase steadily decreases. At 460 K, the monotonously decreasing nature of balance curve f can also be ascertained; further the propyne production curve e displays a peak. The effects of side-reactions are even more marked when ZnNaA catalysts are used (Fig. 2).

The isomerization can also be performed over CaA and LiNaA zeolites, but the activities of these catalysts are much lower than that of CoNaA.

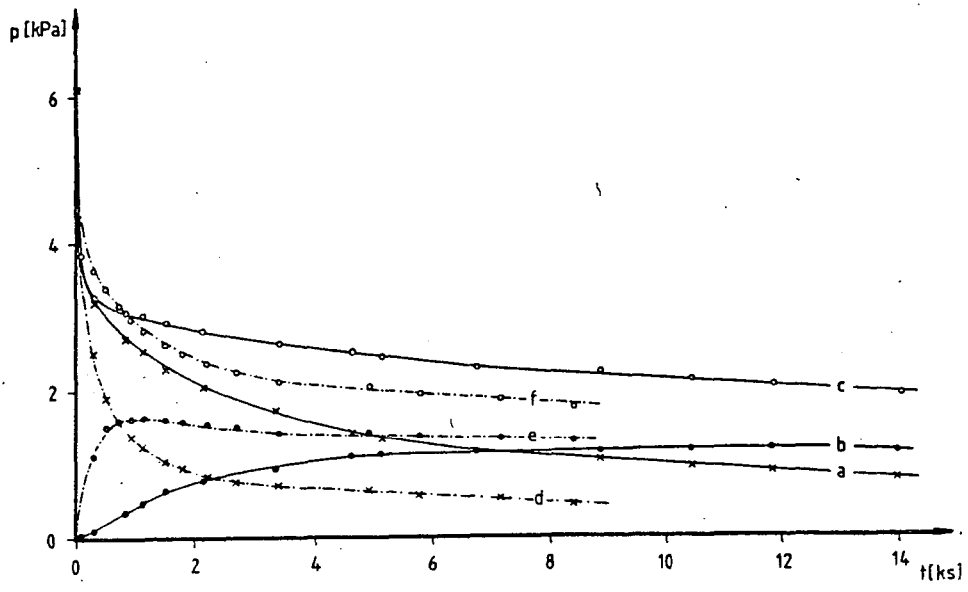

Figure 1.: Kinetic curves of isomerization of allene to propyne over CoNaA catalyst at 395.5 K (——) and at 460 K (-.-), showing partial pressures of allene (a, d), propyne (b, e) and their sum (c, f)

During examinations of the catalytic activity of the NaA base zeolite (LINDE 4A) that had been used to prepare the other catalyst samples, the curves of Fig. 3 were obtained. These show that this zeolite is also an active catalyst of the allene to propyne isomerization. The total pressure c passes through a minimum after the quick decrease caused by the sorption step, and then reaches a constant value.

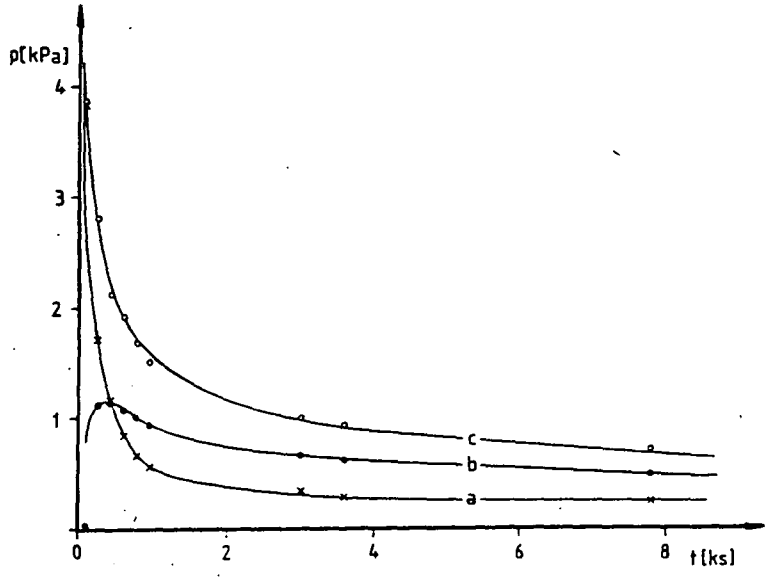

Figure 2.: Kinetic curves of allene isomerization over ZnNaA catalyst at 395.5 K, showing partial pressures of allene (a), propyne (b) and their sum (c)

Since the commercial Na-form zeolites generally contain Ca^{2+} and/or H^{+} ions in traces, which may originate from the washing water during preparation or can be ascribed to partial hydrolysis, respectively, it seemed meaningful to prepare a "clean" sample of NaA. This was obtained by repeated ion-exchanges of the original NaA using NaCl solution. Figure 4 depicts kinetic curves ob-

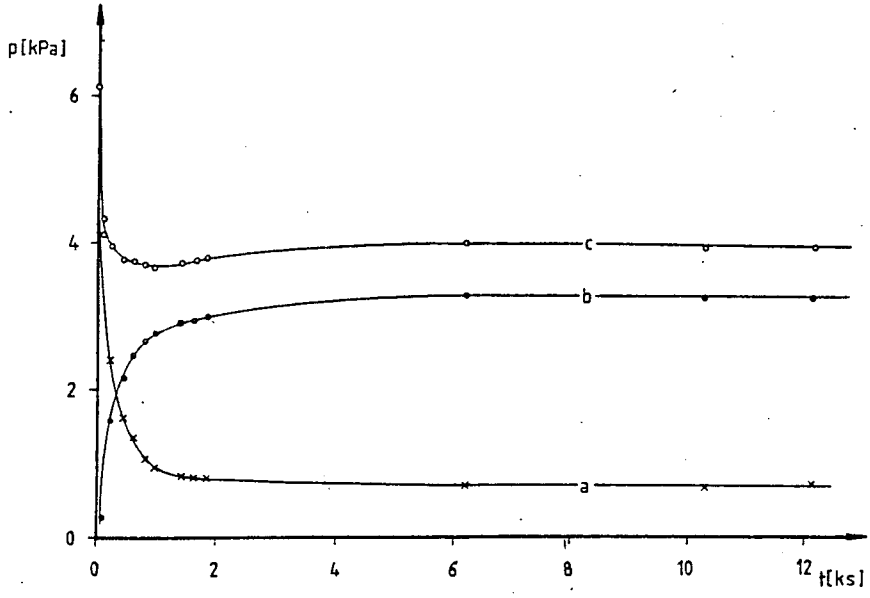

Figure 3.: Kinetic curves of transformation of allene to propyne over LINDE 4A zeolite at 395.5 K

tained from reactions carried out over NaA zeolite prepared in this way. It is obvious that curve c, representing the total pressure, has no minimum, i.e. the total amount of the gas phase does not alter during the whole experiment, apart from the fast initial decrease. Furthermore, the shapes of curves a and b, representing the diminishing of allene and the production of propyne, respectively, do not contradict the qualitative picture of apparent first-order kinetics.

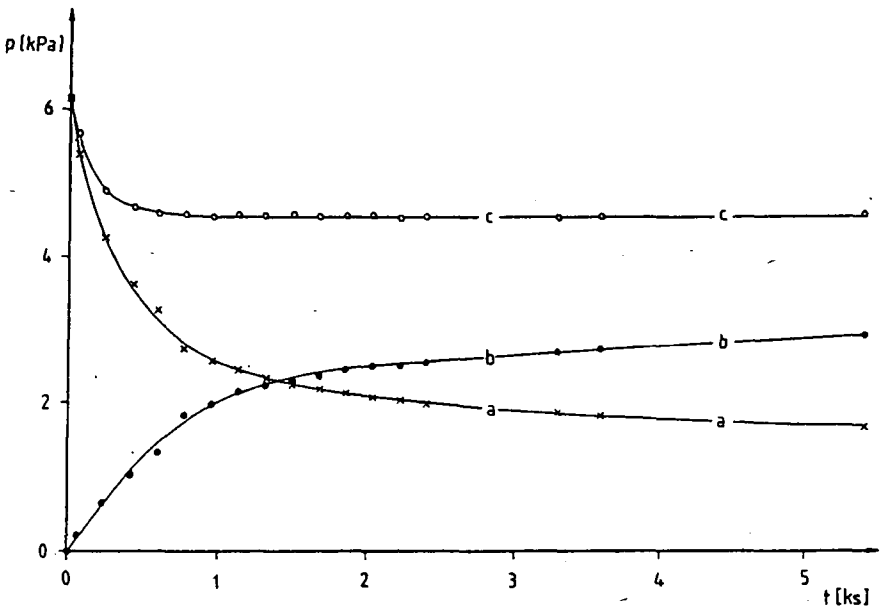

Figure 4.: Kinetic curves of allene to propyne isomerization over Na-exchanged NaA Zeolite catalyst

Discussion

Under the conditions used in this study, allene undergoes a comparatively fast isomerization over CoNaA and ZnNaA catalysts, accompained by other reaction steps. These can be

polymerization steps producing condensed substances, and/or oligomerization reactions the products of which remain irreversibly sorbed on the surface of the catalyst, so that they cannot be detected in the gas phase. These products gradually reduce the activity of the catalyst by occupying some of the active sites, and they also cause a deficiency in the mass balance, which makes evaluation of the kinetic measurements practically impossible. Therefore, these catalysts are not suitable in an experimental model of the ideal A ⇌ B type heterogeneous catalytic reaction.

Since Li^+ ions are smaller and more compact than Na^+ ions, the LiNaA catalyst was expected to be very active in the isomerization. Its peculiar behaviour, i.e. its weak activity, was in accordance with the results found by the investigation of the isomerization of cyclopropane to propene [10].

Over the original NaA catalyst, the initial decrease in the total pressure is related to the adsorption of allene. The succeeding increase (Fig. 3) can be explained by the difference between the sorption capabilities of the reactants.

The shapes of the kinetic curves obtained over Na^+--exchanged NaA catalyst are in accordance with the kinetics of a homogeneous reversible reaction of apparent first order in both directions, except for the initial part referring to the adsorption step.

Thus, we found that all of the investigated A-type zeolites were active to various extents in the isomerization, but only the NaA samples offered the conversion and selectivity required for investigations of the kinetics of the allene to propyne isomerization.

References

[1] *Levush, S.S., S.S. Abadzhev, C.U. Shevchuk*: Neftekhimiya *9*, 215 (1969).
[2] *Lifshitz, A., M. Frenklach, A. Burcat*: J. Phys. Chem. *79*, 805 (1975).
[3] *Bradley, J.N., K.O. West*: J. C. S. Faraday Trans. I, *71*, 967 (1975).
[4] *Hidaka, Y., T. Chimori, M. Suga*: Chem. Phys. Letters, *119*, 435 (1985).
[5] *Walsh, R.*: Trans. Faraday Soc., *67*, 2085 (1971).
[6] *Chang, C.C., R.J. Kokes*: J. Am. Chem. Soc. *92*, 7517 (1970).
[7] *Cordes, J.F., H. Günzler*: Chem. Ber. *92*, 1055 (1959).
[8] *Parmentier, J.H., H.G. Peer, L. Shuttle*: J. Catal. *22*, 213 (1971).
[9] *Fejes, P., I. Kiricsi, Gy. Tasi, K. Varga*: Zeocat'85 Int. Conf. on Zeolite Catal., 1985 Siófok, Hungary, Proceedings, 405.
[10] *Fejes, P., I. Kiricsi, H. Förster, J. Seebode*: Zeolites, *4*, 259 (1984).

ИЗОМЕРИЗАЦИЯ АЛЛЕНА В ПРОПИН НА ЦЕОЛИТАХ ТИПА А.

П. Кош, И. Киричи, К. Варга и П. Фееш

Изучена алленето-пропиновая изомеризация на различных катион-замещенных цеолитах типа А. Все изученные образцы катализаторов оказались более или менее активными, однако, в большинстве случаев изомеризация сопровождалась побочными реакциями. Очищенный цеолит $Na_{12}A$ оказал конверсию и селективность, необходимые для изучения настоящей кинетики изомеризации.

ISBN 963 481 631 2
Acta Phys. et Chem. Szeged 33 119-124 $1987)

MESOGENIC ANDROSTANE DERIVATIVES

By

J.A. SZABÓ, A.I. ZOLTAI and G. MOTIKA

Department of Organic Chemistry, József Attila University
Szeged, Hungary

(Received 5 October 1987)

A homologous series of 4-alkoxybenzoic acid diesters with androst-5--ene-3β,17β-diol have been prepared and their mesogenic properties studied.

The literature contains a number of publications relating to the effects of the structure of the 17β-side-chain of sterols on the mesogenic properties of these compounds [1-3]. Most of these investigations concern the structural requirements of the cholesterol-like molecules, and relatively few articles deal with other biologically important steroidal compounds.

Therefore, we have synthetized a homologous series of diester derivatives of androst-5-ene-3β,17β-diol with 4-alkoxybenzoic acids, which are well-known mesogenic compounds. All compounds prepared exhibited mesogenic properties in relatively wide ranges of temperature. In the case of lower alkoxy derivatives, only a relatively simple phase sequence appeared: Cr——Ch——I (from methoxy- to heptyloxybenzoic acid esters), while for higher homologues the

cholesteric mesophase was accompanied by a monotropic smectic phase. These derivatives showed the characteristic light reflexion. The cholesteric mesophases had oily-streaks in the textures, while the smectic phases appeared as

Table I

Thermal data from polarizing microscopic measurements on compounds investigated

Compound	R	Cr	S	Ch	I
1	methyl	198		277	
2	ethyl	215		265	
3	n-propyl	214		236	
4	n-butyl	165		218	
5	n-pentyl	110		155	
6	n-hexyl	102		175	
7	n-heptyl	103		173	
8	n-octyl	105	(84)	165	
9	n-nonyl	110	(82)	154	
10	n-decyl	110	(84)	146	
11	n-undecyl	112	(108)	129	

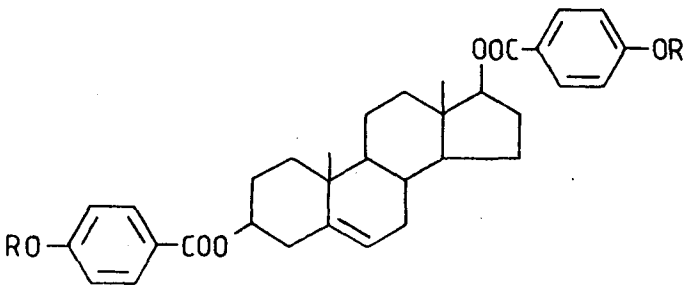

Compounds 1-11

(R varies from methyl to n-decyl)

schlieren textures. In the calorimetric measurements, all compounds showed nearly the same phase-transition temperatures as observed optically with a polarizing microscope in the case of the crystalline-cholesteric and the cholesteric-smectic transitions, but no thermal effect appeared at the cholesteric-isotropic transition. Therefore, this transition is considered to be of a higher (infinite)--order type [4]. The optically observed transition temperatures are listed in Table 1.

At higher temperatures (about 200 °C), the samples decomposed slowly (the 17 β -ester pyrolyzed) when the isotropic liquid state was reached. In the cholesteric region qualitative TLC observation indicated that the decomposition was absent.

Experimental

All esters were prepared in the usual way from specially purified 4-n-alkoxybenzoic acids [5] via the acid chlorides and androst-5-ene-3β,17β-diol in dry pyridine solution at room temperature. In the crude esters were contaminated with the corresponding acid anhydrides, which were hydrolyzed by boiling in aqueous pyridine solutions.

These samples were purified by low-pressure column chromatography on Kieselgel G (Merck) adsorbents, and were crystallized from rectified spirit. The purities were checked on precoated TLC plates (Kieselgel HF, Merck). The analytical data on compounds I-II are shown in Table 2. The IR and NMR spectra of the compounds were recorded with Carl Zeiss Jena 75/IR and JEOL 60 HL NMR spectrometers. The calorimetric investigations were performed with a Perkin-Elmer DSC-2 instrument. Microscopic investigations were conducted on a PMHK-5 (Dresden) hot-stage.

Acknowledgements

The authors are indebted to Mrs. Dr. G. Bartók-Bozóki for microanalyses, and to Mrs. Kertész-Csányi and Mrs. E. Tóth for technical assistance.

Table II

Analytical data on compounds 1-11

Compound	Formula	Calcd. C	Calcd. H	Found C	Found H
1	$C_{35}H_{42}O_6$	75.24	7.58	75.11	7.57
2	$C_{37}H_{46}O_6$	75.74	7.90	75.40	7.77
3	$C_{39}H_{50}O_6$	76.19	8.20	76.00	8.03
4	$C_{41}H_{54}O_6$	76.60	8.47	76.70	8.51
5	$C_{43}H_{58}O_6$	76.98	8.71	77.03	8.82
6	$C_{45}H_{62}O_6$	77.32	8.94	77.31	8.97
7	$C_{47}H_{66}O_6$	77.64	9.15	77.42	9.21
8	$C_{49}H_{70}O_6$	77.94	9.35	78.11	9.45
9	$C_{51}H_{74}O_6$	78.22	9.53	78.03	9.61
10	$C_{53}H_{78}O_6$	78.48	9.69	78.51	9.48
11	$C_{55}H_{82}O_6$	78.72	9.83	78.83	9.71

References

[1] *Gray, G.W.*: Molecular Geometry and the Properties of Non-Amphiphilic Liquid Crystals in Advances of Liquid Crystals (Ed: G.H. Brown) Vol. 2 pp. 62-67. Academic Press, New York (1976).

[2] *Elser, W., Ennulat R.D.*: Selective Reflection of Cholesteric Liquid Crystals, in Advances of Liquid Crystals (Ed: G. H. Brown) Vol. 2 pp. 99-121. Academic Press, New York (1976).

[3] *Demus, D., Zaschke H.*: Flüssige Kristalle in Tabellen. Vol. 1 pp. 276-307 VEB Deutscher Verlag für Grundstoffindustrie. Leipzig (1974). Vol. 2 pp. 408-436. VEB. Deutscher Verlag für Grundstoffindustrie, Leipzig. (1984).

[4] *Kelker, H., Hatz R.*: Handbook of Liquid Crystals Ch. 8. pp. 340-372 Verlag Chemie, Weinheim (1980).

[5] *Gray, G.W., Jones B.*: J. Chem. Soc. 1953, 4199.

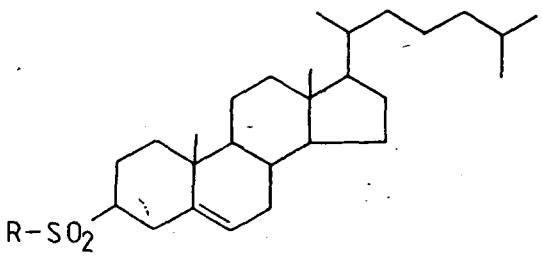

Compounds 1-10
(R varies from methyl to n-decyl)

is a monotropic smectic substance, while the higher members (8-10) are enantiotropic smectic. These smectic phases exhibited characteristic focal-conic fan textures, and all of them were supercoolable to various extents, depending on the cooling rate, e.g. at a cooling rate, of about $10^{\circ}sec^{-1}$ compounds 8 and 10 supercooled by nearly 30° under the observed C—S transition temperatures, while compound 9 did so by only 10°. The compounds displayed crystal polymorphism, frequently with metastable crystal modofications, e.g. compound 5 has a $Cr_I \longrightarrow Cr_{II}$ transition at about 105-115°, while compound 4 shows three modifications, with transition temperatures of about 110°, 136° and 146°.

Table I

The mesogenic properties of compounds 1-10

Compound	R	Cr	S	I
1	methyl	172	.	.
2	ethyl	. 161	.	.
3	n-propyl	. 157	.	.
4	n-butyl	. 166	.	.
5	n-pentyl	. 173	.	.
6	n-hexyl	. 159	. (156)	.
7	n-heptyl	. 160	.	.
8	n-octyl	. 137	. 166	.
9	n-nonyl	. 142	. 167	.
10	n-decyl	. 143	. 169	.

Experimental

Preparation of sulphones: To a 0.01 M ethanolic solution of the thioether (about 30 cm^3), 3 cm^3 30 percent H_2O_2 (about 0.026M) and 1 cm^3 1 % aqueous ammonium molybdate solution (about 0.04 M based on $(NH_4)_2MoO_4$) were added. The samples were allowed to stand for 1-5 days at room temperature, then poured onto ice-water and the solid was filtered off, dried, and chromatographed on Kieselgel 60 (Merck) with benzene. The pure fractions were evaporated and crystallized from aqueous ethanolic solution.

The textural investigations were made a PMHK 5 (Dresden) polarizing microscope hot-stage. In the calorimetric meas-

urements, a Perkin-Elmer DSC-2 instrument was applied. The spectra were recorded with Specord 75IR (Jena) and Jeol 60 HL NMR spectrometers.

Table II

Analytical data

Compound	Formula	Calcd. C	Calcd. H	Found C	Found H
1	$C_{28}H_{48}O_2S$	75.00	10.69	75.30	10.62
2	$C_{29}H_{50}O_2S$	75.26	10.81	75.15	10.91
3	$C_{30}H_{52}O_2S$	75.56	10.90	75.48	10.58
4	$C_{31}H_{54}O_2S$	75.85	11.00	75.91	10.93
5	$C_{32}H_{56}O_2S$	76.12	11.10	76.21	11.07
6	$C_{33}H_{58}O_2S$	76.38	11.18	76.05	11.34
7	$C_{34}H_{60}O_2S$	76.62	11.26	76.40	11.53
8	$C_{35}H_{62}O_2S$	76.85	11.33	76.62	11.27
9	$C_{36}H_{64}O_2S$	77.07	11.41	76.78	11.49
10	$C_{37}H_{66}O_2S$	77.28	11.48	76.85	11.61

Acknowledgements

The authors are indebted to Mrs. G. Bozóki-Bartók for the microanalyses, to Mr. Gy. Dombi and Mr. J. Kiss for the spectra, and to Mrs. J. Csányi-Kertész and Mrs. Szomor-Szeli for technical assistance.

References

[1] *Szabó, J.A., A.I. Zoltai, P.M. Agócs and G. Motika*: in Advances in Liquid Crystal Research and Applications (Ed: L. Bata) Pergamon Press, Oxford; Akadémiai Kiadó Budapest (1979) pp. 1049-1058.
[2] *Demus, D. and H. Zaschke*: Flüssige Kristalle in Tabellen Vol. II p. 418, VEB Deutscher Verlag für Grundstoffindustrie, Leipzig (1984).
[3] *Kelker, H. and R. Hatz*: Handbook of Liquid Crystals Ch. 2.12. pp. 67-113. Verlag Chemie, Weinheim (1980).

ЖИДКОКРИСТАЛЛИЧЕСКИЕ ХОЛЕСТЕРИЛ-СУЛЬФОНЫ

Й.А. Сабо, А.И. Золтаи, Г. Мотика

Авторы синтетизировали серию тождественных н-алкилзамещенных холестерил-сульфонов и изучили мезогенные свойства этих соединений.

ISBN 963 481 632 0
Acta Phys. et Chem. Szeged 33 131-144 (1987)

THE ZX 81 AS AN INTEGRATOR

By

T. KATONA and I. PÁLINKÓ

Department of Organic Chemistry, József Attila University
Szeged, Hungary

(*Received 6 October 1987*)

The paper summarizes the application of a ZX 81 microcomputer as an integrator. The necessary modifications in the hardware, the principles of the integration and the actual integration software are briefly described. Experience revealed that this computer-integrator is a useful tool in both qualitative and quantitative evaluation of even complicated chromatograms, though it is less accurate than a professional integrator.

Introduction

Gas chromatography permits the analysis of complex mixtures both qualitatively and quantitatively. Qualitative analysis requires a knowledge of the retention times, while for quantification the areas of the peaks are needed. These data are measured by specially built computers, which can even control the gas chromatograph. The modern instruments have built-in computers, while specially built simple computers developed for integration purposes can be attached to the older models.

In the following, a cheap and simple integration method will be presented. An integration program has been written

which runs on a simple and cheap home computer (ZX 81).

The computer allows fast data acquisition, a suitable program facilitates the data processing, the results can be stored (and reprocessed with other parameters if necessary), and other programs can be run on the computer as well.

The advantage of writing an individual program is the higher flexibility, and the possibility of fitting it exactly to the problem to be solved. Of course, drawbacks also exist. The main problem is the lack of the sophisticated software which the powerful integrators have; however, these software products are usually well protected by the manufacturer. Therefore, only a few detailed descriptions of such software are to be found in the literature. The manuals of the integrators emphasize the practical aspects; they show how to use the software, but they do not give a description of it [1, 2].

This paper describes the hardware, the elementary steps of the integration procedure, their actual representation on the ZX 81, and finally our experience with the computer-integrator.

Hardware

The CPU (Central Processing Unit) of the ZX 81 is a Z 80A microprocessor. This is used in most of the microcomputers found in Hungary. This model has been developed especially for home computers (HC). It is simple and cheap, though it has all the necessary features. Thus, it can be used as an integrator [3].

The set-up consists of the following parts:

ZX 81 - home computer
16 K RAM - memory extension

SEIKOSHA 50 - dot matrix printer
JUNOSTY - television
MK 29 - tape recorder

The hardware has been modified somewhat to enhance the reliability of the computer. The original keyboard has been changed to a push-button one, the memory extension has been built into the box of the computer, and a RESET button has been added.

The analog-digital converter (ADC) is a product of INTERSIL. This is a converter with 12 bits, working in the DUAL-SLOPE mode with a 30 ms conversion time. The ADC has been attached to the computer through an 8255 PPI circuit. The ZX 81 has a simple address decoding system, therefore the A5, A6 and A7 address lines and the RD, WR and IORQ lines have proved satisfactory. The output signal goes through an amplifier attached to the RECORDER output of the gas chromatograph [1, 4, 5].

Integration

The integration of the gas chromatographic peaks was earlier performed by two methods. The first was the measurement of the weights of the cut out peaks on an analytical balance, while the second was a simple mathematical operation, i.e. multiplying the peak height by its half-width. The former method can be applied well if the chromatogram consists of asymmetrical peaks; the latter gives satisfactory results if the peaks can be approximated by Gaussian curves. If the above conditions are not met, the determina-

tion may contain considerable error [6, 7].

Our integration method resembles the latter procedure, as the computer measures the peak height at given time intervals, performing the integration by the addition of partial peak areas. The data acquisition occurs on-line. There are two processing methods: one is a real-time method, while the other proceeds after the collection of a sufficient number of data (they are stored temporarily by the computer). The accuracy depends on the accuracy of the peak height measurement (i.e. how many meaningful digits are contained by the number formed as the result of the conversion) and on the time interval between samplings (which is determined by the speed of data acquisition).

In our case the AD conversion occurs on 12 bits, which means decomposition of the analog signal to $2^{12}=4096$ parts. The speed of data acquisition is limited by the sum of the conversion time of the ADC and the time required for temporary data storage. Obviously, the frequency of sampling is limited by the capacity of the accessible memory of the computer. This factor is quite significant, because we have only a 16 kbyte RAM.

The reliability of the integration largely depends on the program's being able to distinguish between the baseline and the peaks. For this, we need criteria which allow straightforward evaluation without too many operations.

Baseline corrections

The stability of the baseline is an absolute must during the measurements, but it often changes, and increasing attenuation makes it noisy. There are three methods to re-

cord the baseline.

The simplest method is to take its initial values constant throughout the analysis. The disadvantage of this method is that changes in the baseline are not taken into account, and the criterion of reaching the baseline is recovery of the initial value (Figure 1).

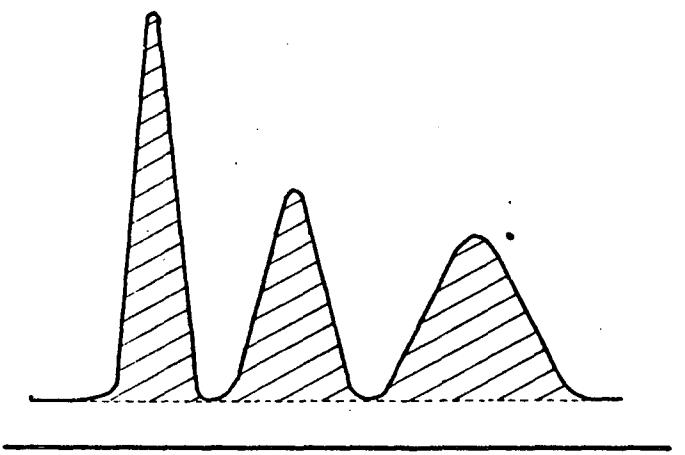

Figure 1.: Integration taking into account the initial value of the baseline.

The second method takes into account the value of the baseline at the end of the chromatogram as well. The change between the initial and the end values is taken as linear and the peak areas are corrected accordingly (Figure 2).

This method can be applied if the baseline is constant, or its tendency to change is constant throughout the analysis.

The third method assigns two baseline values to each peak, one before and another after the peak. Thus, the

variation in the baseline can be tracked accurately, and therefore the peak areas can be corrected precisely (Figure 3).

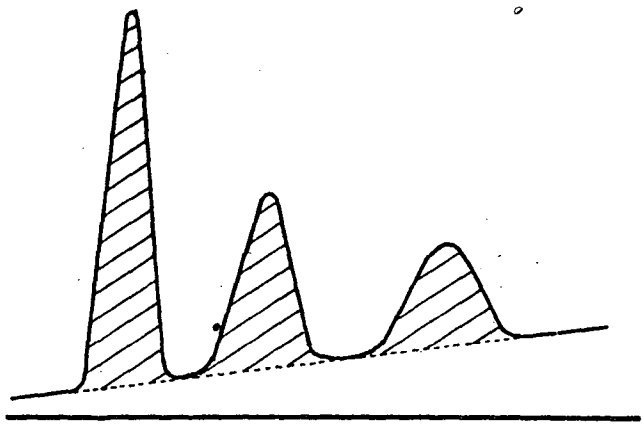

Figure 2.: Integration following the initial change in the baseline.

Peak recording

There are three methods for recording the peaks. They are closely related to the methods of baseline correction.

The first method takes the baseline as constant and records every signal above a given value as a peak. This method can only be used if the resolution is perfect and the baseline is stable (Figure 4).

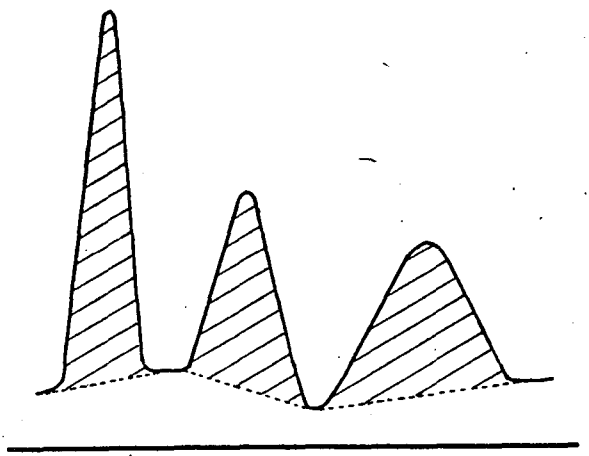

Figure 3.: Integration taking into account the baseline values before and after the peak.

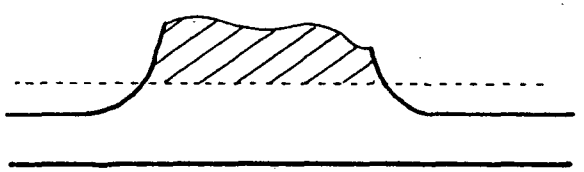

Figure 4.: Peak recording using the constant threshold value.

The second method takes the initial change in the baseline and extrapolates it to the endpoint of the peak (Figure 5).

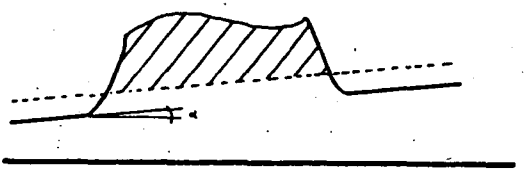

Figure 5.: Peak recording with the extrapolation of the initial value.

The third pays no attention to the baseline, as it monitors the tendency of the variation of the subsequent inputs to vary. A peak is taken as complete when this tendency is below a given value. This method corresponds to the third baseline detecting technique (Figure 6).

The integration software has been compiled in accordance with the third method.

How does the software work?

The integration can be performed in two ways. The first involves parallel data acquisition and data processing, while the second postpones the latter procedure until after the data acquisition. The ZX 81 is quite slow, and so we had to use the second route. The ADC is controlled by an Assembly routine, which runs fast enough to establish 15 inputs/s. The 16 K memory could be filled

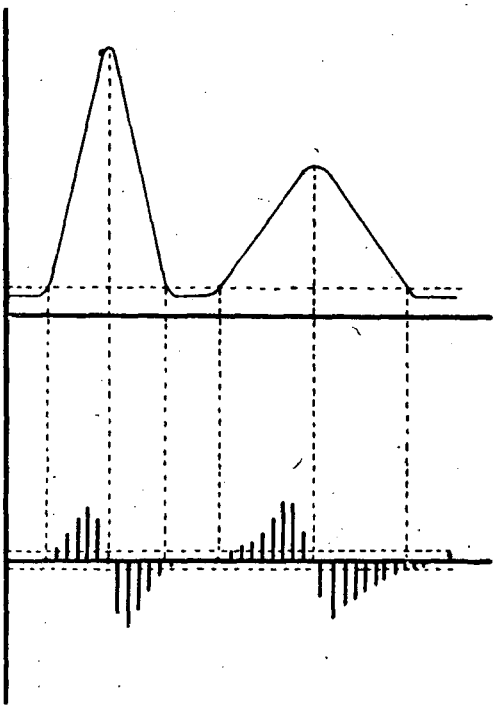

Figure 6.: Peak recording using the changing tendencies.

up quickly in this way, and therefore a cycle in the routine puts the average of more than one inputs into the memory. Accordingly a memory overflow will not occur and the speed of data acquisition can also be varied.

Our experience has shown that the accurate quantitative analysis of a peak with a small retention time requires at least 10 inputs, which means 3 inputs/s if the half-width of the peak is 1,5-2,5 s. If 8 K out of 16 K is reserved for storing the data, then a 12-minute long chromatogram can be recorded. The storage capability has been enhanced by 25 % by shifting and masking the bits

not used, thereby saving the valuable digits only.

The control program has been completed with QUICK SAVE and QUICK LOAD routines to save the stored data. We have found that this fast storing capability is suitably reliable. Another addition is the high-resolution graphics, which allows a plot of the chromatogram. This routine requires 8 K RAM, and therefore the input data must be stored on the DISPLAY FILE. This results in a decrease of the resolution to 8 bits and hence this routine can only be used if the accuracy is satisfactory [8, 9].

Another routine sets the FRAMES control register, and its combination with suitable arithmetic and PRINT routines permits the continuous display of the retention time and the input values during the recording of the chromatogram.

The Assembly routines have been compiled into a REM line, and the data processing is done by a BASIC routine [12, 13].

The BASIC routine

The operation of the BASIC routine is based upon the "window" method. A window moves along the chromatogram, so that a relatively small portion of the chromatogram can be examined at a given time. Our program uses three windows: A, B and C. B is the window for the current operations, while A is the previous and C is the next one. Let us see how an integration proceeds.

At the beginning of the peak (Figure 7), the difference between the input sum for C and the sum for B ex-

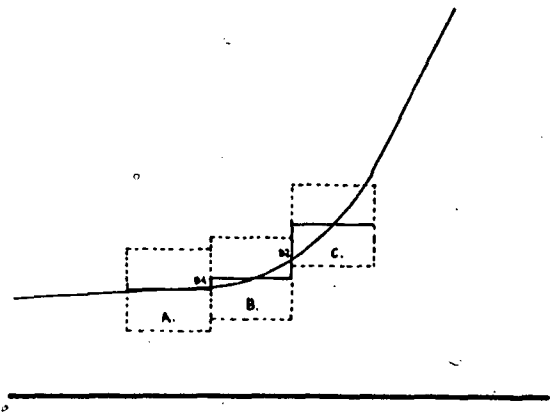

Figure 7.: Integration using the three windows method.

ceeds the threshold value. Window A will give the initial value of the baseline, and B will give the first partial area. At the end of the peak, the difference between C and B decreases to the baseline value, C will give the baseline value and B will give the last partial area. The window method helps the modular programming, and the integration criteria can be reliably programmed as well.

It is also possible to integrate poorly resolved peaks. The software divides them into two parts, with a vertical line at the minimum between the peaks (Figure 8).

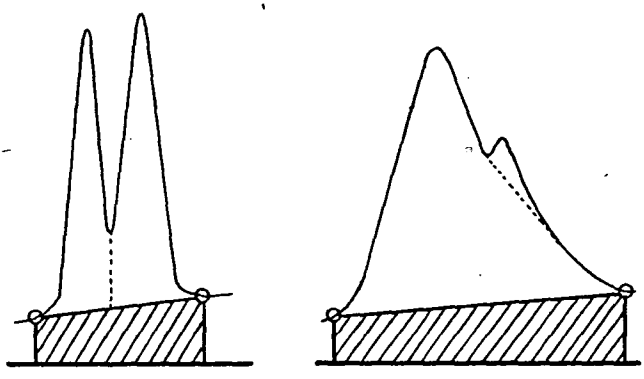

Figure 8.: Integration when resolution is poor

The computer-integrator in practice

The performance of our system had been tested with a mixture of homologous alcohols, the composition of which has been determined with a professional integrator. The variance of the PERKIN ELMER integrator was $\pm$0.5 %, while that of the ZX 81 was at most $\pm$ 2.5 %. The maximum error occurred when the resolution was intentionally worsened.

References

[1] *Chan, C.Z., R. Irwin and R. O'Brien*: International Laboratory 11-12, 54 (1981).
[2] *Hettinger, J.*:-Autolab Technical Bulletin 111, 74.
[3] ZX 81 Users Manual.
[4] ICL 7109 Specifications.
[5] Prof. *G. Buist*, Chemistry Dept., University of Surrey Guilford, Surrey, GU 25 XH, personal communication.
[6] *Stolyarov, B., T.M. Sabinov and A.G. Vitenberg*: Rukovodstvo k prakticheskim rabotam po gazovoi khromatografii., University of Leningrad, Leningrad, 1973.
[7] *Vigdergauz, M.*: Gázkromatográfiai számítások., Müszaki Könyvkiadó, Budapest, 1983.
[8] Mikroszámitógép magazin, Budapest, 4, 23, (1986).
[9] Mikroszámitógép magazin, Budapest, 4, 43 (1986).
[10] *Bóc, I.*: ZX 81 BASIC és ASSEMBLER., Müszaki Könyvkiadó, Budapest, 1985.
[11] *Rákosi, M.*: ASSEMBLER., Müszaki Könyvkiadó, Budapest, 1977.
[12] *Sztrókay, K.*: A Z 80 ASSEMBLER., Müszaki Könyvkiadó, Budapest, 1985.
[13] *Alcock, D.*: Ismerd meg a BASIC nyelvet., Müszaki Könyvkiadó, Budapest, 1983.

ИСПОЛЬЗОВАНИЕ ВЫЧИСЛИТЕЛЬНОЙ МАШИНЫ X 8I В КАЧЕСТВЕ ИНТЕГРАТОРА.

Г. Катона, И. Палинко

В статье обобщены результаты использования микровычислительной машины X 8I в качестве интегратора. Кратко описаны необходимые модификации хардвера, общие принципы и программа актуальной интеграции. Экспериментально подтверждено, что предлагаемый вычислитель-интегратор пригоден для качественной и количественной оценки даже сложных хроматограмм, несмотря на то, что точность его уступает специальным интеграторам.

INDEX

Fk: Dr. Gécseg Ferenc
Készült a JATE Sokszorosító Üzemében, Szeged
Engedélyszám: 84/88. Méret: B/5
Példányszám: 425 Fv: Lengyel Gábor